Smart Hydrogels Based on Responsive Star-Block Copolymers

Dissertation

Zur Erlangung des akademischen Grades eines Doktors der Naturwissenschaften (Dr. rer. nat.) im Fach Chemie der Fakultät für Biologie, Chemie und Geowissenschaften der Universität Bayreuth

vorgelegt von

Alexander Schmalz

geboren in München

Bayreuth, 2011

Die vorliegende Arbeit wurde in der Zeit von Juli 2007 bis Oktober 2011 in Bayreuth am Lehrstuhl für Makromolekulare Chemie II unter der Betreuung von Herrn Prof. Dr. Axel H.E. Müller angefertigt.

Vollständiger Abdruck der von der Fakultät für Biologie, Chemie und Geowissenschaften der Universität Bayreuth genehmigten Dissertation zur Erlangung des akademischen Grades eines Doktors der Naturwissenschaften (Dr. rer. nat.)

Dissertation eingereicht am:	06.12.2011
Zulassung durch die Promotionskommission:	14.12.2011
Wissenschaftliches Kolloquium:	02.03.2012
Amtierender Dekan:	Prof. Dr. Beate Lohnert

Prüfungsausschuss:

Prof. Dr. Axel H.E. Müller (Erstgutachter)

Prof. Dr. Thomas Hellweg (Zweitgutachter)

Prof. Dr. Birgit Weber

Prof. Dr. Carlo Unverzagt (Vorsitzender)

In the beginning the Universe was created. This has made a lot of people very angry and has been widely regarded as a bad move.

Douglas Adams

Table of Contents

1 Introduction

1.1. Star-shaped polymers

Polymers are primarily classified by their composition, topology and functionality, with topology being the relevant subject here. There are two classes of topology, linear and branched. Star-shaped polymers form a subclass of branched polymers on one side of the spectrum with only a single branching point. The remaining subclasses are brush-like and hyperbranched polymers (Figure 1.1).

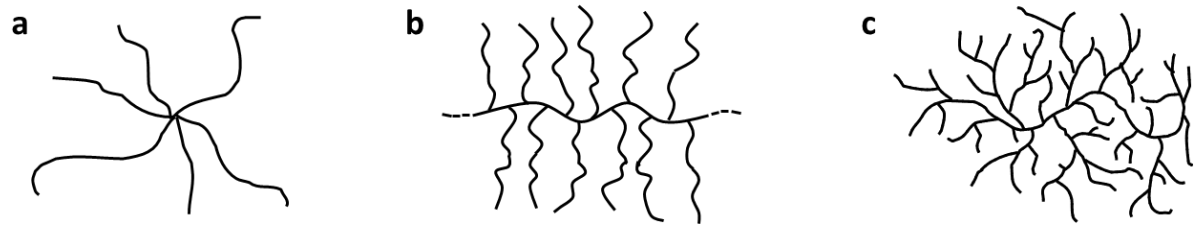

Figure 1.1. Different subclasses of branched polymers with a) star-shaped, b) comb-like and c) randomly branched (dendritic) polymers.

All branched polymers are characterized by the number and functionality of their branching points and the length of their arms or segments. As already mentioned, star-shaped polymers are defined as having only one, at least tri-functional, branching point. A second important characteristic for star-like behavior is the size of the core compared to the size of the whole star. When the core is at least one order of magnitude smaller than the star, its influence can be disregarded.[1,2] Star polymers can be divided into two categories with respect to their chemical composition or topological distribution. One category is symmetrical stars, where all arms are made of the same monomer, the arms have the same length and all stars have the same number of arms. The second category is composed of all stars which show an asymmetry in any of their attributes. These asymmetries can be chemical in nature, *i.e.* different arms are made of different monomers, or topological, *i.e.* there are distributions in the arm length or arm number. The synthesis of well-defined symmetrical stars has long been of interest.[3]

There are three basic strategies for the synthesis of star polymers independent of the actual polymerization technique used and they mainly differ in the sequence in which the core and the arms are formed (Figure 1.2).[4-7] The "grafting-from" or "core-first" approach employs small-molecule multifunctional initiators to grow arms from by various techniques. For the "arm-first" method there are two variants: The "grafting-through" method utilizes pre-formed living polymers which are linked to form the star polymer usually with a divinyl compound. In the "grafting-onto" or "coupling-onto" methodology linear polymers carrying a functional endgroup are attached through ligation reactions onto a multifunctional core.

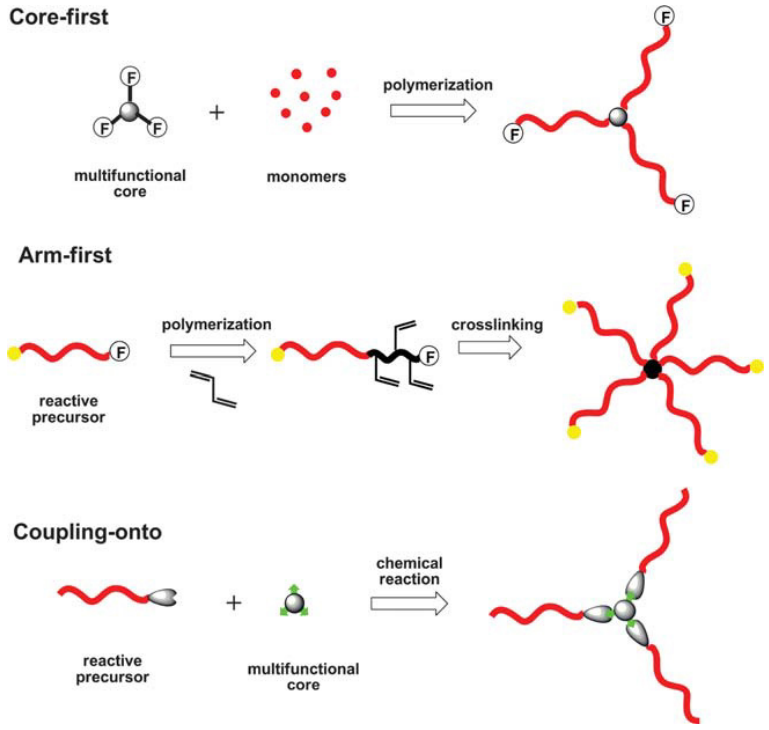

Figure 1.2. General strategies for the synthesis of star polymers.[5]

Each of these methods has disadvantages which limit its use depending on the specific circumstances. The "grafting-through"/"arm-first" method produces stars which have a broad distribution in arm number and therefore also in molecular weight due to a random distribution of arms during the crosslinking of the core. The "grafting to"/"coupling-onto" approach requires functional groups at the chain end and on the core itself, which have to be introduced. In recent years, there have been significant improvements made to increase the

coupling efficiency of the ligation reactions.[5] The "core-first" method is prone to coupling reactions between the stars when employing controlled radical techniques, leading again to broad molecular weight distributions. This tendency can be offset by limiting the monomer conversion to low values (<30%). All of these methods have been proven to be suitable for creating well-defined star polymers. For this work the "core-first" method was chosen because the aim was to synthesize narrow distributed, small arm-number stars. Additionally, the initiators needed for the "core-first" approach can be readily synthesized for atom transfer radical polymerization (ATRP).[8]

1.2. Atom transfer radical polymerization (ATRP)

Atom transfer radical polymerization (ATRP) is one of the techniques known as controlled/"living" radical polymerizations.[9] The controlled radical polymerizations (CRPs) are capable of producing polymers with high molecular weight and narrow molecular weight distributions similar to ionic polymerization techniques. The big advantage of CRP is its high tolerance towards functional groups and impurities. Introduced 10-15 years ago, these methods have become facile and versatile ways to prepare functional materials in a variety of fields.[9] All CRPs are based on a dynamic equilibrium between propagating radicals and various dormant species, with the equilibrium strongly favoring the dormant side. The characteristics for CRPs are a fast initiation, low overall concentration of free radicals and only a minimum of termination reactions. The exchange rate between active and dormant species must be faster than the rate of propagation to insure that all chains grow equally.

ATRP specifically is based on a redox reaction between a solubilized transition metal ion and an alkyl halide to regulate the equilibrium between its reactive and dormant species (Figure 1.3).

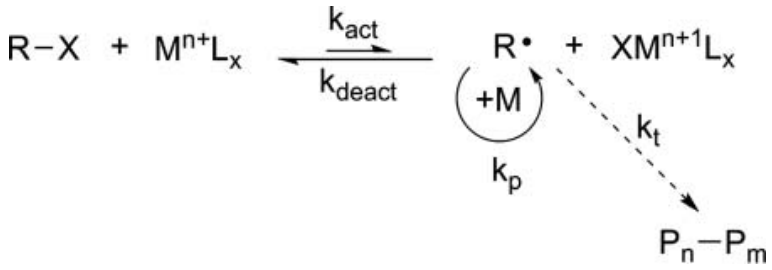

Figure 1.3. Equilibrium between active and dormant species in the ATRP mechanism. R-X: alkyl halide; M^{n+}: transition metal ion; L_x: ligand.[10]

During this reversible redox process the transition metal complex undergoes a one-electron oxidation with the accompanying abstraction of a halogen atom (X) from the dormant species. The first dormant species is the initiator to generate the equilibrium and after the first addition step, the growing chain end becomes the dormant species. The chain grows through consecutive addition steps of the monomer. Termination in ATRP mostly occurs through radical coupling and disproportionation.

A wide variety of transition metals have been found to be able to facilitate ATRP during the last 15 years.[9,10] By virtue of commercial availability, price and properties the copper-catalyzed ATRP has become the most widely used variant. Similarly, a large number of compounds are suitable as ligands. Again for reasons of availability and price, nitrogen containing molecules are the dominant ligands for copper catalyzed ATRP (Figure 1.4). The ATRP system has even more parameters than metal and ligand which influence the equilibrium and determine the success of the ATRP. The structure of the initiator, the solvent, the temperature of the reaction, the presence of ions in the oxidated state and the ratio of ligand to transition metal all play a role in the overall result of the polymerization.

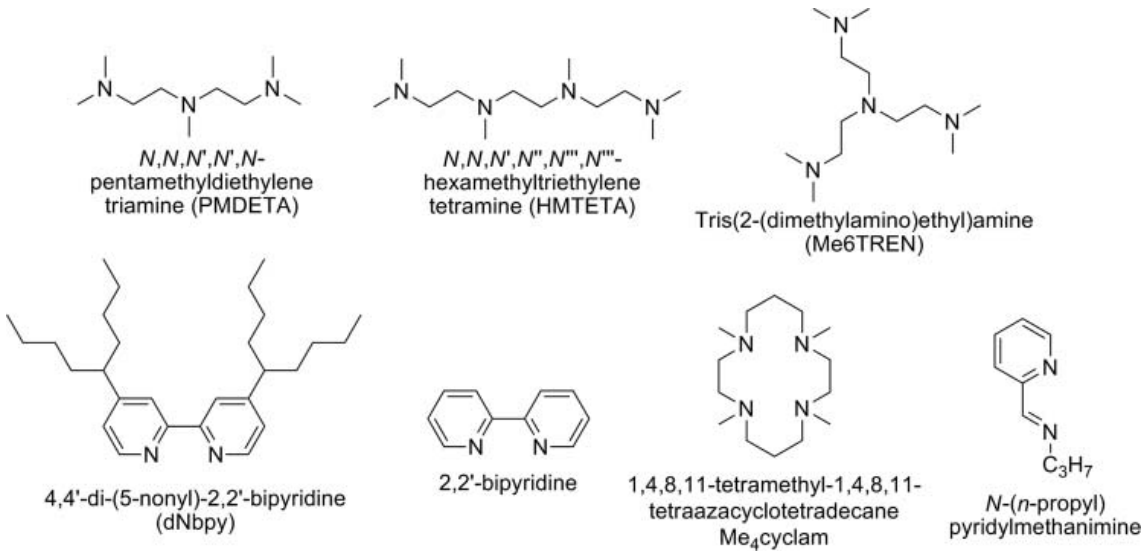

Figure 1.4. Commonly used ligands for ATRP.[10]

1.3. Stimuli-responsive polymers

Stimuli-responsive polymers are defined as polymers that undergo large and abrupt changes, either physical or chemical, in response to small external changes in the environment. Other descriptions have also been used to describe this phenomenon, such as "stimuli-sensitive", "environmentally sensitive", "intelligent" and "smart". There are numerous external stimuli which have been utilized to manipulate these materials, such as temperature, pH, light, electric and magnetic fields, redox reactions as well as ionic strength. They can be divided into two categories, chemical and physical stimuli. Chemical stimuli, such as pH or ionic strength, change the interactions between discrete repeating units or between polymer chains and the solvent. Physical stimuli, like temperature, electric and magnetic fields, influence the strength of the existing interactions.[11]

The chemical structures of the most common stimuli-sensitive polymers are shown in Figure 1.5. In the following only the most frequently employed stimuli, and thus the most studied ones, will be discussed further. These stimuli are temperature and pH, the only stimuli utilized during this work.

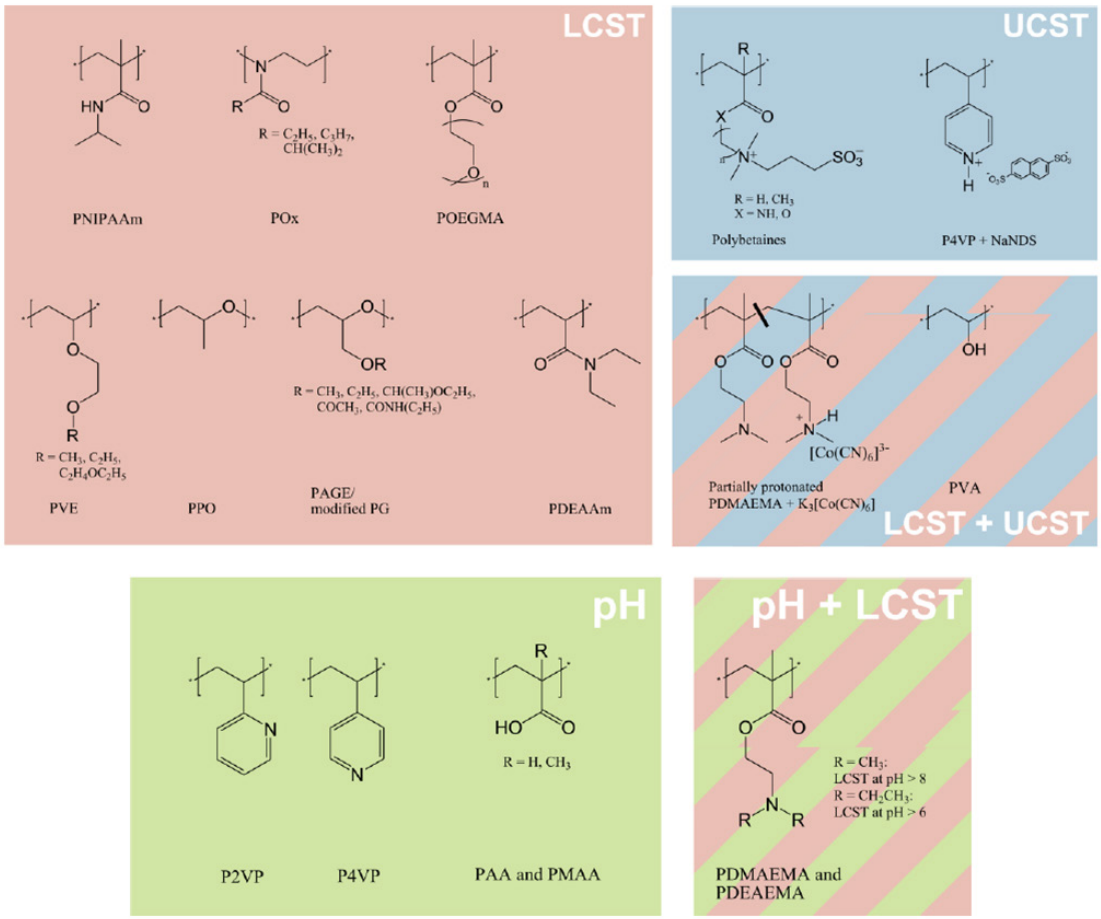

Figure 1.5. Chemical structures of the most common stimuli sensitive polymers, divided by type or types of stimuli.[12] Reprinted with permission from Stefan Reinicke.

1.3.1. Temperature-responsive polymers

Temperature-sensitive polymers undergo a coil-to-globule transition upon a change in the solution temperature. The coil-to-globule transition is generally characterized by a change of the solvent quality from good to poor. If the transition occurs upon cooling, then it is associated with an upper critical solution temperature (UCST) and occurs because of increasing attractive interactions between different polymer segments. The transition upon increased temperature is associated with a lower critical transition temperature (LCST) and is driven by unfavorable entropy of mixing. This phenomenon has been extensively studied over the last decade and was the subject of numerous reviews.[11,13-17] Figure 1.6 shows the idealized phase diagrams for the UCST and LCST type transitions in dependence of polymer concen-

tration and temperature. The UCST and LCST temperatures are defined as the highest and lowest points on the binodal, respectively.

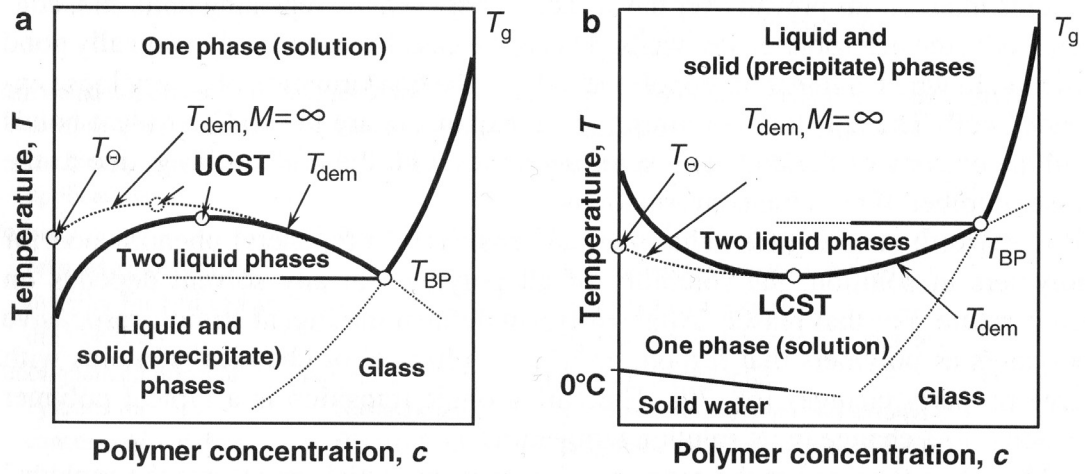

Figure 1.6. Idealized phase diagrams for the a) UCST- and b) LCST-type transitions. T_{dem} is the demixing temperature, T_Θ is the theta temperature and T_{BP} is the temperature corresponding to the Berghmans point.[13] Reprinted with permission from Springer.

The by far most studied thermo-responsive polymer is poly(N-isopropylacrylamide) (PNiPAAm), because of its sharp coil-to-globule transition at 32°C.[14-16,18-20] Heating aqueous solutions of PNiPAAm above the LCST leads to the formation of intra- and intermolecular hydrogen bonds between the amide groups of the repeating units while reducing the number of hydrogen bonds between the same amide groups and water. Only around 15% of these polymer/water hydrogen bonds are replaced by polymer/polymer hydrogen bonds, but this is believed to be the cause for the coil-to-globule transition.[21] The transition temperatures of temperature-sensitive polymers can be tuned by a range of parameters, such as molecular weight, architecture, ionic charges, concentration and functionalized end groups.

1.3.2. pH-responsive polymers

pH-responsive polymers are weak polyelectrolytes whose solubility and conformation can be reversibly manipulated by changes in the external pH value.[22] Changes in pH alter the ionic interactions, hydrogen bonding and hydrophobic interactions of the polymers with the solvent or itself. The repeating units can change from uncharged hydrophobic groups to charged hydrophilic groups, depending on the protonation/deprotonation of the functional groups. The pH responsive polymers can be divided into two categories, polyacids and polybases. The most common pH-responsive polymers are poly((meth)acrylic acid) (P(M)AA) as polyacid and poly(vinyl pyridine) (PVP) as polybase (Figure 1.5).

1.3.3. Multi-responsive systems

There are two methods to introduce two or more stimuli into a polymer. First there is the possibility to copolymerize monomers that respond to different stimuli, either as a random copolymer[23-26] or as a block copolymer.[27,28] Second, there are polymers, the repeating units of which are responsive to different stimuli. One example, which combines sensitivity to temperature and pH, is poly(2-(dimethylamino)ethyl methacrylate) (PDMA). Plamper *et.al.* showed that the LCST of linear and star-shaped PDMA depends strongly on the degree of protonation of the chain, which is controlled by the solution pH.[29-31] A number of reviews deal with this type of polymers.[16,32]

1.4. Hydrogels

1.4.1. Definition of a gel

A structural definition of a gel describes it as a three-dimensional network, swollen in a solvent to a certain finite extent.[33] A more common definition is that a gel consists of two components, a solid and a liquid, where the solid is the minority component and the liquid the majority component. The solid phase extends through the entire volume of the gel.[34] In a recent review, Nishinari defines a gel as a system of molecules, particles, chains, etc. which are partially connected to each other in a fluid medium.[35] A more detailed definition can be

derived from the rheological properties of the gel systems. Almdal and Kramer defined that the storage modulus *G'* should be independent of the frequency at least on the order of seconds and the loss modulus *G"* should be considerably lower than the storage modulus.[34] However, some systems do not follow all of these criteria, *e.g.* the storage modulus is only slightly higher than the loss modulus even though the gel appears to be free-standing. These systems have been characterized as "weak" gels.[36] The most commonly used definition of hard or weak gels goes back to the work of Hvidt *et.al.*, who categorized gels with a storage modulus on the order of 10^4 Pa as "hard" gels and gels with a storage modulus on the order of 10^1 Pa as "weak" gels. The critical point for differentiation between "hard" and "soft" gels was defined as the threshold of 10^3 Pa.[37] Over time exceptions have been found for every definition of the gel point previously presented, making a simple universal definition next to impossible. It is therefore only sensible to look for definitions pertaining to particular types of systems and their behavior. Nishinari went so far as to state that a gel might be present if the system does not flow under gravity.[35]

1.4.2. Smart hydrogels

Hydrogels belong to a class of soft matter which has attracted a lot of attention in the recent years. There are two principal classes of hydrogels, covalently crosslinked and physically crosslinked ones. Particularly stimuli-responsive and physically crosslinked hydrogels have many potential applications in biomedicine and have been the subject of intense scrutiny from the scientific community.[38-43]

The first report of temperature-sensitive microgel particles based on crosslinked PNiPAAm was published in 1986[44] and since then there have been numerous publications on this subject. Progress has been made regarding the synthesis[45] and the characterization of microgels and nanoparticle microgel hybrids.[46] Covalently crosslinked gels such as these show only one reaction to a stimulus, which is swelling/deswelling. The degree and kinetics of this swelling have been extensively studied.[47-53] In the last decade, there have been many applications for which these gels have been used[54-56] and PNiPAAm has also been copolymerized with a wide variety of other monomers, *i.e.* poly(4-vinylpyridine) or poly(acrylic acid).[57,58]

Other polymers besides PNiPAAm have also been studied in the form of covalently cross-linked hydrogels, such as poly(diethylene glycol methyl ether methacrylate) (PDEGMA).[59]

In the following a brief overview is given over the state of the art of physically cross-linked stimuli-responsive hydrogels. There have also been many reviews covering this topic.[11,60-62] All stimuli presented in the following are based upon hydrophobic interactions and other types of interactions, *e.g.* ionic interactions,[63,64] will not be mentioned.

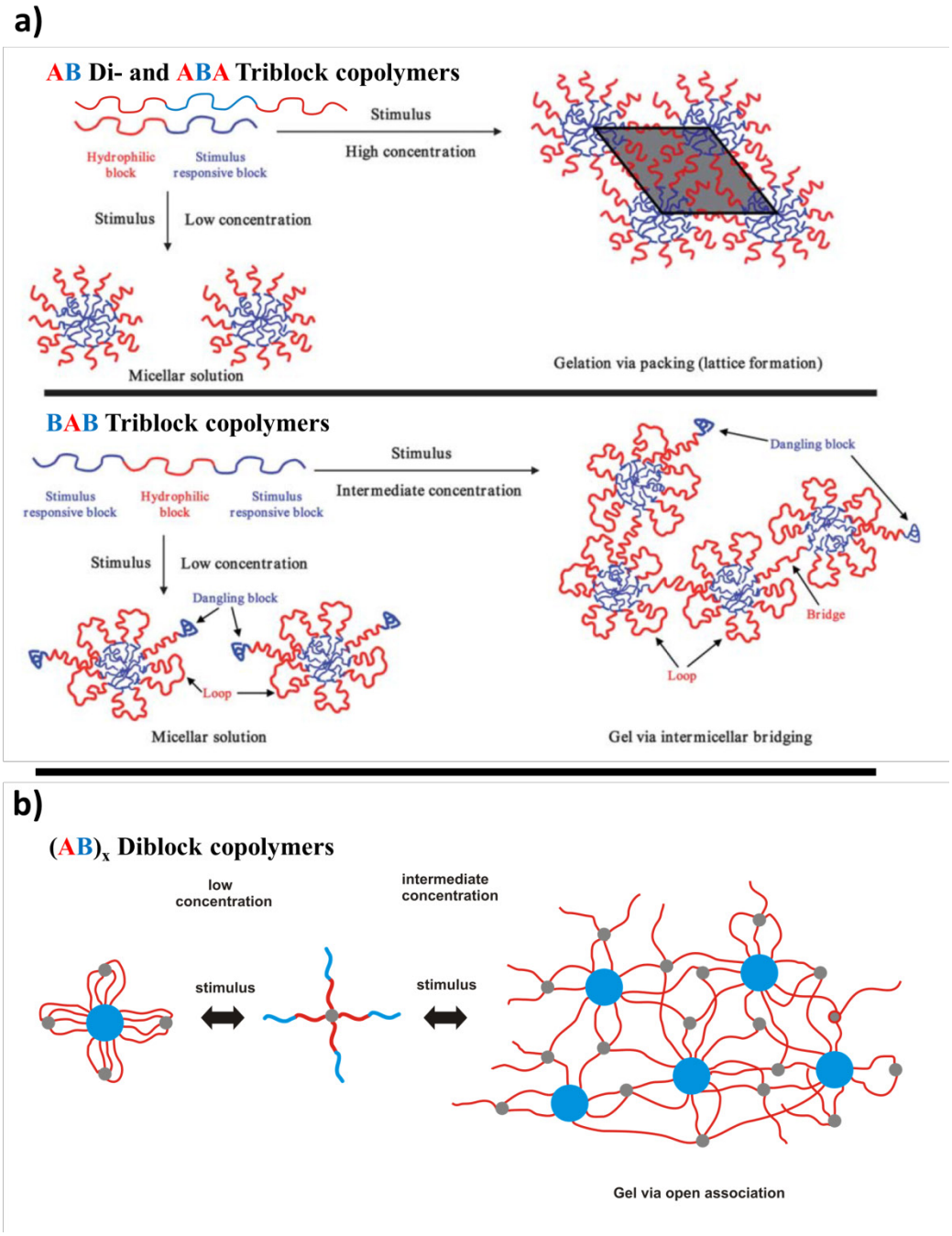

Figure 1.8. Gelation mechanism for a) stimuli-responsive di- and triblock copolymers, where the A block is hydrophilic and the B block is stimuli-responsive. Adapted from Ref. [58]. b) stimuli-responsive $(AB)_x$ diblock copolymers, where the A block is hydrophilic and the B block is stimuli-responsive

Hydrogels based on AB, ABA and BAB block copolymers. Linear stimuli-responsive block copolymers typically follow a micellar gelation mechanism, where the crosslinks can be formed either by micelle jamming, where gelation occurs when the micellar coronas overlap, or by intermicellar bridging (Figure 1.8).[65] The first mechanism is usually observed for AB diblock and ABA triblock copolymers where the A block is hydrophilic and the B block hydrophobic. They form micelles in water and at a sufficiently high concentration the micelles form a closely packed system, their coronas start to overlap, and this causing gelation.[65-67] Micelle bridging is commonly observed for the inverse BAB triblock copolymers (Figure 1.8). There are three possibilities for the triblock copolymers to arrange themselves in aqueous solution in this scenario, both B blocks can occupy the same flower-like micelle, they can connect two adjacent micelles or one of the B blocks forms a dangling collapsed chain end. All three states have been proven to exist.[60] Micelle bridging refers to the case where the chains connect adjacent micelles and this favors gel formation. There are two ways to increase the extent of micellar bridging in such systems. First, if the A block has polyelectrolyte character, as the electrostatic repulsion between the charged chains reduces the possibility of back-folding.[68] Second, using multi-arm $(AB)_x$ type copolymers lowers the critical gelation concentration by eliminating the micelle formation step.[69-71] This will be discussed below.

Temperature-dependent gelators. PNiPAAm has been used numerous times to prepare temperature-dependent gelators. Armes *et.al.* have prepared hydrophilic poly(2-(methacryloyloxy)ethyl phosphoryl choline) (PMCP) end-functionalized with short PNiPAAm blocks at both ends. This BAB triblock copolymer forms a network of bridged flower-like micelles above 32 °C at a concentration as low as 5 wt%.[72] The same polymer was also synthesized with a biodegradable unit inside the A block. The resulting gel formed under physiological conditions at 37 °C and could be turned into a free-flowing liquid through the addition of glutathione, which cleaved the disulfide bond introduced into the central A block.[73] McCormick *et.al.* reported on the gelation behavior of BAB triblock copolymers with PNiPAAm outer blocks and water-soluble poly(*N,N*-dimethylacrylamide) (PDMAAm) inner

block. The copolymer forms free-standing gels in PBS buffer at 37 °C at concentrations of 10 wt% and their mechanical properties are interesting for tissue engineering.[74] The inverse ABA copolymers with PDMAAm outer blocks and PNiPAAm inner blocks also form thermo-responsive gels due to jamming, but at higher concentrations.[66] There have also been studies of P(DEGMA-*co*-OEGMA) as a stimuli responsive block for hydrogels. Both linear BAB triblock and star-shaped $(AB)_x$ diblock copolymers with an A block of poly(ethylene oxide) (PEO) have been prepared. The star-shaped copolymers were able to form gels upon heating in PBS buffer solutions at concentrations of 15 wt%, while their linear ABA counterparts did not lead to highly cohesive networks even at concentrations of 30wt%.[69]

pH-responsive gelators. A number of pH-responsive gelators have been prepared using tertiary amine methacrylate monomers, like DMA, poly(2-(diethylamino)ethyl methacrylate) (PDEA) and poly(2-(diisopropylamino)ethyl methacrylate) (DPA). A triblock with the structure poly(methyl methacrylate)-poly(2-dimethylamino)ethyl methacrylate)-poly(methyl methacrylate) P(MMA_{32}-DMA_{224}-MMA_{32}) forms a hard gel in salt free aqueous solutions of 1 wt% at pH 4 where the amino group is protonated. When the pH is increased the solution turns into a viscous fluid because the protonation of the PDMA chain decreases and its flexibility increases. When the pH is decreased below 4, the ionic strength of the solution increases and leads to screening effects which cause a decrease in viscosity.[75] In a different approach, PDEA as well as PDPA were used as responsive B blocks in BAB triblocks with a PMPC middle block. A 10 wt% solution of PDPA-PMPC-PDPA forms a liquid at pH 2 due to the protonation of the amino groups, but gelation occurs when the pH is increased to pH 7. The reason for this is the deprotonation of the DPA moieties and the formation of bridged “flower-like” micelles. To achieve comparable results with PDEA-PMPC-PDEA, the block length of the outer pH responsive blocks had to be increased as well as a higher pH was needed. This is due to the less hydrophobic character of the PDEA chains compared to the PDPA chains.[76,77]

The use of polyelectrolytes as the central block surrounded by temperature sensitive blocks in BAB triblock copolymers leads to temperature and pH responsive hydrogels. A double hydrophilic triblock copolymer with a long PAA inner block and an outer block of poly(N,N-diethylacrylamide) (PDEAAm) (LCST≈32 °C) forms hydrogels at physiological pH and 60 °C at concentrations of 3 wt%. Due to the high stretching of the PAA block at this pH, bridging is

favored over looping, as can be seen in a high plateau modulus and a low critical gelation concentration (cgc). Both the conformation of the inner block and the LCST of the outer block are sensitive to ionic strength, adding another parameter that can influence the behavior of this system.[78]

Hydrogels based on ABC triblock terpolymers. pH- and temperature-sensitive systems designed around the ABC triblock terpolymer concept have also been reported. Reinicke *et.al.* prepared ABC triblock terpolymers comprised of P2VP-PEO-P(GME-*co*-EGE) blocks, with a pH-sensitive block (poly(2-vinylpyridine)), a hydrophilic block (PEO) and a temperature-responsive poly(glycidyl methyl ether-*co*-ethyl glycidyl ether) copolymer block. The LCST of the last block can be easily controlled by the copolymer composition. At pH 7 and a concentration of 18 wt%, this block terpolymer undergoes a gel-sol-gel transition upon heating. At low temperatures the gel is formed by a bcc packing of core-shell-corona micelles with a hydrophobic P2VP core, and at elevated temperatures, the gel turns into a viscous liquid but at 60 °C the gel state is restored because at that temperature the P(GME-*co*-EGE) block becomes insoluble and a network is formed through bridging. An additional gel state can be found for pH 3 and high temperatures, when only the P(GME-*co*-EGE) block is insoluble and again core-shell-corona micelles are formed, this time with a hydrophobic P(GME-*co*-EGE) core. The gel also results from micellar jamming.[79] The same group has prepared other ABC systems with different thermoresponsive C blocks, P2VP-PEO-PDMA and P2VP-PEO-P(DEGMA-*co*-OEGMA).[80] The P2VP-PEO-P(DEGMA-*co*-OEGMA) system behaves similar to the P2VP-PEO-P(GME-co-EGE) system, as it undergoes a gel-sol-gel transition at pH 7 with a concentration of 20 wt%. The system with PDMA as the C block behaves differently because of the dual-responsive nature of the PDMA, its LCST being strongly dependent upon pH. Samples prepared at pH 8 showed a strong gel at room temperature and a gel-sol transition upon heating, but no second gel phase was found, this is due to the electrostatic repulsion between the micelles because of residual protonation of the DMA block. At pH 9 the terpolymer forms a weak gel at room temperature, because the PDMA block is almost completely deprotonated and therefore hydrophobic. Upon increasing the temperature, a gel-sol transition is visible, followed very quickly by another sol-gel transition to a strong gel above 32 °C.

Hydrogels based on $(AB)_x$ star-shaped block copolymers. There is also a number of reports for star-shaped block copolymers as gelators. Li *et.al.* reported the synthesis of three-arm star copolymers with inner blocks of PMPC and the outer blocks composed of statistical copolymers of PDMA, PDEA and monomethoxy capped poly(poly(propylene oxide) methacrylate) (PPOMA). $(PMPC_{125}\text{-}(PDMA_{50}\text{-}co\text{-}PDEA_{50}))_3$ formed free-standing hydrogels at 37 °C at physiological pH and a concentration of 7 wt%, while the incorporation of only 3 wt% of hydrophobic PPOMA lead to free-standing gels at 5 wt% under the same conditions. In contrast, $(PMPC_{125}\text{-}PDPA_{100})_3$ forms free-standing gels at 5 wt%, but only at 20 °C and pH 8.2.[81] Lin et.al. reported on linear and star-shaped block copolymers of PEO and PNiPAAm and found that $(PEO\text{-}PNiPAAm)_4$ showed a sol-gel transition to a strong gel at 37 °C and exhibited the highest moduli compared to the other polymers.[71] Fechler et.al. reported 4-arm stars with PEO inner blocks and P(DEGMA-*co*-OEGMA) outer blocks, which formed fully reversible free-standing hydrogels at 15 wt% upon heating.[69] All three groups describe that the star-shaped gelators are more efficient than their linear counterparts. Pérez et.al. reported hydrogels based on covalently linking a collagen-based peptide to an 8-arm poly(ethylene glycol) star polymer. These polymer-peptide conjugates formed a hydrogel at room temperature at a concentration of 4 wt% and underwent a reversible gel-sol transition upon heating above 50 °C, due to the denaturation and refolding of the collagen peptide triple heilx.[82]

There are many more examples for hydrogel formation published, including a variety of other stimuli, but for the sake of brevity they have not been discussed here. For further information please refer to the relevant literature.[11,38-43,60-62]

1.5. Objective of this thesis

Since there are still many unsolved problems in the field of smart hydrogels ranging from synthesis to characterization, the German Science Foundation in 2006 launched a priority program to develop intelligent hydrogels (SPP 1259), aimed at creating new ways to synthesize and characterize these novel systems.

This work was part of a project in the priority program with the intent to create double responsive systems based on star-shaped block copolymers. The goal was to create efficient

gelators, which would form hydrogels based on one trigger where the gel strength would still respond independently to another trigger. The initial design called for both blocks of the diblock copolymer arms of the stars to be double-responsive themselves. This strategy was later expanded to include one block that was only responsive to temperature. These systems were synthesized by ATRP and characterized in dilute and concentrated aqueous solution to determine the parameters which control their gelation behavior and gel strength. The initial monomers chosen were DMA and DEA, because of our knowledge of the double-responsive behavior of PDMA and because we suspected that PDEA would behave in a similar matter. Due to the fact that PDEA is more hydrophobic than PDMA, we predicted that the pH-dependent transition temperatures of PDEA would be consistently lower than those of PDMA, making it possible to trigger them independently.

1.6. References

1. N. Dan and M. Tirrell, *Macromolecules*, 1992, **25**, 2890-2895.
2. G. S. Grest, K. Kremer and T. A. Witten, *Macromolecules*, 1987, **20**, 1376-1383.
3. M. Mishra and S. Kobayashi, *Star and hyperbranched polymers*, Marcel Dekker, Inc., New York, 1999,
4. D. J. A. Cameron and M. P. Shaver, *Chem. Soc. Rev.*, 2011, **40**, 1761-1776.
5. O. Altintas, A. P. Vogt, C. Barner-Kowollik and U. Tunca, *Polym. Chem.*, 2011.
6. K. Matyjaszewski and N. V. Tsarevsky, *Nat. Chem.*, 2009, **1**, 276-288.
7. N. Hadjichristidis, H. Iatrou, M. Pitsikalis and J. Mays, *Prog. Polym. Sci.*, 2006, **31**, 1068-1132.
8. F. A. Plamper, H. Becker, M. Lanzendörfer, M. Patel, A. Wittemann, M. Ballauff and A. H. E. Müller, *Macromol. Chem. Phys.*, 2005, **206**, 1813-1825.
9. W. A. Braunecker and K. Matyjaszewski, *Prog. Polym. Sci.*, 2007, **32**, 93-146.
10. N. Ayres, *Polym. Rev.*, 2011, **51**, 138-162.
11. E. S. Gil and S. M. Hudson, *Prog. Polym. Sci.*, 2004, **29**, 1173-1222.
12. S. Reinicke, *Dissertation*, University of Bayreuth, 2010.
13. V. Aseyev, H. Tenhu and F. Winnik, in *Adv. Polym. Sci.*, Springer Berlin / Heidelberg, 2011, vol. 242, pp. 29-89.
14. R. Liu, M. Fraylich and B. Saunders, *Colloid. Polym. Sci.*, 2009, **287**, 627-643.
15. S. Aoshima and S. Kanaoka, in *Adv. Polym. Sci.*, Springer Berlin / Heidelberg, 2008, vol. 210, pp. 169-208.
16. I. Dimitrov, B. Trzebicka, A. H. E. Müller, A. Dworak and C. B. Tsvetanov, *Prog. Polym. Sci.*, 2007, **32**, 1275-1343.
17. D. Schmaljohann, *Adv. Drug Delivery Rev.*, 2006, **58**, 1655-1670.
18. D. Kuckling, C. D. Vo, H. J. P. Adler, A. Völkel and H. Cölfen, *Macromolecules*, 2006, **39**, 1585-1591.
19. X.-Z. Zhang and R.-X. Zhuo, *Eur. Polym. J.*, 2000, **36**, 643-645.
20. T. G. Park and A. S. Hoffman, *J. Polym. Sci., Part A: Polym. Chem.*, 1992, **30**, 505-507.
21. Y. Maeda, T. Higuchi and I. Ikeda, *Langmuir*, 2000, **16**, 7503-7509.
22. I. Roy and M. N. Gupta, *Chem. Biol.*, 2003, **10**, 1161-1171.
23. M. Karg, I. Pastoriza-Santos, B. Rodriguez-González, R. von Klitzing, S. Wellert and T. Hellweg, *Langmuir*, 2008, **24**, 6300-6306.
24. X.-Z. Zhang, Y.-Y. Yang, F.-J. Wang and T.-S. Chung, *Langmuir*, 2002, **18**, 2013-2018.
25. K. Kratz, T. Hellweg and W. Eimer, *Colloids Surf. A: Physicochem. Eng. Aspects*, 2000, **170**, 137-149.
26. M. S. Jones, *Eur. Polym. J.*, 1999, **35**, 795-801.
27. C. M. Schilli, M. Zhang, E. Rizzardo, S. H. Thang, Y. K. Chong, K. Edwards, G. Karlsson and A. H. E. Müller, *Macromolecules*, 2004, **37**, 7861-7866.
28. V. Bütün, M. Vamvakaki, N. C. Billingham and S. P. Armes, *Polymer*, 2000, **41**, 3173-3182.
29. F. A. Plamper, A. Schmalz, E. Penott-Chang, M. Drechsler, A. Jusufi, M. Ballauff and A. H. E. Müller, *Macromolecules*, 2007, **40**, 5689-5697.
30. F. A. Plamper, A. Schmalz, M. Ballauff and A. H. E. Müller, *J. Am. Chem. Soc.*, 2007, **129**, 14538-14539.

31. F. A. Plamper, M. Ruppel, A. Schmalz, O. Borisov, M. Ballauff and A. H. E. Müller, *Macromolecules*, 2007, **40**, 8361-8366.
32. S. Dai, P. Ravi and K. C. Tam, *Soft Matter*, 2008, **4**, 435-449.
33. J. P. Gong, *Dictionary of Polymers*, Asakura Shoten, Tokyo, 2005, p 208.
34. K. Almdal, J. Dyre, S. Hvidt and O. Kramer, *Polym. Gels Netw.*, 1993, **1**, 5-17.
35. K. Nishinari, *Prog. Colloid Polym. Sci.*, 2009, **136**, 87-94.
36. A. Clark and S. Ross-Murphy, in *Biopolymers*, Springer Berlin / Heidelberg, 1987, vol. 83, pp. 57-192.
37. S. Hvidt, E. B. Joergensen, W. Brown and K. Schillen, *J. Phys. Chem.*, 1994, **98**, 12320-12328.
38. C. He, S. W. Kim and D. S. Lee, *J. Controlled Release*, 2008, **127**, 189-207.
39. N. A. Peppas, J. Hilt, A. Khademhosseini and R. Langer, *Adv. Mater.*, 2006, **18**, 1345-1360.
40. C. Alarcon, H. de Las, S. Pennadam and C. Alexander, *Chem. Soc. Rev.*, 2005, **34**, 276-285.
41. E. Ruel-Gariepy and J.-C. Leroux, *Eur. J. Pharm. Biopharm.*, 2004, **58**, 409-426.
42. A. S. Hoffman, *Adv. Drug Deliv. Rev.*, 2002, **43**, 3-12.
43. C. T. Huynh, M. K. Nguyen and D. S. Lee, *Macromolecules*, 2011, **44**, 6629-6636.
44. R. H. Pelton and P. Chibante, *Colloids Surf.*, 1986, **20**, 247-256.
45. P. Robert, *Adv. Colloid Interface Sci.*, 2000, **85**, 1-33.
46. M. Karg and T. Hellweg, *Curr. Opin. Colloid Interface Sci.*, 2009, **14**, 438-450.
47. A. Panda, S. B. Manohar, S. Sabharwal, Y. K. Bhardwaj and A. B. Majali, *Radiat. Phys. Chem.*, 2000, **58**, 101-110.
48. R. Kishi, O. Hirasa and H. Ichijo, *Polym. Gels Networks*, 1997, **5**, 145-151.
49. M. Shibayama and T. Tanaka, in *Adv. Polym. Sci.*, Springer Berlin / Heidelberg, 1993, vol. 109, pp. 1-62.
50. C. Wu, *Polymer*, 1998, **39**, 4609-4619.
51. M. Hahn, E. Görnitz and H. Dautzenberg, *Macromolecules*, 1998, **31**, 5616-5623.
52. D. Kuckling, H.-J. P. Adler, K.-F. Arndt, L. Ling and W. D. Habicher, *Macromol. Chem. Phys.*, 2000, **201**, 273-280.
53. Y. Liu, J. L. Velada and M. B. Huglin, *Polymer*, 1999, **40**, 4299-4306.
54. Y. Zhang, S. Sinha-Ray and A. L. Yarin, *J. Mater. Chem.*, 2011, **21**, 8269-8281.
55. Y. Samchenko, Z. Ulberg and O. Korotych, *Adv. Colloid Interface Sci.*, 2011, **168**, 247-262.
56. Y. Guan and Y. Zhang, *Soft Matter*, 2011, **7**, 6375-6384.
57. H. Nur, V. T. Pinkrah, J. C. Mitchell, L. S. Benée and M. J. Snowden, *Adv. Colloid Interface Sci.*, 2010, **158**, 15-20.
58. D. Kuckling, A. Richter and K.-F. Arndt, *Macromol. Mater. Eng.*, 2003, **288**, 144-151.
59. J. A. Yoon, C. Gayathri, R. R. Gil, T. Kowalewski and K. Matyjaszewski, *Macromolecules*, 2010, **43**, 4791-4797.
60. J. Madsen and S. P. Armes, *Soft Matter*, 2012, Advance Article.
61. J.-F. Lutz, *Adv. Mater.*, 2011, **23**, 2237-2243.
62. C. Tsitsilianis, *Soft Matter*, 2010, **6**, 2372-2388.
63. V. A. Kabanov, A. B. Zezin, V. B. Rogacheva, T. V. Panova, E. V. Bykova, J. G. H. Joosten and J. Brackman, *Faraday Discuss.*, 2005, **128**, 341-354.
64. A. B. Zezin, V. B. Rogacheva and V. A. Kabanov, *J. Intell. Mater. Syst. Struct.*, 1994, **5**, 144-146.

65. I. W. Hamley, *The Physics of Block Copolymers*, Oxford University Press, Oxford, 1998,
66. S. Kirkland-York, K. Gallow, J. Ray, Y.-l. Loo and C. McCormick, *Soft Matter*, 2009, **5**, 2179-2182.
67. L. Klouda and A. G. Mikos, *Eur. J. Pharm. Biopharm.*, 2008, **68**, 34-45.
68. A. S. Kimerling, W. E. Rochefort and S. R. Bhatia, *Ind. Eng. Chem. Res.*, 2006, **45**, 6885-6889.
69. N. Fechler, N. Badi, K. Schade, S. Pfeifer and J.-F. Lutz, *Macromolecules*, 2009, **42**, 33-36.
70. N. Badi and J.-F. Lutz, *J. Controlled Release*, 2009, **140**, 224-229.
71. H.-H. Lin and Y.-L. Cheng, *Macromolecules*, 2001, **34**, 3710-3715.
72. C. Li, Y. Tang, S. P. Armes, C. J. Morris, S. F. Rose, A. W. Lloyd and A. L. Lewis, *Biomacromolecules*, 2005, **6**, 994-999.
73. C. Li, J. Madsen, S. P. Armes and A. L. Lewis, *Angew. Chem. Int. Ed.*, 2006, **45**, 3510-3513.
74. S. E. Kirkland, R. M. Hensarling, S. D. McConaughy, Y. Guo, W. L. Jarrett and C. L. McCormick, *Biomacromolecules*, 2007, **9**, 481-486.
75. F. Bossard, T. Aubry, G. Gotzamanis and C. Tsitsilianis, *Soft Matter*, 2006, **2**, 510-516.
76. V. Castelletto, I. W. Hamley, Y. Ma, X. Bories-Azeau, S. P. Armes and A. L. Lewis, *Langmuir*, 2004, **20**, 4306-4309.
77. Y. Ma, Y. Tang, N. C. Billingham, S. P. Armes and A. L. Lewis, *Biomacromolecules*, 2003, **4**, 864-868.
78. S. A. Angelopoulos and C. Tsitsilianis, *Macromol. Chem. Phys.*, 2006, **207**, 2188-2194.
79. S. Reinicke, J. Schmelz, A. Lapp, M. Karg, T. Hellweg and H. Schmalz, *Soft Matter*, 2009, **5**, 2648-2657.
80. S. Reinicke and H. Schmalz, *Colloid. Polym. Sci.*, 2011, **289**, 497-512.
81. Y. Li, Y. Tang, R. Narain, A. L. Lewis and S. P. Armes, *Langmuir*, 2005, **21**, 9946-9954.
82. C. M. Rubert Pérez, A. Panitch and J. Chmielewski, *Macromol. Biosci.*, 2011, **11**, 1426-1431.

2 Overview of this thesis

The work presented in this thesis is aimed at the creation of double stimuli responsive star-shaped polymers that are able to form dual-responsive hydrogels. The stimuli utilized are temperature and pH. The thesis contains three publications, which are presented in chapters 3 to 5.

Linear and star-shaped poly(*N,N*-diethylaminoethyl methacrylate) (PDEA) was synthesized by ATRP using the core-first method with sugar-based multifunctional initiators. The double responsiveness of the polymer to both temperature and pH is investigated and compared to the properties of the well-known double-responsive polymer poly(*N,N*-dimethylaminoethyl methacrylate (PDMA) (Chapter 3).

The established synthesis protocol was extended to produce double stimuli responsive star-shaped block copolymers consisting of PDMA inner blocks and PDEA outer blocks. These diblock copolymer stars show temperature- and pH-dependent aggregation in dilute aqueous solution and hydrogel formation in concentrated aqueous solution. The influence of pH, PDEA block length and arm number on the gelation behavior is investigated (Chapter 4).

After being able to prove our concept for the formation of dual responsive hydrogels based on star-shaped block copolymers, we broadened the range of monomers to include others that are only thermo-responsive as the outer block. In this particular case we used poly(diethylene glycol methylether methacrylate) (PDEGMA) as the outer block to produce $(DMA_nDEGMA_m)_x$ diblock copolymer stars. They show double stimuli responsive behavior and form hydrogels that are able to change their mechanical properties in response to a second stimulus (Chapter 5).

In this chapter an overview of the work completed in this project is presented.

2.1 Double Stimuli-Responsive Behavior of Linear and Star-Shaped Poly(*N,N*-Diethylaminoethyl Methacrylate) in Aqueous Solution

The aim of this project was to investigate the stimuli responsive behavior of poly(*N,N*-diethylaminoethyl methacrylate) (PDEA) for a possible use in creating double-responsive block copolymers. ATRP was employed to synthesize well-defined linear and star-shaped polymers using the "grafting-from" approach. The multifunctional initiators were prepared from various sugar molecules to yield initiators with different numbers of initiation functions. The polymers showed low polydispersity indices (1.08 < PDI < 1.35) and the arm numbers of the star-shaped polymers varied between 3 and 8. Figure 2.1 shows the temperature and pH dependent behavior of these polymers.

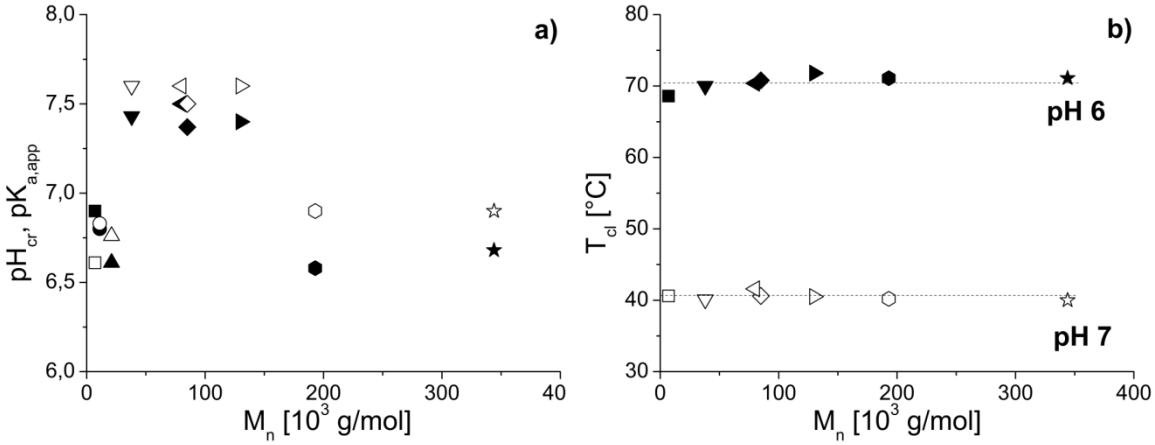

Figure 2.1. a) Critical pH values (pH_{cr}, filled symbols) and apparent pK_a values ($pK_{a,app}$, open symbols) and b) cloud points (Tcl) in pH 6 and 7 buffers as a function of molecular weight for linear and star-shaped PDEA (■,□ DEA_{41}; ●,○ DEA_{59}; ▲,△ DEA_{109}; ▼,▽ $(DEA_{65})_{3.1}$; ◆,◇ $(DEA_{145})_{3.1}$; ◀,◁ $(DEA_{78})_{5.5}$; ▶,▷ $(DEA_{126})_{5.5}$; ⬢,⬡ $(DEA_{119})_{8.6}$; ★,☆ $(DEA_{214})_{8.6}$

The critical pH values pH_{cr}, *i.e.* the pH value at which the polymers become insoluble at 25 °C, are close to the respective apparent pK_a values for all polymers. In most cases they are even below their pK_a, meaning that they become hydrophobic even though they are still more than 50% protonated. This shows that a high charge density is necessary to keep the

polymer in solution, which can be attributed to the hydrophobic ethyl substituents at the amino group. Figure 2b shows the temperature dependent behavior of the polymers at different pH. There is no significant dependence on temperature or architecture, *i.e.* arm number, visible at both pH values, making this a type II transition. Importantly, the cloud point increases considerably with decreasing pH value, again because of the increasing charge density of the polymer chain. At pH 6 we are well below $pK_{a,app}$ for PDEA so that the charge density is high and the electrostatic interactions impede chain collapse and aggregation. The case is different for pH 7, as we are above the $pK_{a,app}$ for most of the polymers we measured, lowering the charge density and the accompanying electrostatic repulsion substantially.

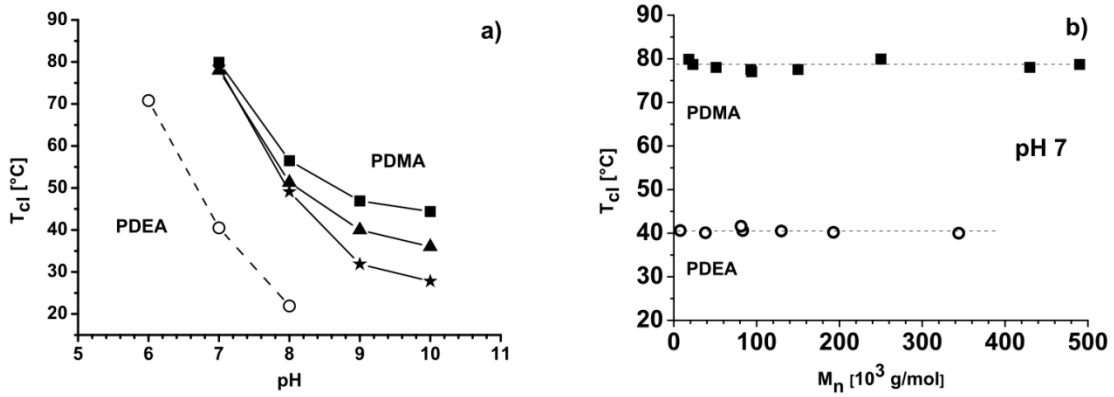

Figure 2.2. 3 a) Cloud points for linear and star-shaped PDEA and PDMA in dependence of pH (○ $(DEA_n)_x$; ■ DMA_{108}; ▲ $(DMA_{100})_{3.1}$; ★ $(DMA_{170})_{18}$), and b) cloud points plotted against molecular weight for linear and star-shaped PDEA (○) and PDMA (■) at pH 7. The lines are only a guide to the eye.

Finally, the results for PDEA were compared with earlier work performed in our group on poly(*N,N*-dimethylaminoethyl methacrylate) (PDMA) (Figure 2.2), which carries only methyl substituents and is therefore less hydrophobic than PDEA. Figure 2.2a shows the cloud points of PDEA and PDMA for various pH values and the solubility of PDMA is much greater than that of PDEA. A direct comparison is made and the cloud point of PDEA is 30 °C lower than that PDMA at pH 8 and 40 °C lower at pH 7, due to the higher hydrophobicity of DEA (Figure 2.2).

2.2 Double-responsive hydrogels based on tertiary amine methacrylate star block copolymers

This project focused on the synthesis of double-responsive star-shaped block copolymers capable of forming reversible hydrogels. Our strategy was based upon our knowledge of PDMA and PDEA homopolymers and their pH- and temperature dependent solution behavior. As shown in the previous chapter, it is possible to select conditions under which the different polymers collapse at very different temperatures. A star-block copolymer, where the arms are composed of a PDMA inner block and a PDEA outer block should be able to form hydrogels under conditions where a sequential collapse of the blocks from the outside in takes place.

The synthesis of the star-shaped block copolymers is based on the protocol for the synthesis for the star-shaped homopolymers of PDMA and PDEA with one change: the catalyst employed is copper chloride to facilitate a halogen exchange at the chain end from bromine to chlorine. This increases the chain stability and the block efficiency for the second block. The resulting polymers are well-defined with PDIs between 1.11 and 1.27 and average arm numbers of 4 and 6.

The solution and gelation behavior of the star block copolymer stars was investigated by turbidimetry, dynamic light scattering (DLS), tube-inversion experiments and rheology. The turbidity measurements did not reveal much information because they showed cloud points very similar to those of the PDMA homopolymers, which is due to the short length of the outer PDEA blocks and the inability of the turbidity setup to detect small changes in aggregate size. For this reason DLS measurements were carried out for PDMA homopolymer stars and $(DMA\text{-}DEA)_x$ block copolymer stars to compare their respective behavior. At pH 7, under conditions where the PDMA block is soluble over the whole measured temperature range, the block copolymer stars show an increase in hydrodynamic radius of 50% around 40 °C, which coincides with the cloud point of PDEA at this pH. The PDI of the structures detected in DLS also decreases significantly in the same temperature range. Additionally, angle-dependent DLS measurements were carried out at pH 7 and 60 °C, conditions where the outer PDEA block should be totally insoluble while the inner PDMA block is still soluble and

partially stretched. The observed linear dependence of the decay rate on the squared scattering vector points to a purely translational diffusion of the formed flower-like aggregates in dilute solution upon the collapse of the outer block.

The behavior in concentrated solution was first investigated with tube-inversion experiments, some of which are shown in Figure 2.3.

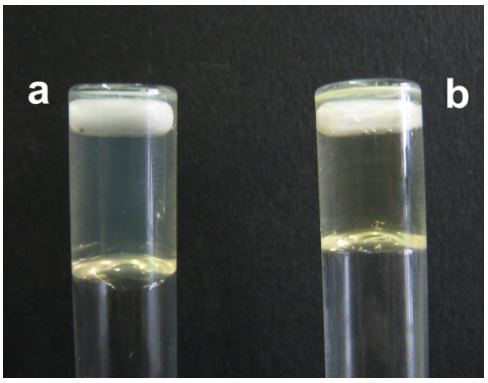

Figure 2.3. Tube-inversion experiments at pH 8 and 40 °C for a) a 20 wt% solution of $(DMA_{130}DEA_{16})_6$ and b) a 10 wt% solution of $(DMA_{110}DEA_{43})_4$.

Tube-inversion experiments revealed that there is a minimum PDEA block length that is necessary to form a hydrogel. We also observed an influence of the DEA molar fraction on the critical gelation concentration (cgc). An increase of the fraction of DEA leads to a decrease in the cgc. To gain more information on the sol-gel transition, selected polymer samples were subjected to oscillatory shear experiments using a cone-plate cell geometry (Figure 2.4).

Two measurements of the six-arm star $(DMA_{130}DEA_{16})_6$ at pH 8 are shown in Figures 2.4a and b, for 15 wt% and 20 wt%, respectively. They show the influence of polymer concentration on the gel strength and the sol-gel transition temperature, T_{sg}. The gel strength increases with increasing concentration because the amount of physical crosslinking points increases and T_{sg} decreases slightly with increasing concentration because of the concentration dependence of the cloud point as one moves along the binodal. The transition temperatures are also significantly higher than the cloud point of the PDEA block, this is attributed to

the influence of the inner hydrophilic PDMA block. In both measurements only weak gels are detected for pH 8, even at 20 wt%. However, a strong free-standing gel is formed at pH 7 and 20 wt% (Figure 2.4c), illustrating the influence of pH on this system. This phenomenon is caused by the high charge density of the inner PDMA block, whose pK_a value is around 6.2, causing a stretching of the PDMA block due to increased electrostatic repulsion and the osmotic pressure of the counterions.

An important difference between the measurements at pH 7 and pH 8 is the fact that both moduli decrease significantly above 50 °C in the case of pH 8 and this behavior is not seen at pH 7. We attribute this to the inner PDMA blocks which start to collapse above their cloud point of $T_{cl} \approx 50$ °C at pH 8, leading to a weakening of the gel. At pH 7 the cloud point of PDMA is above 80 °C and thus outside our measurement range. These findings support our claim that the block copolymer stars can reversibly form hydrogels that are able to change their mechanical properties because of the double-responsive nature of the inner blocks.

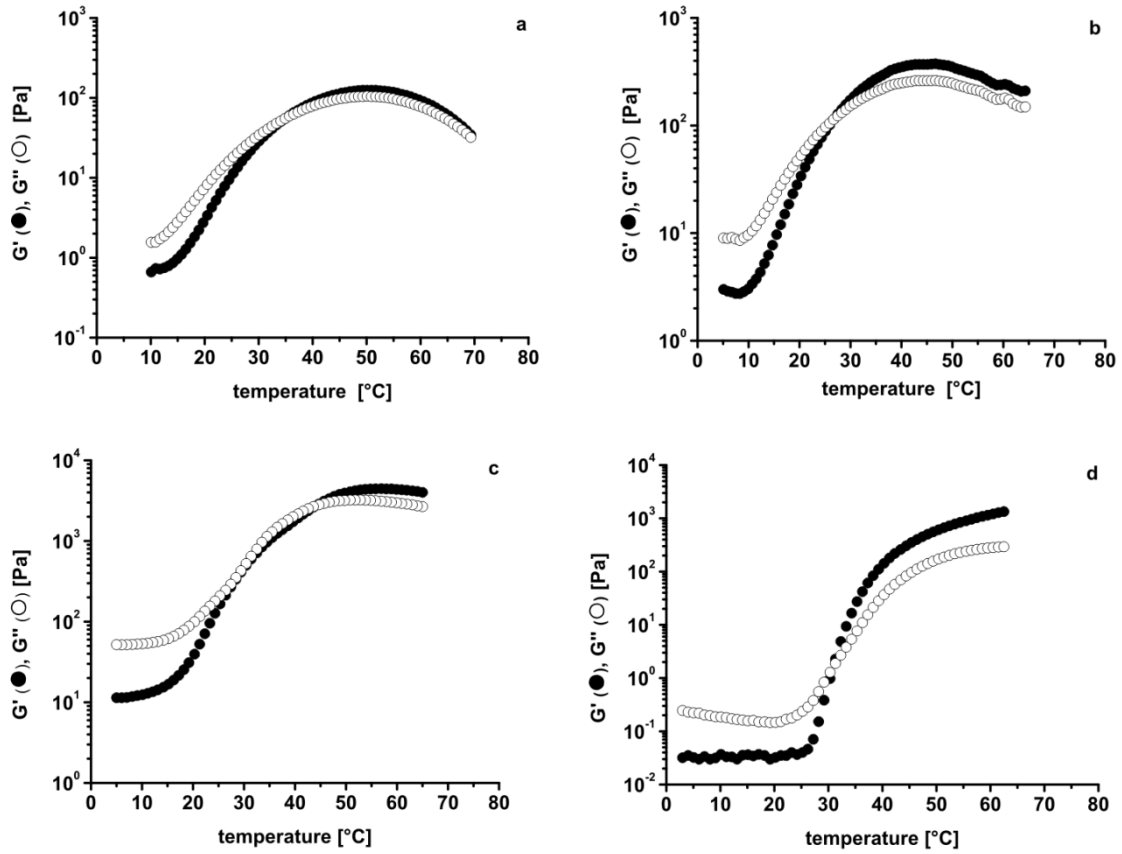

Figure 2.4. Temperature-dependent storage (G') and loss (G'') moduli of a) a 15 wt% solution of $(DMA_{130}DEA_{16})_6$ at pH 8, b) a 20 wt% solution of $(DMA_{130}DEA_{16})_6$ at pH 8, c) a 20 wt% solution of $(DMA_{130}DEA_{16})_6$ at pH 7 and d) a 10 wt% solution of $(DMA_{110}DEA_{43})_4$ at pH 8.

The block length of the outer PDEA block also plays a significant role in the properties of the gels. When the block length is increased, the gel strength increases and the cgc decreases (Figure 2.4d). The sol-gel transition temperature of $(DMA_{110}DEA_{43})_4$ is still higher than the cloud point of PDEA, but it is significantly lower than for $(DMA_{130}DEA_{16})_6$, which is due to the high molar fraction of DEA.

2.3 Smart hydrogels based on dual responsive star block copolymers

To extend our concept and possibly simplify it, the decision was made to change the outer block of our diblock stars to a polymer that only responds to a single stimulus, in our case temperature. The identical PDMA homopolymer stars as in the previous work were employed as precursors and poly(diethylene glycol methyl ether methacrylate) was chosen as the temperature-responsive polymer. The synthetic protocol had to be adjusted slightly to compensate for the new monomer but the synthesis was carried out successfully and produced well defined block copolymers with a high blocking efficiency.

Four different diblock stars were synthesized to investigate the parameters that control the gelation behavior, $(DMA_{150}DEGMA_{40})_4$, $(DMA_{150}DEGMA_{100})_4$, $(DMA_{130}DEGMA_{60})_6$ and $(DMA_{130}DEGMA_{140})_6$. Based upon our previous work we expected the behavior of the stars to follow the mechanism depicted in scheme 2.1.

Scheme 2.1. Aggregation and network formation of dual-responsive star block copolymers in dependence of concentration and pH.

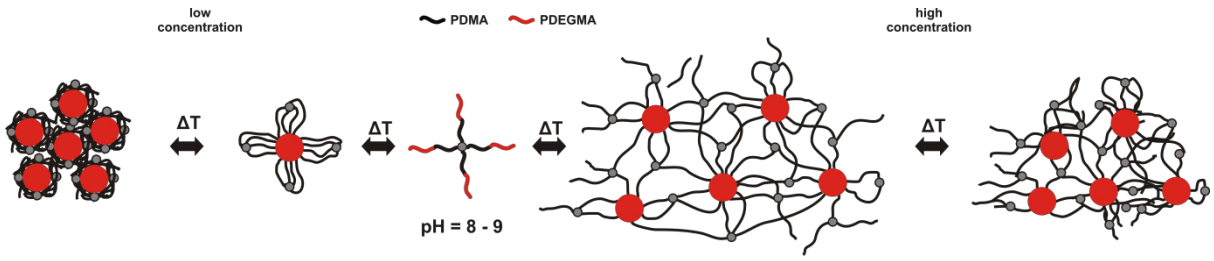

Turbidity and DLS measurements were used to investigate the behavior in dilute aqueous solution. Both methods reveal the double-responsive nature of the star block copolymers. The collapse of the outer block leads to the formation of small flower-like aggregates ($R_{h,app} \approx 34$ nm) regardless of the solution pH. The inner block of PDMA on the other hand is sensitive to both temperature and pH, meaning that at intermediate pH, *e.g.* pH = 7, PDMA is protonated enough so its cloud point is very high (≈ 80°C) and no second transition is ob-

served in our experimental setup. At elevated pH on the other hand, *e.g.* pH = 8, DMA is less protonated and the cloud point is decreased (≈ 50°C) so that an additional transition is visible in the measurements. This transition is the collapse of the PDMA block and as a result, larger and larger aggregates are formed and the polymer precipitates with time.

Based on these results, hydrogel samples were prepared at pH ≈ 8, to utilize the second transition of the block copolymer stars to manipulate the mechanical properties of the gels. These samples were analyzed using tube-inversion experiments and rheology measurements. The tube-inversion revealed that only three of the stars formed gels under the conditions tested. The star with the lowest fraction of DEGMA, $(DMA_{150}DEGMA_{40})_4$, does not form gels at all. This suggests that a minimum fraction of DEGMA, f_{DEGMA}, exists to successfully form hydrogels. The two stars with the next higher f_{DEGMA} form strong free-standing gels at concentrations of 15 wt% and the star with the highest f_{DEGMA} forms gels at concentrations as low as 10 wt%. To obtain a more detailed picture, rheology measurements were performed. Figure 2.5 shows the temperature-dependent storage (G') and loss (G'') moduli and an isothermal frequency sweep for the star with the highest f_{DEGMA}, $(DMA_{130}DEGMA_{140})_6$.

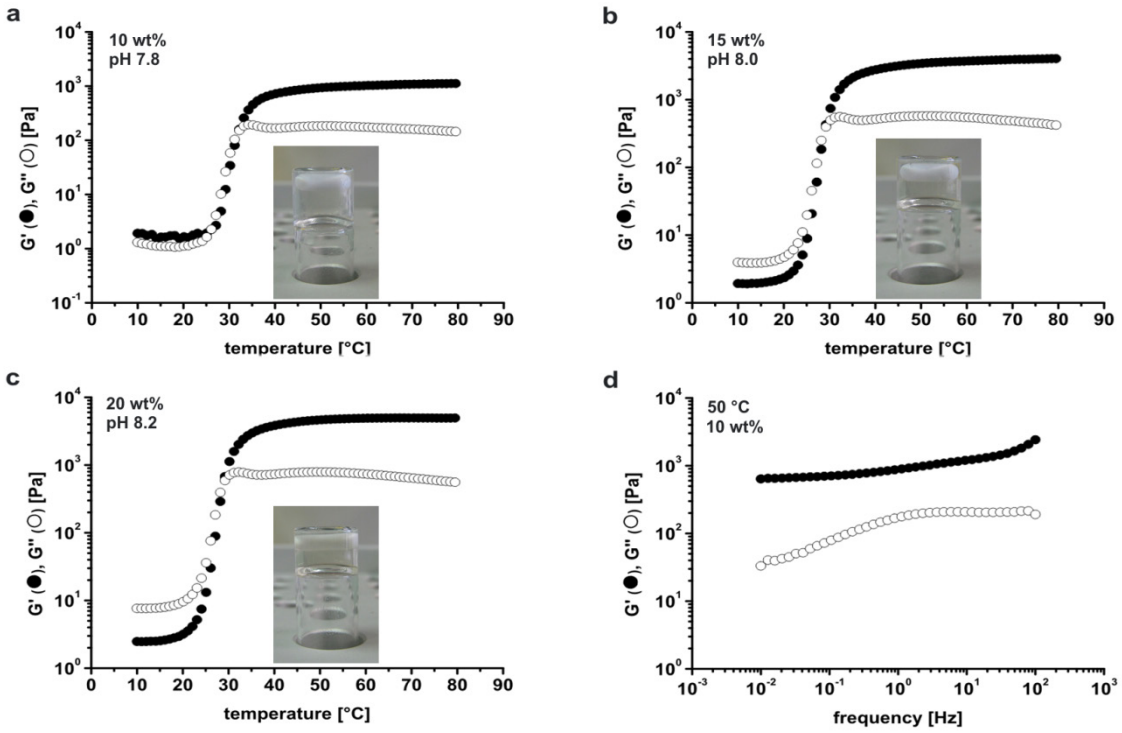

Figure 2.5. Temperature-dependent storage and loss moduli of $(DMA_{130}DEGMA_{140})_6$ at a concentration of a) 10 wt% at a pH of 7.8, b) 15 wt% at a pH of 8.0, c) 20 wt% at a pH of 8.2 and d) an isothermal frequency sweep at 50 °C of the 10 wt% sample. Insets depict digital photographs of tube-inversion experiments of the respective samples at 50 °C.

The gels at all three concentrations are free-standing and strong, as the plateau values of *G'* are above 1 kPa and *G'* is higher than *G''* for the whole frequency range measured in the frequency sweep. Unexpectedly, the gels do not show any change in the moduli when the temperature is increased above 50 °C; we attribute this to the high gel strength, which can impede structural changes. However, when the samples are prepared at higher pH values, *e.g.* close to 9 the situation changes. The increase in pH causes a decrease in protonation, which in turn leads to a decrease in the effective volume fraction of the stars and finally to a softening of the gels. In addition, the transition temperature of the PDMA block is lowered to around 30 °C, as seen for the cloud point in turbidimetry. At such pH values, a change in both moduli can be observed for temperatures above 35 °C or 40 °C, depending on the polymer concentration (Figure 2.6). *G'* and *G''* eventually reach a plateau, because the PDMA block cannot collapse completely since the polymer is already in the gel state.

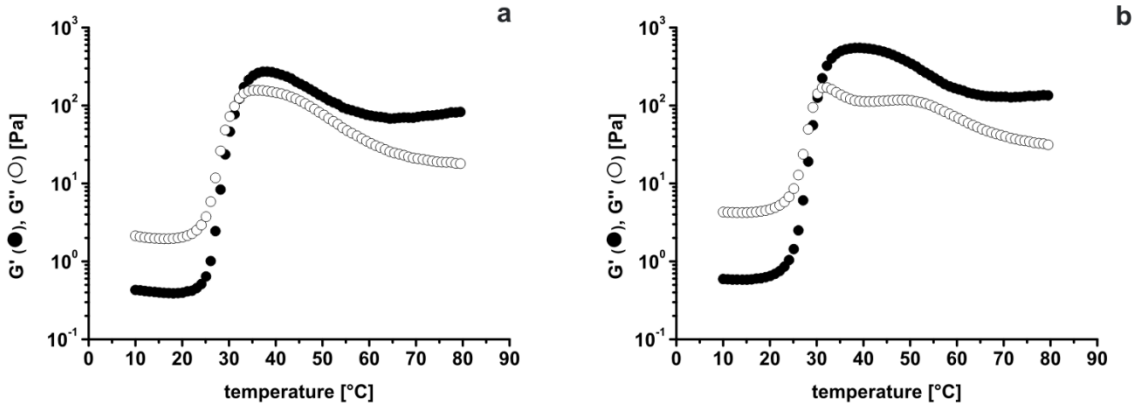

Figure 2.6. Temperature-dependent storage and loss modulus of $(DMA_{130}DEGMA_{140})_6$ for concentrations of a) 15 wt% at a pH of 8.8 and b) 20 wt% at a pH of 8.7.

These results confirm that our mechanism is correct even though the pH at which a dual-responsive gel exists is higher than expected.

To broaden our approach even more, the inner PDMA block was quaternized and transformed into a strong polycation. The increased electrostatic repulsion and the osmotic pressure of the counterions cause a stretching of the DMA chains, which leads to an increase of the effective volume fraction and to a significant reduction of the critical gelation concentration. The quaternized six-arm star $(qDMA_{130}DEGMA_{140})_6$ for example forms hydrogels at concentration as low as 2 wt%. Additionally, the quaternized block can be utilized for the incorporation of nanoparticles or the introduction of light-sensitivity through light-sensitve multivalent counterions, generating an LCST behaviour.

In conclusion, our concept for the formation of smart hydrogels based on dual-responsive star-shaped block copolymers has proven to be mostly correct in predicting the behavior of the synthesized stars. This concept can thus be extended further by replacing PDMA and PDEGMA with other polymers that are responsive to one or more stimuli.

2.4 Individual contributions to joint publications

The results presented in this thesis were obtained in collaboration with others and have been published or are submitted for publication as indicated below. In the following, the contributions of all the coauthors to the different publications are specified. The asterisk denotes the corresponding author.

Chapter 3

This work was published in *Polymer* **2010**, *51*, 1213-1217 under the title:

"Double Stimuli-Responsive Behavior of Linear and Star-Shaped Poly(N,N-Diethylaminoethyl methacrylate) in Aqueous Solution"

by Alexander Schmalz, Mathias Hanisch, Holger Schmalz* and Axel H.E. Müller*

I conducted all the experiments and wrote the publication.

Mathias Hanisch was involved in the synthesis of the DEA polymers.

Holger Schmalz and Axel H.E. Müller were involved in the discussions and the correction of the manuscript.

Chapter 4

This work is accepted by Z. Phys. Chem. under the title:

"Double-responsive hydrogels based on tertiary amine methacrylate star block copolymers"

by Alexander Schmalz, Holger Schmalz* and Axel H.E. Müller*

I conducted all the experiments and wrote the manuscript.

Holger Schmalz and Axel H.E. Müller were involved in the discussions and the correction of the manuscript.

Chapter 5

This work is published in *Soft Matter*, 2012, *8* (36), 9436-9445 under the title:

"Smart Hydrogels based on dual responsive star block copolymers"

by Alexander Schmalz, Holger Schmalz* and Axel H.E. Müller*

I conducted all the experiments and wrote the manuscript.

Holger Schmalz and Axel H.E. Müller were involved in the discussions and the correction of the manuscript.

3 Double Stimuli-Responsive Behavior of Linear and Star-Shaped Poly(*N,N*-Diethylaminoethyl Methacrylate) in Aqueous Solution

Alexander Schmalz, Mathias Hanisch, Holger Schmalz*, Axel H. E. Müller*

Makromolekulare Chemie II, Universität Bayreuth, D-95440 Bayreuth

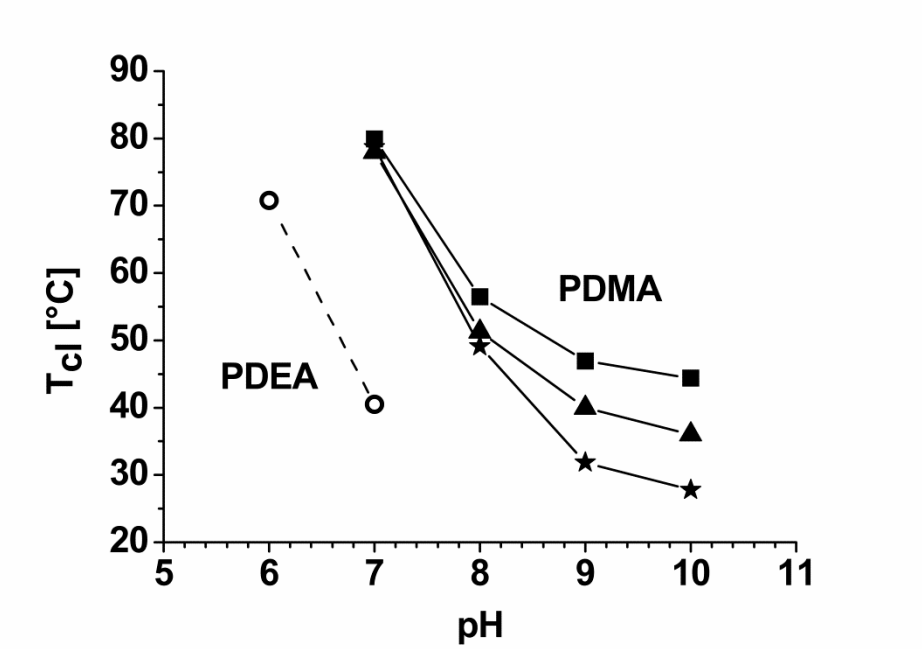

Abstract

We report on the synthesis and characterization of linear and star-shaped poly(*N,N*-diethylaminoethyl methacrylate) (PDEA). The synthesis was accomplished by Atom Transfer Radical Polymerization (ATRP) via a core-first approach using sugar-based multifunctional initiators. The investigation of the solution properties in water shows that PDEA is both pH- and temperature-responsive, analogous to the behavior of poly(*N,N*-dimethylaminoethyl methacrylate) (PDMA). In literature, PDEA is frequently referred to as being only pH-sensitive. The critical pH values for the aggregation are close to the apparent pK_a values in all cases, i.e. a high charge density is necessary to keep the polymers soluble. The cloud points show a strong dependence on the pH value of the solution but no dependence on either molecular weight or architecture. Thus, the two polymers differ only quantitatively as PDEA has cloud points about 40 K lower than PDMA and critical pH values which are 1.5 - 2 units lower than PDMA.

3.1. Introduction

Stimuli-responsive polymers have received much attention in the last years because of their use in hydrogels, actuators, membranes and other applications [1-6]. The most extensively studied thermo-responsive polymer is poly(*N*-isopropylacrylamide) due to its lower critical solution temperature (LCST) at around 32 °C in water [7-9]. In the field of pH responsiveness a typical polymer is poly(methacrylic acid) [10]. Moreover, double stimuli-sensitive polymers are of increasing interest, because some applications may require an independent response to several factors [11]. Since the number of double stimuli-responsive monomers is very limited, a thermo-sensitive monomer is often copolymerized with a pH-sensitive one, e.g., acrylic acid, to obtain a double stimuli-responsive polymer [12-14].

One class of promising candidates as double stimuli-responsive monomers are *N,N*-dialkylaminoethyl methacrylates. A well studied example of this type of polymer is poly(*N,N*-dimethylaminoethyl methacrylate) (PDMA), but it has been used mostly for its thermo-responsiveness [15-21]. Only recently, the focus has shifted to its responsiveness to both pH and temperature [22-34].

In contrast, the analogous poly(*N,N*-diethylaminoethyl methacrylate) (PDEA), differing only in the type of alkyl substituent at the amino group, is mostly described as pH-sensitive [35-38]. It has often been used to facilitate micellisation in conjunction with PDMA [39], since their responsive behavior is similar but triggered under different conditions.

However, because of their similar structure it might be expected that PDEA exhibits a double responsive behavior just like PDMA. Since DEA carries a more hydrophobic side group compared to DMA we expect an earlier collapse of the PDEA chains.

Already, there are several promising applications for PDEA, e.g. as stabilizers [40], nano-gels [41], hydrogels [42], dental applications [43] or intraocular lens biomaterials [44]. These might benefit from the possibility of a second stimulus.

In this paper we report the synthesis of well-defined PDEA stars with 3 to 8 arms by ATRP using multifunctional initiators. We investigated their solubility in dependence of pH, temperature, molecular weight and architecture using turbidimetry. The results are compared to previous investigations of PDMA stars [33]. We show that the two polymers differ only quantitatively.

3.2. Experimental

Materials. Anisole (p.a.), ethyl-α-bromoisobutyrate, *N,N,N′,N′,N‴,N‴*-hexamethyl-triethylenetetramine (HMTETA), copper(I)chloride, methyl iodide, and trimethylsilyldiazo-methane were purchased from Aldrich and used without further purification. The other solvents used (acetone, tetrahydrofuran, 1,4-dioxane) were of p.a. quality. The monomer *N,N*-diethylaminoethyl methacrylate (98%, Aldrich) was destabilized before use by passing through an alumina B column. The synthesis of the sugar-based initiators with 5, 8 and 21 initiation sites, based on glucose, saccharose and β-cyclodextrin, respectively, is described in a previous publication [45]. For dialysis, regenerated cellulose membranes (ZelluTrans with MWCO 4000-6000) were used.

Synthesis of Star-Shaped Poly(*N,N*-diethylaminoethyl methacrylate). In a typical reaction the monomer N,N-diethylaminoethyl methacrylate (64.47 g, 0.348 mol), the solvent

anisole (164 g) and the initiator (e.g. 236 mg of the β-cyclodextrin-based initiator, 1.16 mmol initiation sites) were deoxygenated by purging with nitrogen for 30 min. Afterwards the solution was heated to 60 °C by immersion in an oil bath. Simultaneously, another 15 g of anisole and the ligand HMTETA (321 mg, 1.39 mmol) were degassed with nitrogen. After 15 min the catalyst copper(I)chloride (138 mg, 1.39 mmol) was added and the mixture was again purged with nitrogen for another 15 min. For the transfer of the copper complex solution to the preheated reaction vessel a syringe was used, ensuring as little contact with air as possible. The reaction solution immediately turned green. For conversion determination a sample was taken directly after injection of the catalyst solution and every 30 min thereafter. This was done using a syringe under nitrogen counter flow. The molar ratios between monomer, initiation sites, catalyst and ligand were kept constant for all reactions at $[M]_0$:$[I]_0$:[Cat]:[L]=300:1:1.2:1.2 at $[M]_0$ ~1.4 mol/L.

The conversion was calculated using ^{1}H NMR spectroscopy by comparing the integrals of the vinyl protons of the monomer (5.6 and 6.2 ppm) with the integral of the aromatic protons of the solvent (7.2-7.5 ppm). From each reaction two star polymers with different arm lengths were obtained by removing approximately half of the reaction solution at a conversion of approximately 15%. The remaining solution was allowed to react to a conversion of ca. 30%. For the workup, the reaction solutions were passed through a silica column to remove the catalyst and concentrated using a rotary evaporator. The resulting clear viscous solutions were dialyzed against THF for 3 days to remove low molecular weight impurities. Afterwards, the solutions were concentrated again and added drop wise into basic water (pH 12-14). The precipitated polymer was filtrated off and freeze-dried from dioxane.

The arms of the star polymers were cleaved off by an alkaline ester hydrolysis. The first step was a quaternization of the amino-groups with methyl iodide to increase the water solubility of the polymer. For the actual cleaving concentrated sodium hydroxide was used. Finally, the obtained poly(methacrylic acid) was transformed to poly(methyl methacrylate) using trimethylsilyldiazomethane, enabling an easier molecular weight determination via SEC. The whole procedure is described in detail by Plamper et al. [31]. The actual arm number (Table 1) was calculated by a comparison of theoretical (obtained from conversion data) and experimental molecular weights.

^{1}H NMR spectroscopy. All measurements were performed using a Bruker AC 250 spectrometer with deuterated chloroform as solvent.

Size Exclusion Chromatography (SEC). The apparent molecular weight distributions of the star-shaped PDEA polymers were determined by SEC using dimethylacetamide (DMAc) with 0.05% lithium bromide as eluent at a flow rate of 0.8 mL/min. The equipment consisted of one pre-column and two analytical columns (PSS GRAM, 10^2 and 10^3 Å pore size, 7 µm particle size) and an Agilent 1200 RI detector. The measurements were performed at 60 °C.

The PMMA samples obtained from the arm cleavage were analyzed using a THF-SEC with a flow rate of 1 mL/min. This setup was equipped with one pre-column, four analytical columns (PSS SDV, 10^2, 10^3, 10^4 and 10^5 Å pore size, 5 µm particle size) and an Shodex 101 RI detector. The measurements were performed at 40 °C.

For data evaluation a calibration with linear PMMA standards was used in all cases.

Titration and Cloud Point Measurements. The pH and temperature dependent solution behavior was investigated using an automatic titrator (Titrando 809) from Metrohm. For the titration experiments 30 mg of polymer were dissolved in 30 ml of a hydrochloric acid solution (pH 2). The solution was degassed by applying vacuum (50-100 mbar) for 15 minutes at room temperature in order to minimize bubble formation during the experiments. The measurements were carried out with 1N NaOH (Merck) as titer, using a homemade thermostatable vessel equipped with a turbidity sensor (Spectrosense electrode, λ_0=523 nm, Metrohm), a pH sensor (Aquatrode, Metrohm), and a titration unit (Dosino 800, Metrohm). The setup was kept at a constant temperature of 25 °C. The apparent pK_a values were extracted from the titration curves at degree of neutralization α=0.5.

For the cloud point determination 30 mg of polymer were dissolved in 30 ml of buffer solution of pH 6 (citric acid/NaOH, Riedel-de-Haën) or pH 7 (NIST buffer, Titrinorm VWR). The sample preparation was identical to the one described for the titration measurements. For the experiments a constant heating rate of 1 K/min was applied.

3.3. Results and Discussion

Star-shaped PDEA polymers were synthesized by atom transfer radical polymerization (ATRP) using the core-first approach with sugar-based multifunctional initiators, bearing 2-bromoisobutyryl initiation sites. Linear PDEA was synthesized by ATRP using ethyl α-bromoisobutyrate as initiator. All reactions were performed in anisole at 60 °C with CuCl as catalyst and HMTETA as ligand. The use of a copper chloride catalyst in combination with a bromine initiator leads to cross-halogenation[46]. This can lead to an increase in control and the resulting chlorine chain-end is more stable, against a possible side reaction with a pendant amino side group, than a bromine chain-end. To avoid star-star coupling, the reactions were terminated at a maximum conversion of 30%. Additionally, at approximately 15% conversion about half of the solution was withdrawn so that each reaction resulted in two star polymers with different arm lengths but identical arm-number.

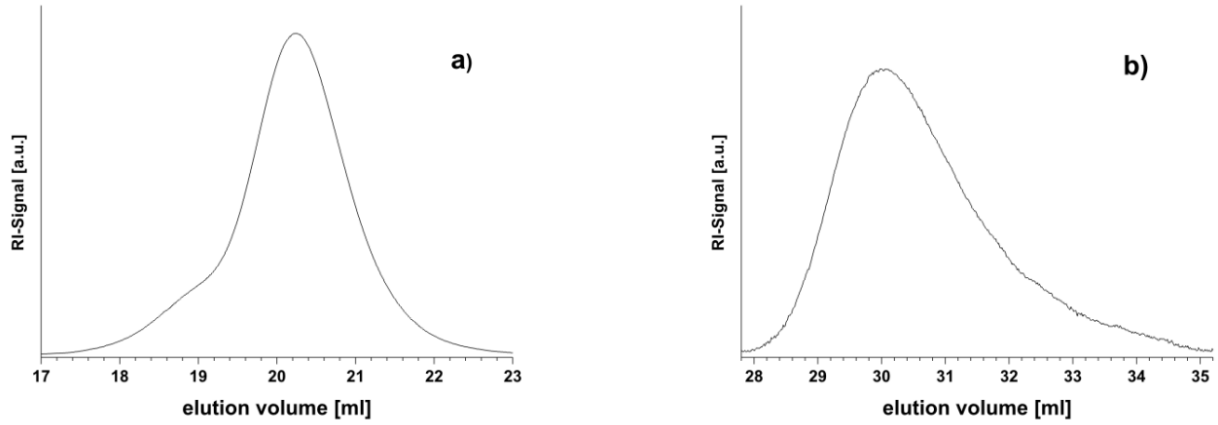

Fig. 3.1 SEC traces of a) $(DEA_{126})_{5.5}$ in DMAc and b) cleaved-off and reesterified arms (MMA_{126}) of the same star in THF.

The stars were characterized by SEC calibrated with linear PMMA standards. A typical eluogram for a PDEA star is depicted in Figure 3.1a. A small fraction of star-star coupling is observed as a shoulder at lower elution volumes, i.e. higher molecular weights. A multi peak fit analysis of the SEC traces revealed the mole fraction of coupled stars to be ca. 3%. This can be due to recombination of active chain end radicals, which should be negligible for

methacrylates, or the nucleophilic attack of a pendant amino group on the chain end halogen [47]. Due to the applied linear calibration SEC gives only apparent molecular weights.

To determine the actual arm numbers of the stars, the arms were detached from the core by alkaline ester hydrolysis and analyzed separately. The obtained linear poly(methacrylic acid) (PMAA) was reesterified to linear poly(methyl methacrylate) (PMMA), and subsequently analyzed by THF-SEC. Figure 3.1b shows a typical eluogram of the cleaved-off arms after conversion to PMMA. There is no discernable shoulder detectable on the low elution volume side. Thus, either the amount of coupled chains is too small, or they were split again in the cleavage reaction, which would point to a coupling by nucleophilic attack of a pendant amino group on the chain-end. From the molecular weight of the cleaved arms, obtained by SEC, and the conversion data from NMR the actual molecular weight of the stars can be calculated, as well as the initiation efficiency and arm number (Table 3.1) [31].

Table 3.1 Molecular characterization of linear and star-shaped poly(*N,N*-diethylaminoethyl methacrylate)

initiator functions	x_P [%] [a]	I_{eff} [b]	arm number [c]	DP (Arm) [d]	M_n [10^3 g/mol][e] (PDI)[f]	formula [g]
1	15	0.95	1	41	7.7 (1.22)	DEA_{41}
1	53	0.96	1	59	11.0 (1.22)	DEA_{59}
1	61	0.95	1	109	20.3 (1.36)	DEA_{109}
5	13	0.61	3.1	65	38.0 (1.35)	$(DEA_{65})_{3.1}$
5	30	0.61	3.1	145	83.1 (1.10)	$(DEA_{145})_{3.1}$
8	18	0.69	5.5	78	81.1 (1.08)	$(DEA_{78})_{5.5}$
8	29	0.69	5.5	126	129.7 (1.09)	$(DEA_{126})_{5.5}$
21	16	0.41	8.6	119	192.7 (1.10)	$(DEA_{119})_{8.6}$
21	29	0.41	8.6	214	344.0 (1.18)	$(DEA_{214})_{8.6}$

[a] monomer conversion, as determined by ^{1}H NMR; [b] initiator efficiency calculated from the ratio of theoretical and experimental molecular weight of arms; [c] number of initiation functions multiplied by the initiation efficiency; [d] calculated from M_n(PMMA) after arm cleavage; [e] calculated according to DP(Arm) x arm number x $M_{DEA;}$ [f] PDI of stars as measured by SEC in DMAc using PMMA calibration; [g] $(DEA_n)_f$: n = number-average degree of polymerization per arm; f = number-average arm number.

For the analysis of the pH-responsive behavior the polymer was dissolved in water at pH 2 (1 g/L) and then titrated with 1 M NaOH to pH 12. At a critical pH value, pH_{cr}, the polymer becomes insoluble. This can be monitored by a change in transmittance. The critical value was defined as the intercept of the tangents at the onset of turbidity. In addition, the apparent pK_a value, $pK_{a,app}$, is determined from the titration curves analogous to the method used by Plamper et al. [33]. In Figure 3.2a the obtained critical pH (pH_{cr}) and $pK_{a,app}$ are plotted against the molecular weight of the corresponding polymers.

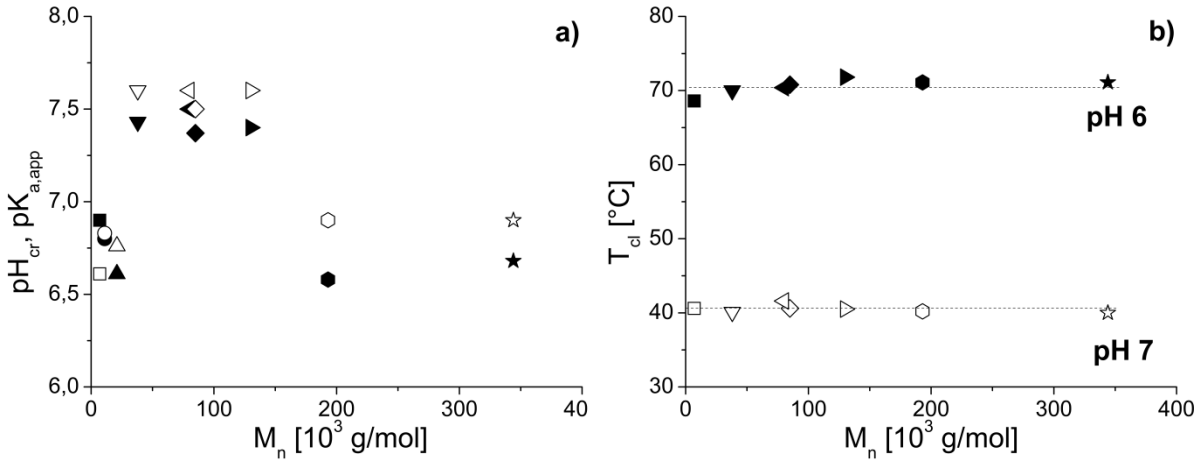

Fig. 3.2 a) Critical pH-values (pH_{cr}, filled symbols), apparent pK_a values ($pK_{a,app}$, open symbols), and b) cloud points (T_{cl}) in pH 6 and pH 7 buffers as a function of molecular weight for linear and star-shaped PDEA (■,□ DEA_{41}; ●,○DEA_{59}; ▲,△DEA_{109}; ▼,▽$(DEA_{65})_{3.1}$; ◆,◇$(DEA_{145})_{3.1}$; ◀,◁$(DEA_{78})_{5.5}$; ▶,▷ $(DEA_{126})_{5.5}$; ⬢,⬡ $(DEA_{119})_{8.6}$; ★,☆ $(DEA_{214})_{8.6}$).

The graph shows that the critical pH values are close to the apparent pK_a values in every case, i.e. aggregation occurs when roughly half of the amino groups are deprotonated. This indicates that a high charge density is necessary to provide the solubility of the polymers in water, which can be attributed to the hydrophobicity of the ethyl substituents at the amine group. PDMA, which carries less hydrophobic substituents, is soluble over the whole pH-range at 25 °C.

To prove the assumption that PDEA shows temperature-responsive behavior too, the polymer was dissolved in buffer solutions of pH 6 and pH 7 (1 g/L), respectively. The samples were heated from 20°C to 90°C at a rate of 1 K/min, and the changes in turbidity were measured. The cloud points, T_{cl}, were determined using the onset method [33].

Figure 3.2b shows the results of the temperature-dependent measurements. For both pH values the cloud points do not show a significant dependence on molecular weight and architecture, i.e. arm number. However, a clear dependence on pH can be detected. The cloud points decrease from around 70 °C for pH 6 to around 40 °C for pH 7. This is most likely due to the charge density inside the stars, as electrostatic interactions would prevent the aggregation of the polymer chains, and the charge density is higher for pH 6. This behavior agrees well with results previously reported by our group for PDMA [31, 33]. A comparison of the pH dependent behavior between star-shaped PDEA and PDMA (Figure 3.3a) shows similar trends. The cloud point of PDMA shows a slight dependence on molecular weight [33]. However, this is only observed at high pH values, i.e. lower protonation, which is inaccessible for PDEA. At pH 7 the cloud points of PDMA vary between 77 °C and 80 °C, whereas the values for PDEA are around 40 °C (Fig. 3.3b). This can be attributed to the more hydrophobic alkyl substituents at the amino group of the repeating unit.

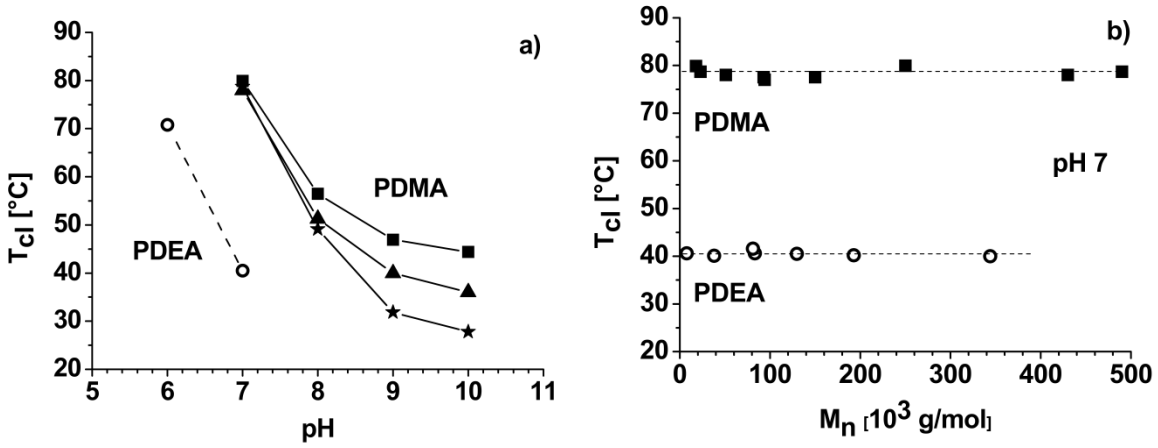

Fig. 3.3 a) Cloud points for linear and star-shaped PDEA and PDMA in dependence of pH (○ $(DEA_n)_x$; ■ DMA_{108}; ▲ $(DMA_{100})_{3.1}$; ★ $(DMA_{170})_{18}$), and b) cloud points plotted against molecular weight for linear and star-shaped PDEA (○) and PDMA (■) at pH 7. The lines are only a guide to the eye. Results for PDMA taken from reference [33].

The measurements for PDMA were performed at 0.1 g/L whereas the measurements for PDEA were performed at 1.0 g/L. There is a concentration dependence of the cloud point as we move along the bimodal, which has its minimum in the LCST. But since the effect is only in the order of a few Kelvin in the relevant concentration range [33], it is not discussed here.

Plamper et al. [33] were able to measure PDMA stars in buffer solutions of a pH up to 10 (Figure 3.3a). This was impossible for PDEA because of the poor solubility for a pH > 7. In addition, PDMA loses its LCST below pH 7 (i.e. T_{cl} > 100 °C), whereas PDEA still exhibits a cloud point at pH = 6. Under identical conditions, PDEA always shows lower critical values. At a given pH, e.g. pH 7, the cloud point of PDEA is ca. 40 K lower than that of PDMA, and for high temperatures, the critical pH value of PDEA is 1.5 – 2 units below that of PDMA.

3.4. Conclusions

Star-shaped PDEA was successfully synthesized by the core-first method employing ATRP. The initiators and conditions used resulted in star polymers with arm numbers ranging from 3 to 8, and polydispersity indices between 1.08 and 1.35. Our experiments showed that PDEA is a double stimuli-responsive polymer in contrast to literature, where it has only been described as pH-sensitive. In fact, it responds to both variations in pH and temperature, just like the analogous PDMA. Consequently, the differences between these two polymers are purely quantitative in nature and not qualitative, as they only differ in the magnitude of their critical values. PDEA exhibits a critical pH at which the protonation of its pendant amino groups is no longer sufficient to keep it soluble in water. At this pH the chains collapse and aggregate. The temperature-responsive behavior of PDEA does not depend on molecular weight or architecture, i.e. arm number. However, the cloud point does strongly depend on pH, as it affects the overall charge of the star. Upon lowering the pH from 7 to 6 the cloud point increased dramatically from 40°C to 70°C.

In comparison to PDMA, all critical values for PDEA are lower. The cloud points at a given pH lie 40 K below those of PDMA, and the critical pH values of PDEA are 1.5 – 2 units lower, regardless of architecture or molecular weight.

Acknowledgements: We thank the German Science Foundation (DFG) for financial support within the Priority Program SPP 1259.

3.5. References

[1] Yu L, Ding J. Chem. Soc. Rev. 2008;37:1473-1481.

[2] Hart DS, Gehrke SH. J. Pharm. Sci. 2007;96:484-516.

[3] Guenther M, Kuckling D, Corten C, Gerlach G, Sorber J, Suchaneck G, Arndt KF. Sens. Actuators B 2007;126:97-106.

[4] Calvert P, Patra P, Duggal D. Proc. SPIE-Int. Soc. Opt. Eng. 2007;6524:M1-6.

[5] Tachibana Y, Kurisawa M, Uyama H, Kakuchi T, Kobayashi S. Chem. Lett. 2003;32:374-375.

[6] Beebe DJ, Moore JS, Bauer JM, Yu Q, Liu RH, Devadoss C, Jo B-H. Nature 2000;404:588-590.

[7] Kuckling D, Vo CD, Adler HJP, Völkel A, Cölfen H. Macromolecules 2006;39:1585-1591.

[8] Zhang X-Z, Zhuo R-X. Eur. Polym. J. 2000;36:643-645.

[9] Park TG, Hoffman AS. J. Polym. Sci., Part A: Polym. Chem. 1992;30:505-507.

[10] He H, Li L, Lee LJ. Polymer 2006;47:1612-1619.

[11] Dong L-C, Hoffman AS. J. Controlled Release 1991;15:141-152.

[12] Xu F-J, Kang E-T, Neoh K-G. Biomaterials 2006;27:2787-2797.

[13] Bae SJ, Joo MK, Jeong Y, Kim SW, Lee WK, Sohn YS, Jeong B. Macromolecules 2006;39:4873-4879.

[14] Lin HH, Cheng YL. Macromolecules 2001;34:3710-3715.

[15] Xia J, Johnson T, Gaynor SG, Matyjaszewski K, DeSimone J. Macromolecules 1999;32:4802-4805.

[16] Zeng F, Shen Y, Zhu S, Pelton R. Macromolecules 2000;33:1628-1635.

[17] Fang Z, Kennedy JP. J. Polym. Sci., Part A: Polym. Chem. 2002;40:3679-3691.

[18] Lee Sang B, Russell Alan J, Matyjaszewski K. Biomacromolecules 2003;4:1386-1393.

[19] Zheng G, Stoever HDH. Macromolecules 2003;36:7439-7445.

[20] Mao B, Gan L-H, Gan Y-Y, Li X, Ravi P, Tam K-C. J. Polym. Sci., Part A: Polym. Chem. 2004;42:5161-5169.

[21] Lee H-I, Pietrasik J, Matyjaszewski K. Macromolecules 2006;39:3914-3920.

[22] Schacher F, Müllner M, Schmalz H, Müller AHE. Macromol. Chem. Phys. 2009;210:256-262.

[23] Schacher F, Ulbricht M, Müller AHE. Adv. Funct. Mater. 2009;19:1040-1045.

[24] Huang J, Cusick B, Pietrasik J, Wang L, Kowalewski T, Lin Q, Matyjaszewski K. Langmuir 2007;23:241-249.

[25] Yamada K, Shibuya M, Takagi C, Hirata M. J. Appl. Polym. Sci. 2006;99:381-391.

[26] Teoh SK, Ravi P, Dai S, Tam KC. J. Phys. Chem. B 2005;109:4431-4438.

[27] Lee SB, Russell AJ, Matyjaszewski K. Biomacromolecules 2003;4:1386-1393.

[28] Shen Y, Zeng F, Zhu S, Pelton R. Macromolecules 2001;34:144-150.

[29] Bütün V, Armes SP, Billingham NC. Polymer 2001;42:5993-6008.

[30] Plamper FA, Walther A, Müller AHE, Ballauff M. Nano Letters 2007;7:167-171.

[31] Plamper FA, Schmalz A, Penott-Chang E, Drechsler M, Jusufi A, Ballauff M, Müller AHE. Macromolecules 2007;40:5689-5697.

[32] Plamper FA, Schmalz A, Ballauff M, Müller AHE. J. Am. Chem. Soc. 2007;129:14538-14539.

[33] Plamper FA, Ruppel M, Schmalz A, Borisov O, Ballauff M, Müller AHE. Macromolecules 2007;40:8361-8366.

[34] Plamper FA, Müller AHE, Ballauff M. Polym. Mater. Sci. Eng. 2007;96:799.

[35] Ma Y, Tang Y, Billingham NC, Armes SP, Lewis AL. Biomacromolecules 2003;4:864-868.

[36] Liu S, Weaver JVM, Tang Y, Billingham NC, Armes SP, Tribe K. Macromolecules 2002;35:6121-6131.

[37] Mao BW, Gan LH, Gan YY, Tam KC, Tan OK. Polymer 2005;46:10045-10055.

[38] He E, Ravi P, Tam KC. Langmuir 2007;23:2382-2388.

[39] Jiang X, Zhang G, Narain R, Liu S. Soft Matter 2009;5:1530-1538.

[40] Shahalom S, Tong T, Emmett S, Saunders BR. Langmuir 2006;22:8311-8317.

[41] Yusa S-i, Sugahara M, Endo T, Morishima Y. Langmuir 2009;25:5258-5265.

[42] Tuncer Caykara SK, Eylem Turan. Polym. Int. 2007;56:532-537.

[43] Rusen E, Marculescu B, Butac L, Zecheru T, Miculescu F, Rotariu T. J. Optoelectron. Adv. Mater. 2008;10:3436-3441.

[44] Brady C, Bell SEJ, Parsons C, Gorman SP, Jones DS, McCoy CP. J. Phys. Chem. B 2007;111:527-534.

[45] Plamper FA, Becker H, Lanzendörfer M, Patel M, Wittemann A, Ballauff M, Müller AHE. Macromol. Chem. Phys. 2005;206:1813-1825.

[46] Matyjaszewski K, Shipp DA, Wang J-L, Grimaud T, Patten TE. Macromolecules 1998;31:6836-6840.

[47] Zeng F, Shen Y, Zhu S. Macromol. Rapid Commun. 2002;23:1113-1117.

4 Double responsive hydrogels based on tertiary amine methacrylate star block copolymers

Alexander Schmalz, Holger Schmalz*, Axel H. E. Müller*

Makromolekulare Chemie II, Universität Bayreuth, D-95440 Bayreuth

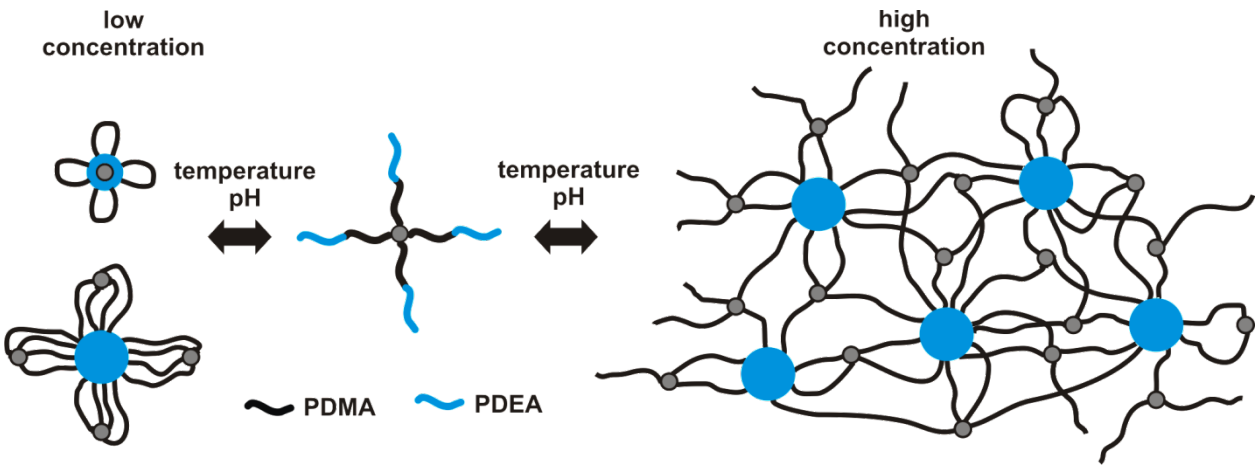

Abstract

Double hydrophilic stimuli-responsive star block copolymers with poly(2-(dimethylamino)ethyl methacrylate) (PDMA) inner blocks and poly(2-(diethylamino)ethyl methacrylate) (PDEA) outer blocks were synthesized using ATRP. Different multifunctional initiators based on sugar scaffolds were employed in a core-first approach with sequential polymerization of both blocks yielding stars with 4 and 6 arms, respectively, and varying length of the PDEA outer block. The star block copolymers show pH- and temperature-responsive aggregation as revealed by dynamic light scattering and turbidimetry. The impact of pH, PDEA block length and arm number on the gelation behavior was investigated by tube inversion and rheology.

4.1. Introduction

'Smart' hydrogels are polymer networks that have the ability to form/break or expand/contract in response to external stimuli. Suitable stimuli are pH, temperature, ionic strength, light, or external magnetic and electric fields.[1,2] The two most commonly applied stimuli are temperature[3] and pH.[4] Responsive hydrogels find widespread applications, *e.g.* in time-controlled release of active compounds,[5-7] tissue engineering[2,8-10] and microfluidics.[11] Over the last years there has been great interest in the mechanisms of gel formation,[2] shape-change of gels in response to an applied field[1] and the controlled disintegration of gels.[12]

There are two classes of networks, chemically and physically cross-linked ones. Chemically cross-linked systems based on poly(N-isopropylacrylamide) (PNIPAAm) have been studied most extensively because of its Lower Critical Solution Temperature (LCST) at around 32 °C in water.[13-15] The advantage of physically cross-linked networks is the reversibility of the gelation process, and the fact that the network formation itself can be triggered by external stimuli.[2,4,7] Mostly linear ABA[16,17] and ABC[18,19] triblock copolymers, based on a hydrophilic middle block B and stimuli-responsive outer blocks A and C, were used to construct physical gels. In addition, star-shaped block copolymers, $(AB)_x$, with stimuli-responsive outer blocks were also used.[20] Considerable work has been devoted to stars where the inner hydrophilic

block is poly(ethylene glycol) (PEG), with thermo-responsive outer blocks of PNIPAAm, [21] poly(oligo(ethylene glycol) methacrylate) (POEGMA)[22], as well as stars with biodegradable outer blocks of poly(lactic acid) (PLA)[23,24] or poly(ε-caprolactone) (PCL).[24,25] For pH responsive star block copolymers P2VP was used as an intelligent block[26] as well as different 2-(dialkylamino)ethyl methacrylates such as poly(2-(dimethylamino)ethyl methacrylate) (PDMA), poly(2-(diethylamino)ethyl methacrylate) (PDEA) and poly(2-(diisopropyl)ethyl methacrylate) (PDPA).[27,28] However, in studies related to star-shaped block copolymers thus far only the formation/disintegration of the network is subject to external parameters, as only the outer blocks of the stars were stimuli responsive. Thus, the resulting gels themselves cannot respond to a second, different stimulus. Nevertheless, if the inner blocks of the stars would exhibit responsive behavior, too, then a second trigger could possibly lead to additional intelligent behavior, such as shrinking. We have recently shown that linear and star-shaped PDMA as well as PDEA homopolymers are responsive to both pH and temperature.[27-32] The cloud points of PDEA are significantly lower than those of PDMA at any pH value. Thus, choosing the proper conditions it should be possible to trigger a consecutive collapse of PDEA and PDMA in respective block copolymer architectures.

In this section we present the synthesis of double stimuli-responsive star-shaped block copolymers based on two different 2-(dialkylamino)ethyl methacrylate monomers, DMA and DEA. Scheme 4.1 illustrates the proposed mechanism, by which network formation or self-assembly occurs depending on polymer concentration, similar to the model described by Stepánek et al. and Taktak et al.[24,33] At low concentrations, intramolecular collapse or aggregation to small micellar aggregates is favored and leads to the formation of flower-like micelles. At high concentrations, on the other hand, intermolecular collapse is preferred, resulting in bridging between multiple hydrophobic domains and thus gelation. Here, we have combined two double responsive monomers to synthesize double stimuli-responsive star-shaped block copolymers, which can reversibly form hydrogels in dependence of pH and temperature.

Scheme 4.1. Aggregation and network formation of double responsive star block copolymers

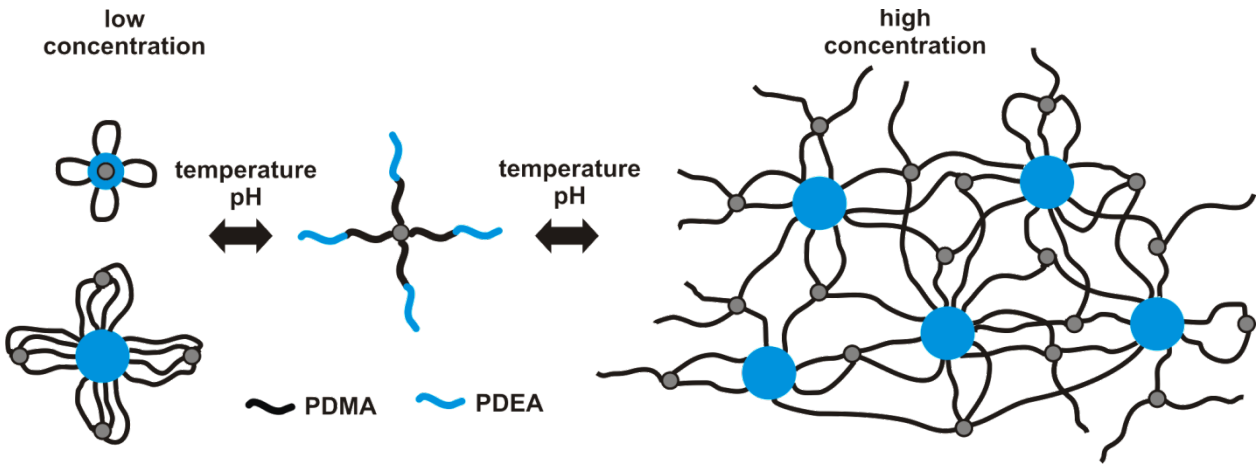

4.2. Experimental

Materials. Anisole (p.a.), ethyl 2-bromoisobutyrate, N,N,N',N'',N''',N'''-hexamethyl-triethylenetetramine (HMTETA), copper(I) chloride, 1,3,5-trioxane, methyl iodide, and trimethylsilyldiazomethane were purchased from Aldrich and used without further purification. The other solvents used (acetone, tetrahydrofuran, 1,4-dioxane) were of p.a. quality. The monomers 2-(dimethylamino)ethyl methacrylate (98%, Aldrich) and 2-(diethylamino)ethyl methacrylate (99%, Aldrich) were destabilized before use by passing through a basic alumina column. The synthesis of the sugar-based initiators with 5 and 8 2-bromoisobutyryl initiation sites, based on glucose and saccharose, respectively, is described in a previous publication.[34] For dialysis, regenerated cellulose membranes (ZelluTrans with MWCO 4000-6000) were used.

Synthesis of star-shaped block copolymers. The core-first approach utilizing sugar-based initiators and sequential polymerization was used in all syntheses. In a typical reaction for the first block, the monomer 2-(dimethylamino)ethyl methacrylate (127.5 g, 0.811 mol), the solvent anisole (995 g), the initiator (500 mg of the pentafunctional glucose-based initiator, 2.7 mmol initiation sites) and 1,3,5-trioxane as internal standard were mixed in the reactor and deoxygenated by three cycles of evacuating and purging the reactor with nitrogen. Afterwards the solution was heated to 60 °C. Simultaneously, another 50 g of anisole and the ligand HMTETA (746.5 mg, 3.24 mmol) were degassed with nitrogen. After 15 min the catalyst copper(I) chloride (320.8 mg, 3.24 mmol) was added and the mixture was again purged with nitrogen for another 15 min. For the transfer of the copper complex solution to the preheated reactor a syringe was used, ensuring as little contact with air as possible. The reaction solution immediately turned green. For conversion determination a sample was taken directly after injection of the catalyst solution and every 30 min thereafter. This was done using a syringe under nitrogen counter flow. The molar ratios between monomer, initiation sites, catalyst and ligand were kept constant for all reactions at $[M]_0$:$[I]_0$:[Cat]:[L]=300:1:1.2:1.2 at $[M]_0$ ~ 0.77 mol/L.

The conversion was determined using ^{1}H-NMR spectroscopy by comparing the integrals of the vinyl protons of the monomer (5.6 and 6.2 ppm) with the internal standard (1,3,5-trioxane, 4.9 ppm). The reactions were terminated at a maximum conversion of about

30%, to avoid or at least minimize star-star coupling. For workup, the diluted reaction solutions were passed through a silica column to remove the catalyst and concentrated again using a rotary evaporator. The polymer was precipitated in *n*-hexane, filtrated off and dried in a vacuum oven at 40 °C. Finally, the polymer was redissolved in dioxane and freeze-dried.

For the second block the same procedure was used. In a typical reaction 20 g of the star-shaped PDMA macroinitiator (~ 0.77 mmol initiation sites), 14.25 g of the monomer 2-(diethylamino)ethyl methacrylate (0.077 mol), 91.4 mg Cu(I)Cl (0.92 mmol) and 212.7 mg HMTETA (0.92 mmol) were used. All reactions for the second block were carried out using a fixed ratio between monomer, initiation sites, catalyst and ligand of $[M]_0$:$[I]_0$:[Cat]:[L]=100:1:1.2:1.2 at $[M]_0$ ~ 0.073 mol/L.

The arms of the resulting PDMA-*b*-PDEA star block copolymers were cleaved off by an alkaline ester hydrolysis. The first step was quaternization of the amino groups with methyl iodide to increase the water solubility of the polymer. For the actual cleaving concentrated sodium hydroxide was used. Finally, the obtained poly(methacrylic acid) was transformed to poly(methyl methacrylate) using trimethylsilyldiazomethane, enabling an easier molecular weight determination via SEC. The whole procedure is described in detail by Plamper et al.[30] The actual arm number (Table 4.1) was calculated by a comparison of theoretical (obtained from conversion data) and experimental molecular weights.

^{1}H-NMR spectroscopy. All measurements were performed with a Bruker AC 250 spectrometer using deuterated chloroform as solvent.

Size Exclusion Chromatography (SEC). The apparent molecular weight distributions of the star-shaped homo- and copolymers were determined by SEC using dimethylacetamide (DMAc) with 0.05% lithium bromide as eluent at a flow rate of 0.8 mL/min. The equipment consisted of one pre-column and two analytical columns (PSS GRAM, 10^2 and 10^3 Å pore size, 7 μm particle size) and an Agilent 1200 RI detector. The measurements were performed at 60 °C.

The PMMA samples obtained from the arm cleavage were analyzed using a THF-SEC with a flow rate of 1 mL/min. This setup was equipped with one pre-column, four analytical columns (PSS SDV, 10^2, 10^3, 10^4 and 10^5 Å pore size, 5 μm particle size) and a Shodex 101 RI

detector. The measurements were performed at 40 °C. For data evaluation a calibration with linear PMMA standards was used in all cases.

Cloud Point Measurements. The temperature-dependent solution behavior was investigated using a titrator (Titrando 809, Metrohm) equipped with a turbidity probe (Spectrosense, Metrohm, λ_0 = 523 nm) and a temperature sensor (Pt1000, Metrohm). The cloud points (T_{cl}) were determined by dissolving 30 mg of polymer in 30 ml of buffer solutions ranging from pH 7 to pH 10 (NIST buffer, Titrinorm VWR). The solutions were degassed by applying vacuum (50-100 mbar) for 15 min at room temperature in order to minimize bubble formation during the measurements. For the experiments a homemade thermostatable vessel was used and a constant heating rate of 1 K/min was applied using a thermostat (Lauda Ecoline Staredition RE 306, +/- 0.01°C). The cloud points were determined from the intersection of the two tangents applied to the two linear regimes of the transmittance curve at the onset of turbidity.

Dynamic Light Scattering. DLS was performed on an ALV DLS/SLS-SP 5022F compact goniometer system with an ALV 5000/E in cross-correlation mode and a HeNe laser (λ_0 = 632.8 nm). The solutions were prepared by dissolving 2 mg of polymer in 2 ml of buffer solution of either pH 7 or 8 (NIST buffer, Titrinorm, VWR) and filtered prior to the measurements with 0.45 μm syringe filters (cellulose acetate, Roth). For temperature-dependent measurements, the decaline bath of the instrument was thermostated using a LAUDA Proline RP 845 thermostat. At each temperature the sample was equilibrated for 10 min prior to data acquisition, which was done five times for the duration of 60 sec each. The autocorrelation functions were recorded individually and evaluated using 2nd order cumulant analysis.

Rheology. Rheology measurements were conducted using a Physica MCR 301 rheometer with a cone-and-plate shear cell geometry (D = 50 mm, cone angle = 1°). For the temperature-dependent measurements a frequency of 1 Hz, a heating rate of 0.5 K/min and a strain of 0.5%, which is inside the linear viscoelastic regime, were applied. The temperature was controlled by a Peltier element. For the isothermal frequency sweeps (10^{-2} to 10^{2} Hz) the desired temperature was adjusted by heating the sample at a rate of 0.5 K/min. The samples were prepared using a Ditabis Cooling-Thermomixer MKR13. The polymers were directly dissolved in water at different low pH values, *i.e.*, pH = 2 or 3, to produce solutions with final

pH values of pH = 7 or 8, respectively. This procedure avoids additional pH adjustments after sample preparation, which would result in salt (NaCl) formation and consequently might influence the solution behavior of the polyelectrolyte blocks. The samples were shaken in the MKR13 at 10 °C for several hours up to several days until the polymer was completely dissolved, and subsequently stored at 3 °C until use.

4.3. Results and Discussion

Synthesis and molecular characterization. We have successfully synthesized star block copolymers of 2-(dimethylamino)ethyl methacrylate (DMA) and 2-(diethylamino)ethyl methacrylate (DEA) via ATRP using the core-first method (Scheme 4.2). Sequential grafting of the two monomers from multifunctional initiators based on sugar scaffolds was combined with the cross-halogenation technique[35] in order to achieve a good control over molecular weight and distribution as well as a high blocking efficiency.

Scheme 4.2. Synthesis of $(DMA_nDEA_m)_x$ star block copolymers

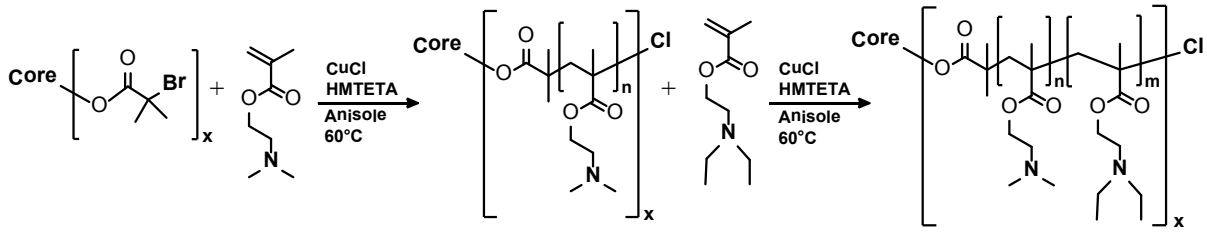

First, a corresponding linear PDMA-*b*-PDEA diblock copolymer was synthesized using a monofunctional ATRP initiator, ethyl 2-bromoisobutyrate, in order to test the efficiency of the applied synthesis route. Only by employing the cross-halogenation approach were we able to achieve a high blocking efficiency. Figure 4.1 shows the SEC traces of the synthesized linear PDMA-*b*-PDEA diblock copolymer together with the respective PDMA precursor. Both SEC traces show narrow (PDI = 1.18 and 1.19, respectively) and monomodal molecular weight distributions, and the SEC trace of the diblock copolymer is completely shifted toward higher molecular weights, *i.e.*, lower elution volumes, revealing a complete blocking.

Consequently, this synthetic protocol was applied to the synthesis of (PDMA-*b*-PDEA)$_x$ diblock copolymer stars.

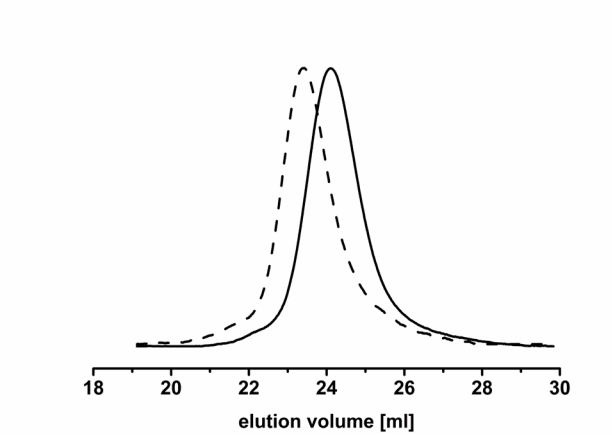

Figure 4.1. SEC traces of the synthesized linear PDMA-*b*-PDEA diblock copolymer (dashed line) and the corresponding PDMA precursor (solid line), using ethyl 2-bromoisobutyrate as the monofunctional initiator and the cross-halogenation technique.

As an example, the SEC trace of the synthesized $(DMA_{130}DEA_{16})_6$ diblock copolymer star is shown in Figure 4.2a. The molecular weight distribution is monomodal with a shoulder at higher molecular weight indicating some star-star coupling. This might be caused by a combination of chain-end radicals or the nucleophilic attack of pendant amino groups on the chain end halogen.[36] However, in a methacrylate polymerization the predominant termination reaction is disproportionation, which is attributed to steric hindrance preventing a combination of two polymer radicals.

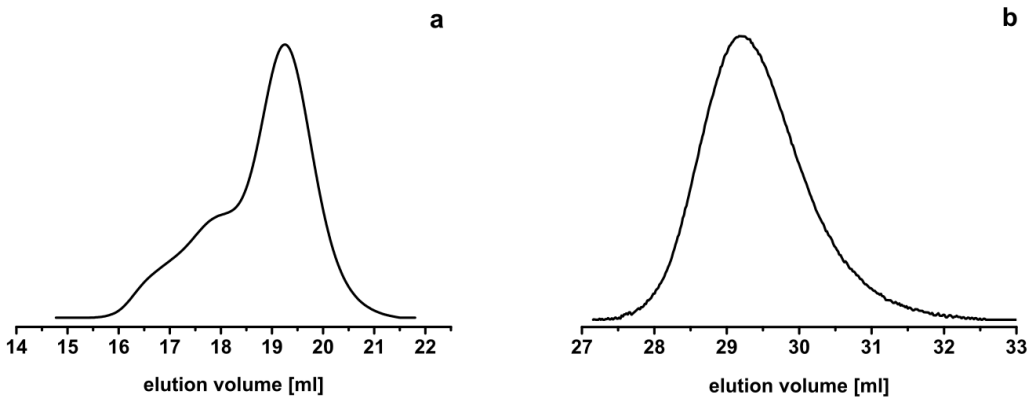

Figure 4.2. SEC traces of a) the star block copolymer $(DMA_{130}DEA_{16})_6$ in DMAc, and b) the corresponding cleaved-off arms which have been transformed to PMMA in THF.

The actual number and length of the arms was determined by detaching the arms from the core via alkaline ester hydrolysis and subsequent reesterification of the resulting poly(methacrylic acid) (PMAA) to poly(methyl methacrylate) (PMMA). The SEC trace of the detached PMMA arms of the $(DMA_{130}DEA_{16})_6$ diblock copolymer star does not show a coupling shoulder at the high molecular weight side (Figure 4.2b). This suggests that the coupling reaction involves intermolecular nucleophilic substitution of chain end halogens by pendant amino groups from different stars, as this linkage is hydrolyzed under the alkaline conditions used for the arm cleavage. Since the SEC trace of the cleaved block copolymer arms is monomodal and does not show a shoulder at the low molecular weight side a blocking efficiency close to unity can be assumed.

All synthesized $(PDMA\text{-}b\text{-}PDEA)_x$ diblock copolymer stars exhibit narrow molecular weight distributions with polydispersity indices between 1.1 and 1.3 (Table 4.1). ^{1}H-NMR measurements were used to confirm the structure of the diblock copolymer stars and to calculate the average degree of polymerization of the PDEA outer blocks. Here, the molecular weight of the PDMA inner block, determined by arm cleavage of the $(PDMA)_x$ precursor stars, was used for internal calibration. Consequently, the peaks at 2.75 and 4.05 ppm, corresponding to *-N(**CH$_2$**-CH$_3$)$_2$* and *-O-**CH$_2$**-CH$_2$-* groups, respectively, were compared to calculate the PDEA block lengths (Figure S1, Supporting Information). The calculated number average arm numbers of the star polymers are consistently lower than the number of initiating sites. This

can be attributed to steric hindrance caused by the bulky nature of the monomer and the relative small size of the initiator. The determined initiation efficiencies for the (PDMA-*b*-PDEA)$_x$ diblock copolymer stars range from 67% to 75%, which is consistent with previous work.[29,30]

Table 4.1. Molecular characteristics of the linear and star-shaped diblock copolymers and their gelation behavior

block polymer[a, b]	M_n [10^3 g/mol][b]	PDI[c]	DEA_{arm} [d]	gelation behavior
$DMA_{143}DEA_{40}$	29.9	1.19	0.22	---
$(DMA_{150}DEA_{12})_4$	104	1.11	0.07	no gelation
$(DMA_{110}DEA_{43})_4$	102	1.16	0.28	free-standing gels
$(DMA_{130}DEA_{16})_6$	142	1.27	0.11	free-standing gels

[a] $(DMA_nDEA_m)_x$: n and m denote the number average degree of polymerization of the blocks, and x is the number average arm number. [b] Calculated by comparing the molecular weight of the arms obtained by arm cleavage with the theoretical molecular weight from conversion data. [c] Determined by DMAc-SEC applying a calibration with linear PMMA standards. [d] Molar fraction of DEA units per arm.

Aggregation in dilute solution. The pH- and temperature-dependent solution behavior of the star block copolymers was investigated by turbidimetry and dynamic light scattering (DLS). Prior investigations (Figure S4.2, Supporting Information p.71) showed that at any given pH value the cloud point of PDEA homopolymer stars is 30 – 40 K lower than that of PDMA stars.[29] This indicates that the region between pH 7 and pH 8 is interesting because the cloud points of both stars are in an accessible temperature range, *e.g.*, 40 °C for PDEA and 80 °C for PDMA at pH 7, and 20 °C for PDEA and 50 °C for PDMA at pH 8, respectively. Consequently, upon increasing the temperature the PDEA outer blocks of the (PDMA-*b*-PDEA)$_x$ diblock copolymer stars are expected to collapse first and thus induce aggregation.

Figure 4.3 shows the cloud points (T_{cl}) of the diblock copolymer stars at different pH values. In analogy to the PDMA and PDEA homopolymer stars[29,30] (Figure S4.2, Supporting Information p.71) the cloud point decreases with increasing pH, with cloud points ranging

from 80 °C at pH 7 to 30 °C at pH 10, respectively. No significant influence of arm number, arm length and DEA content on the cloud point can be detected. Furthermore, irrespective of the lower cloud point expected for PDEA with respect to that of PDMA at a given pH value (Figure S4.2, Supporting Information p.71), the observed values are very close to that of PDMA homopolymer stars. This observation can be explained by the fact that the turbidity sensor used cannot detect the formation of small micellar aggregates with sizes well below the wavelength of visible light, as this does not give rise to an increased turbidity of the solution. Because of the low concentration of the solutions and the low average degree of polymerization of the PDEA outer blocks with respect to that of the PDMA inner blocks, aggregation to small micellar aggregates, *i.e.*, flower-like micelles, is favored over intermolecular aggregation and corresponding bridging between micelles that would give rise to larger structures and, hence, an increase in turbidity (Scheme 4.1). As a result, a significant increase in turbidity is observed only under conditions where the PDMA blocks also become insoluble and thus the diblock copolymer stars collapse completely and form large aggregates.

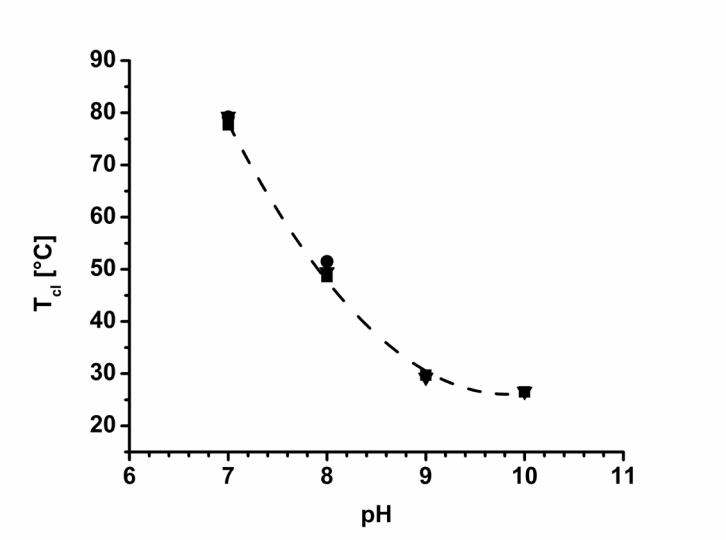

Figure 4.3. pH-dependent cloud points of the synthesized star block copolymers at *c* = 1 g/L (■) $(DMA_{150}DEA_{12})_4$, (●) $(DMA_{110}DEA_{43})_4$ and (▼) $(DMA_{130}DEA_{16})_6$.

A closer insight into the aggregation behavior of the $(PDMA\text{-}b\text{-}PDEA)_x$ diblock copolymer stars in dilute solution can be derived from dynamic light scattering (DLS) experiments (Fig-

ure 4.4). The depicted graphs show the results for the $(DMA_{130})_6$ homopolymer star at pH = 7 and 8 (Figures 4.4a,b) as well as for the star block copolymers $(DMA_{130}DEA_{16})_6$ and $(DMA_{110}DEA_{43})_4$ at pH = 7 (Figures 4.4c,d).

First, the results for the PDMA homopolymer star are discussed. At pH = 7 the apparent hydrodynamic radius, $R_{h,app}$, of the PDMA star decreases slightly with temperature (Figure 4.4a). This corresponds to the expected contraction of the star at temperatures well below its cloud point (T_{cl} = 80 °C at pH = 7). The collapse of the star above its cloud point cannot be detected with the used equipment as it is outside of the accessible temperature range. However, at pH = 8 this transition is shifted to lower temperatures ($T_{cl} \approx 50$ °C) and thus inside the measurement range. The temperature-induced collapse and subsequent aggregation of the PDMA star is clearly demonstrated by the sharp increase in $R_{h,app}$ between 40 °C and 50 °C which is accompanied by a significant narrowing of the size distribution (Figure 4.4b). A similar behavior was reported for hydrophobically modified PNIPAAm and PEG-grafted PNIPAAm, too.[37] It is noted, that the pH = 8 sample becomes turbid under these conditions, which dramatically increases the probability of multiple scattering. Thus, the obtained hydrodynamic radii and polydispersity indices are apparent values as the DLS theory relies on single scattering.

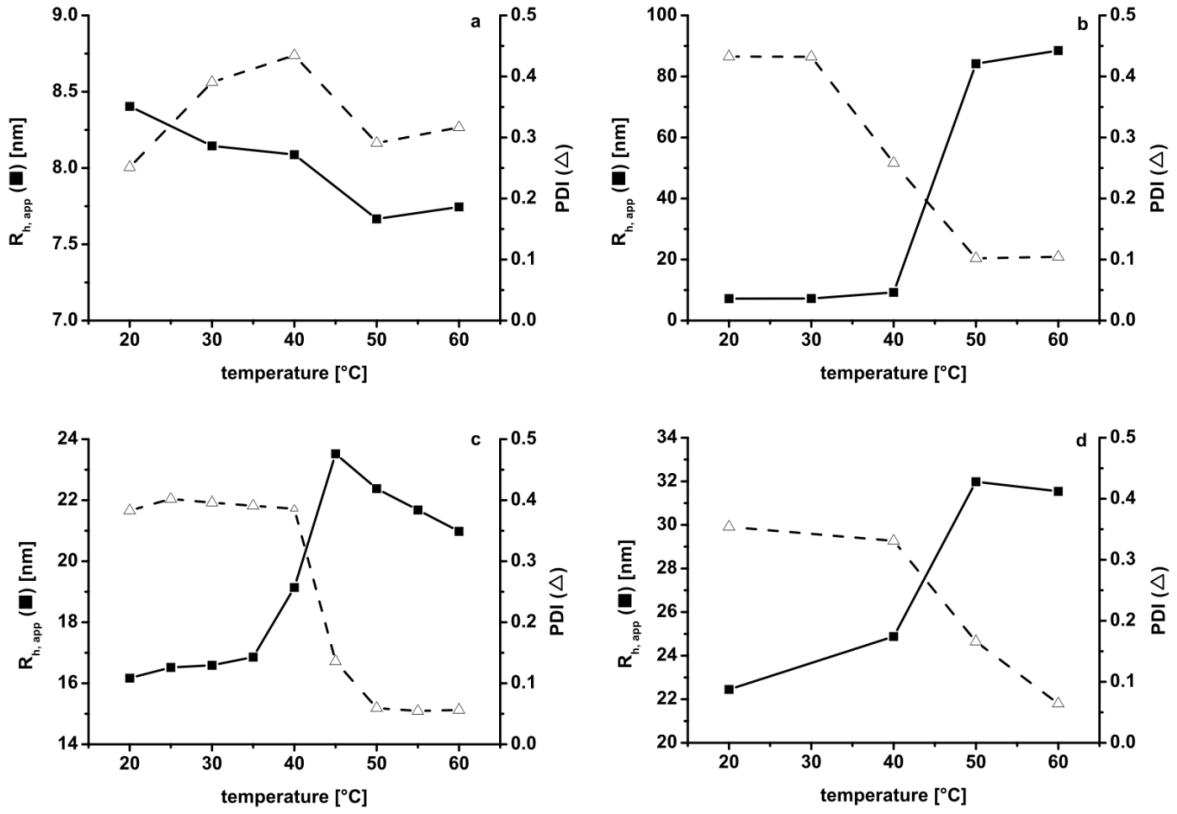

Figure 4.4. Temperature-dependent apparent hydrodynamic radii and polydispersity indices derived from cumulant analysis for a) $(DMA_{130})_6$ at pH = 7, b) $(DMA_{130})_6$ at pH = 8, c) $(DMA_{110}DEA_{43})_4$ at pH = 7 and d) $(DMA_{130}DEA_{16})_6$ at pH = 7 (all measurements were performed at c = 1 g/L and θ = 90°). The lines are guides to the eye.

We now turn to the temperature-dependent aggregation behavior of the (PDMA-*b*-PDEA)$_x$ diblock copolymer stars at pH = 7, *i.e.*, under conditions where the inner PDMA blocks are soluble over the entire investigated temperature range (Figures 4c,d). It is noted that the size of the unimolecularly dissolved $(DMA_{130}DEA_{16})_6$ stars is larger with respect to that of the $(DMA_{110}DEA_{43})_4$ stars at pH = 7 and low temperatures, irrespective of the comparable overall degree of polymerization of the arms in both stars. This is attributed to the higher block length of the PDMA inner block as well as the higher arm number in $(DMA_{130}DEA_{16})_6$. As the pK_a of star-shaped PDMA (pK_a = 6.2)[32] is about 1 unit lower compared to that of PDEA ($pK_a \approx 7 - 7.5$)[29] the PDMA block exhibits a higher degree of protonation at pH = 7, which results in a larger Rh,app value for the star with the longer PDMA inner block. In addition,

the higher arm number is supposed to increase the this effect as electrostatic repulsion between positively charged PDMA units and osmotic pressure of the counter ions increase with the number.[38,39] Both diblock copolymer stars show a roughly 50% increase in $R_{h,app}$ at about 40 °C to 45 °C, which corresponds well to the cloud point of the PDEA outer blocks at pH = 7 (T_{cl} = 40 °C, Figure S4.2, Supporting Information p.71). In addition, the polydispersity index, PDI, decreases substantially at the same time as $R_{h,app}$ increases. Consequently, the observed increase in $R_{h,app}$ can be attributed to the formation of small flower-like aggregates consisting of only a few stars, as depicted in Scheme 4.1. This is consistent with the observations for other diblock copolymer stars reported in literature.[24,40] At temperatures above 50 °C the size of the formed flower-like micelles decreases slightly indicating a further contraction of the inner PDMA block, which is most pronounced for $(DMA_{110}DEA_{43})_4$. This behavior corresponds well to that observed for the PDMA homopolymer star at pH = 7 (Figure 4.4a) and indicates that the block copolymer stars are actually double-responsive, *i.e.*, the inner block is still responsive even after the collapse of the outer block has been triggered.

Angle-dependent DLS measurements provide further evidence for the formation of flower-like micelles upon switching the PDEA outer blocks insoluble. Figure 5 displays the decay rate, Γ, in dependence on the squared scattering vector, q^2, for $(DMA_{130}DEA_{16})_6$ at 60 °C and pH = 7, *i.e.*, the PDEA blocks are expected to be completely collapsed while the inner PDMA blocks are still soluble and at least partly stretched. The observed linear dependence points to a purely translational diffusion of the formed flower-like aggregates and may be taken as a further indication for the assumed spherical shape of the aggregates.[41,42]

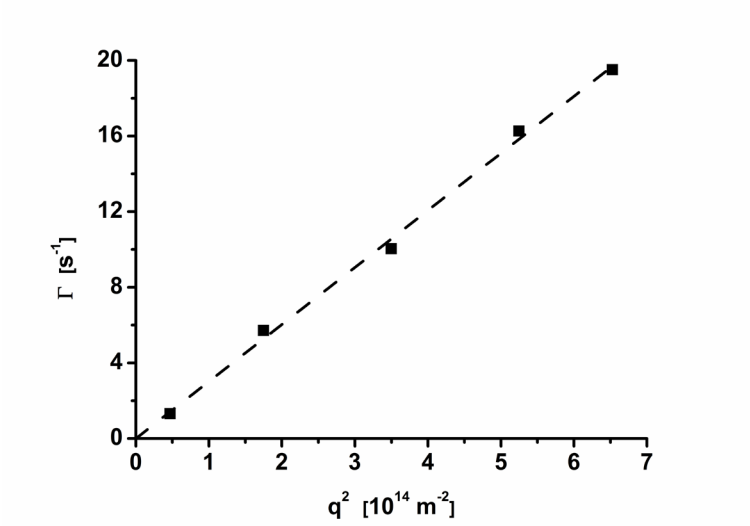

Figure 5. Decay rate vs. squared scattering vector for $(DMA_{130}DEA_{16})_6$ at pH = 7 and 60 °C.

Turbidimetry and DLS measurements on dilute solutions of (PDMA-*b*-PDEA)$_x$ stars have proven that the collapse of the PDEA outer blocks can be triggered independently from the PDMA blocks. This results in the formation of small, flower-like aggregates at low concentrations. Consequently, hydrogel formation via open association is expected at higher concentrations when the PDEA blocks are switched insoluble (Scheme 4.1). Tube-inversion experiments and rheology measurements were carried out to study the gelation behavior of the diblock copolymer stars. To this end, aqueous solutions with concentrations ranging from 10 to 20 wt% were prepared at pH values of 7 and 8. All samples were subjected to tube-inversion experiments and two were further investigated by rheology.

Aggregation in concentrated solution. Tube-inversion experiments (Figure S4.3, Supporting Information p.71) revealed that at pH = 8 and 40 °C, *i.e.*, at temperatures well above the cloud point of the PDEA outer blocks (T_{cl} = 20 °C), $(DMA_{110}DEA_{43})_4$ shows gelation already at 10 wt%, whereas for $(DMA_{130}DEA_{16})_6$ a higher concentration of about 15 wt% is necessary. In contrast, $(DMA_{150}DEA_{12})_4$ shows no gelation within the investigated concentration and temperature range. This suggests that irrespective of the arm number a minimum PDEA block length or molar ratio of DEA repeating units is necessary to form a hydrogel (Table 4.1). Moreover, increasing the DEA molar fraction while keeping the DMA block length constant, like for $(DMA_{130}DEA_{16})_6$ and $(DMA_{110}DEA_{43})_4$, results in a shift of the critical gelation

concentration to lower values. At pH = 7 the sol-gel transition of a 20 wt% solution of $(DMA_{130}DEA_{16})_6$ is shifted to higher temperatures (ca. 50 °C) as compared to pH = 8, which is reasonable as the cloud point of PDEA is shifted to higher temperatures (T_{cl} = 40 °C), too. When samples were prepared at pH > 8 the solutions gelled around or even below room temperature.

To deduce more detailed information on the gelation behavior of concentrated $(DMA_{130}DEA_{16})_6$ and $(DMA_{110}DEA_{43})_4$ solutions, the samples were subjected to oscillatory shear using a cone-plate shear cell geometry (Figure 4.6). Regimes, where the storage modulus, G', exceeds the loss modulus, G'', are defined as the gel state with respect to common definitions, and $G' > 1$ kPa is taken as a characteristic value for strong, free-standing gels.[43-45] Sol states, on the other hand, are characterized by $G'' > G'$. We mainly focused on solutions at pH = 8, as the cloud points of both PDMA and PDEA lie within the accessible temperature range and thus allow us to probe not only the sol-gel transition but also the influence of the responsive PDMA inner block on the mechanical properties of the hydrogels.

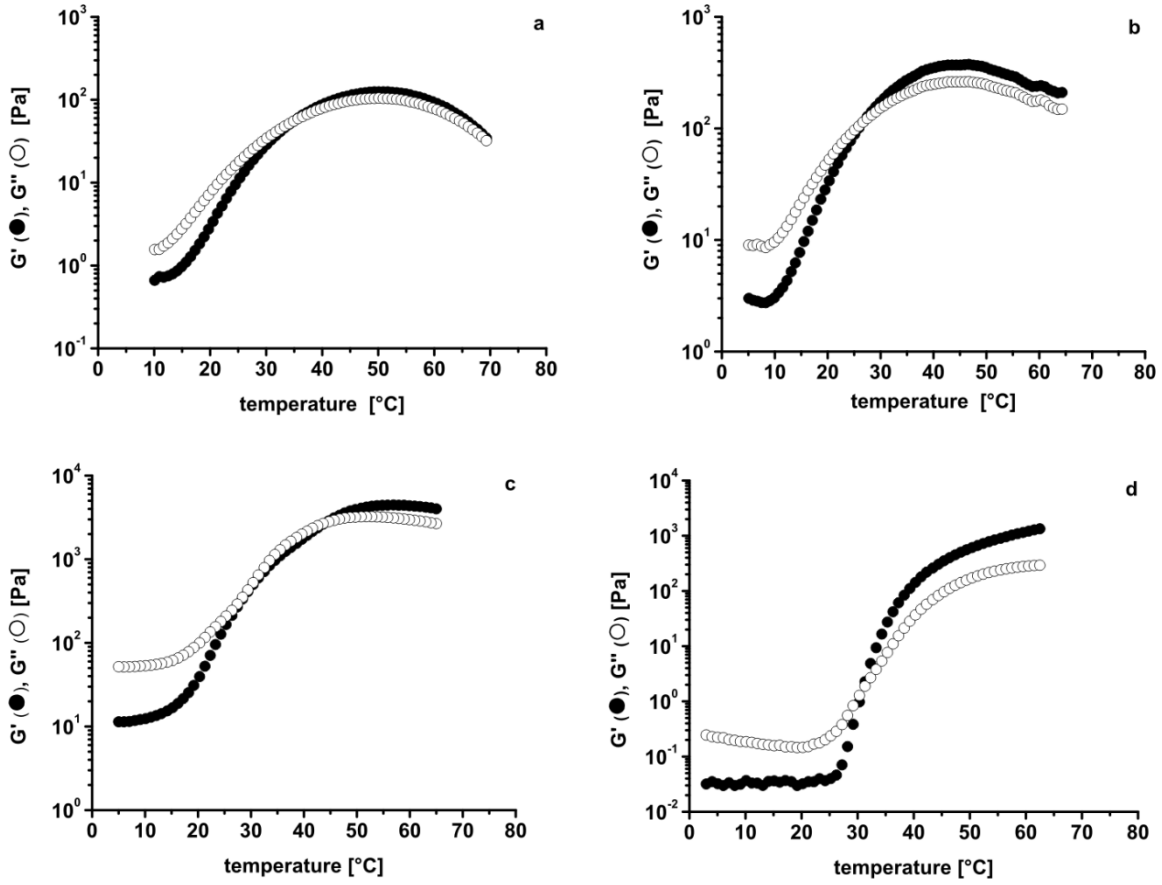

Figure 4.6. Temperature-dependent storage (*G'*) and loss (*G''*) moduli of a) a 15 wt% solution of $(DMA_{130}DEA_{16})_6$ at pH 8, b) a 20 wt% solution of $(DMA_{130}DEA_{16})_6$ at pH 8, c) a 20 wt% solution of $(DMA_{130}DEA_{16})_6$ at pH 7 and d) a 10 wt% solution of $(DMA_{110}DEA_{43})_4$ at pH 8.

Figure 4.6a shows the temperature-dependent storage and loss modulus of a 15 wt% solution of $(DMA_{130}DEA_{16})_6$ at pH = 8, *i.e.*, the lowest concentration for which gelation was observed in the tube-inversion experiments. At temperatures well below 20 °C the loss modulus exceeds the storage modulus which is consistent with the solution being in the sol state. This is the expected behavior, as at pH = 8 the cloud points of both PDMA and PDEA are higher or equal to 20 °C, respectively (Figure S4.2, Supporting Information p.71). Upon heating, both moduli increase with temperature until at 35 °C a cross-over of the *G'* and *G''* traces is observed, which is linked to the sol-gel transition. However, the maximum *G'* value in the gel state ($T > 35$ °C) is only about 100 Pa, showing that at 15 wt% relatively soft gels are formed. At 20 wt% and pH = 8, the sol-gel transition is shifted to lower temperatures

(T_{sg} = 27 °C) and the gel strength is slightly increased, with maximum G' values of about 400 Pa (Figure 4.6b). The formation of a stronger gel is attributed to the higher concentration of the solution, which in turn results in an increased number of physical crosslinking points. For both solutions the sol-gel transition temperatures are significantly higher than the cloud point of the PDEA outer blocks at pH = 8 (T_{cl} = 20 °C). This can be explained by the influence of the polar PDMA inner blocks which cause a shift of the PDEA cloud point to higher temperatures, a common phenomenon that has been observed in previous studies, too.[18,46] The detected decrease of T_{sg} with concentration might be linked to the concentration dependence of the PDEA cloud point, *i.e.*, the cloud point decreases with concentration as we move along the binodal which has its minimum in the LCST.

Figure 4.6c shows a 20 wt% solution of $(DMA_{130}DEA_{16})_6$ at pH = 7. Here, the cross-over of the G' and G'' traces occurs at 44 °C and a strong free-standing gel with G' ≈ 4 kPa is formed. In consistency with the increased cloud point of the PDEA blocks at pH = 7 (T_{cl} = 40 °C), the sol-gel transition is shifted to higher temperatures as compared to that of the sample at pH = 8 (Figure 4.6b). This result is in agreement with the tube-inversion experiments. The significantly increased gel strength of the sample at pH = 7 with respect to that at pH = 8 at identical concentration is attributed to the higher charge density of the inner PDMA blocks at pH = 7 (pK_a(PDMA) ≈ 6.2).[31,32] This, in turn, results in an enhanced stretching of the PDMA chains due to electrostatic repulsion and the osmotic pressure of the bound counter ions,[38,39] and thus in an increased effective volume fraction of the $(DMA_{130}DEA_{16})_6$ diblock copolymer stars. Both measurements on concentrated $(DMA_{130}DEA_{16})_6$ solutions at pH = 8 reveal, that the storage modulus in the gel state first increases until about 50 °C and then decreases again at higher temperatures (Figures 4.6a,b). We attribute this to the inner PDMA blocks, which start to collapse at temperatures above their respective cloud point of T_{cl} ≈ 50 °C at pH = 8, (Figure S4.2, Supporting Information p.71), resulting in a weakening of the gels due to partial syneresis. In contrast, no significant decrease of the modulus was observed in the measurement at pH = 7 (Figure 4.6c), where the cloud point of the PDMA blocks is around 80 °C and thus significantly higher than the applied measurement range. This supports our assumption drawn from the DLS data about the double responsive nature of the (PDMA-*b*-PDEA)$_x$ diblock copolymer stars and, hence, of the corresponding hydrogels. Consequently, gelation can be triggered by selectively switching the PDEA outer blocks in-

soluble, whereas the mechanical properties of the hydrogels might be further tuned utilizing the responsive nature of the PDMA inner blocks.

Figure 4.6d depicts the dynamic moduli of a 10 wt% solution of $(DMA_{110}DEA_{43})_4$ at pH = 8 in dependence of temperature. This sample exhibits a sol-gel transition temperature at T_{sg} = 31 °C and the storage modulus in the gel phase exceeds the limit of 1 kPa for strong free-standing gels at sufficiently high temperatures (T > 55 °C). Again, the sol-gel transition temperature is higher than the cloud point of the PDEA outer blocks (T_{cl} = 20 °C). However, it is still significantly lower than the sol-gel transition observed for the 15 wt% solution of $(DMA_{130}DEA_{16})_6$ (T_{sg} = 35 °C), irrespective of the lower concentration. This is attributed to the fact that the block length of the PDEA outer blocks for $(DMA_{110}DEA_{43})_4$ is higher by a factor of about 3 with respect to $(DMA_{130}DEA_{16})_6$, while the PDMA block length is almost identical. Thus, the molar DEA fraction (Table 4.1) is considerably higher, which presumably reduces the influence of the polar PDMA block on the cloud point of PDEA. Moreover, G' exhibits only a weak dependence on frequency in the gel state at 60 °C and exceeds G'' over the whole investigated frequency range (10^{-2} – 10^{2} Hz) with values >1 kPa, showing the existence of a strong free-standing gel over a broad frequency range (Figure S4.4, Supporting Information p.72). In addition, the hydrogel formed by $(DMA_{110}DEA_{43})_4$ (Figure 4.6d) is significantly stronger than those based on $(DMA_{130}DEA_{16})_6$ (Figures 4.6a,b) at identical pH, despite the lower concentration used for $(DMA_{110}DEA_{43})_4$. This might be attributed to the increased PDEA block length, as a similar dependence on the block length of the responsive block was observed for hydrogels based on triblock terpolymer micelles with a thermo-responsive corona, too.[18,19]

4.4. Conclusion

Both blocks of the star-shaped block copolymers $(DMA\text{-}DEA)_x$ are responsive to pH and temperature, as manifested by a strong pH dependence of the respective cloud points. The collapse of the PDEA outer blocks can be selectively triggered first upon heating. This is due to the significantly lower cloud point of PDEA with respect to that of PDMA at identical pH. Turbidimetry and angle-dependent DLS data point to the formation of flower-like micelles with a collapsed PDEA core and a soluble PDMA corona at temperatures above the cloud

point of PDEA but still below that of PDMA at a given pH. Contraction of the flower-like micelles at temperatures above the cloud point of the PDMA blocks indicates the double responsive nature of the diblock copolymer stars, *i.e.*, both blocks can be addressed separately.

At sufficiently high concentrations, on the other hand, hydrogel formation was observed by tube-inversion and rheology under conditions where only the PDEA outer blocks are insoluble. The ability to form a gel and the critical gelation concentration are mainly influenced by the molar fraction of the DEA units irrespective of the arm number. Consequently, a minimum DEA fraction is necessary for gel formation and the critical gelation concentration decreases with the DEA content. Moreover, the gel strength increases with the DEA content. The second factor controlling the gelation behavior of the diblock copolymer stars is the pH value. The sol-gel transition temperature at a given concentration is shifted to lower values upon increasing the pH value from 7 to 8, which is caused by a corresponding decrease of the PDEA cloud point. In addition, the gel strength increases with decreasing pH value due to an increased charge density and thus enhanced stretching of the PDMA inner blocks. A decrease in the storage modulus with temperature was observed for soft gels, which is attributed to a partial collapse of the PDMA blocks above their respective cloud point. Thus, utilizing diblock copolymer stars with two responsive blocks allows not only to trigger the gel formation by applying an external stimulus, but also to tune the mechanical properties of the hydrogels.

Acknowledgements

The German Science Foundation is acknowledged for financial support within the priority program SPP 1259. We thank Ingo Rehberg and Reinhard Richter (Experimental Physics V, University of Bayreuth) for providing us with access to their rheological equipment and Marietta Böhm (Macromolecular Chemistry II, University of Bayreuth) for performing the SEC measurements. We also thank Werner Köhler (Experimental Physics IV, University of Bayreuth) for very helpful discussions on DLS.

4.5. References

(1) Ahn, S.-K.; Kasi, R. M.; Kim, S.-C.; Sharma, N.; Zhou, Y. *Soft Matter* **2008**, *4*, 1151-1157.
(2) Tsitsilianis, C. *Soft Matter* **2010**, *6*, 2372-2388.
(3) Liu, R.; Fraylich, M.; Saunders, B. *Colloid. Polym. Sci.* **2009**, *287*, 627-643.
(4) Dai, S.; Ravi, P.; Tam, K. C. *Soft Matter* **2008**, *4*, 435-449.
(5) Hatefi, A.; Amsden, B. *J. Controlled Release* **2002**, *80*, 9-28.
(6) Yu, L.; Ding, J. *Chem. Soc. Rev.* **2008**, *37*, 1473-1481.
(7) Schmaljohann, D. *Adv. Drug Delivery Rev.* **2006**, *58*, 1655-1670.
(8) Vogt, A. P.; Sumerlin, B. S. *Soft Matter* **2009**, *5*, 2347-2351.
(9) Huh, K. M.; Bae, Y. H. *Polymer* **1999**, *40*, 6147-6155.
(10) Metters, A. T.; Anseth, K. S.; Bowman, C. N. *Polymer* **2000**, *41*, 3993-4004.
(11) Dong, L.; Jiang, H. *Soft Matter* **2007**, *3*, 1223-1230.
(12) Hawkins, A.; Satarkar, N.; Hilt, J. *Pharm. Res.* **2009**, *26*, 667-673.
(13) Park, T. G.; Hoffman, A. S. *J. Polym. Sci., Part A: Polym. Chem.* **1992**, *30*, 505-507.
(14) Zhang, X.-Z.; Zhuo, R.-X. *Eur. Polym. J.* **2000**, *36*, 643-645.
(15) Kuckling, D.; Vo, C. D.; Adler, H. J. P.; Völkel, A.; Cölfen, H. *Macromolecules* **2006**, *39*, 1585-1591.
(16) Bae, S. J.; Joo, M. K.; Jeong, Y.; Kim, S. W.; Lee, W. K.; Sohn, Y. S.; Jeong, B. *Macromolecules* **2006**, *39*, 4873-4879.
(17) Madsen, J.; Armes, S. P.; Bertal, K.; Lomas, H.; MacNeil, S.; Lewis, A. L. *Biomacromolecules* **2008**, *9*, 2265-2275.
(18) Reinicke, S.; Schmelz, J.; Lapp, A.; Karg, M.; Hellweg, T.; Schmalz, H. *Soft Matter* **2009**, *5*, 2648-2657.
(19) Sugihara, S.; Kanaoka, S.; Aoshima, S. *J. Polym. Sci., Part A: Polym. Chem.* **2004**, *42*, 2601-2611.
(20) Hietala, S.; Mononen, P.; Strandman, S.; Järvi, P.; Torkkeli, M.; Jankova, K.; Hvilsted, S.; Tenhu, H. *Polymer* **2007**, *48*, 4087-4096.
(21) Lin, H. H.; Cheng, Y. L. *Macromolecules* **2001**, *34*, 3710-3715.
(22) Fechler, N.; Badi, N.; Schade, K.; Pfeifer, S.; Lutz, J.-F. *Macromolecules* **2008**, *42*, 33-36.
(23) Buwalda, S. J.; Dijkstra, P. J.; Calucci, L.; Forte, C.; Feijen, J. *Biomacromolecules* **2009**, *11*, 224-232.
(24) Stepánek, M.; Uchman, M.; Procházka, K. *Polymer* **2009**, *50*, 3638-3644.
(25) Lu, C.; Liu, L.; Guo, S.-R.; Zhang, Y.; Li, Z.; Gu, J. *Eur. Polym. J.* **2007**, *43*, 1857-1865.
(26) Kyriazis, A.; Aubry, T.; Burchard, W.; Tsitsilianis, C. *Polymer* **2009**, *50*, 3204-3210.
(27) Iddon, P. D.; Armes, S. P. *Eur. Polym. J.* **2007**, *43*, 1234-1244.
(28) Li, Y.; Tang, Y.; Narain, R.; Lewis, A. L.; Armes, S. P. *Langmuir* **2005**, *21*, 9946-9954.
(29) Schmalz, A.; Hanisch, M.; Schmalz, H.; Müller, A. H. E. *Polymer* **2010**, *51*, 1213-1217.
(30) Plamper, F. A.; Schmalz, A.; Penott-Chang, E.; Drechsler, M.; Jusufi, A.; Ballauff, M.; Müller, A. H. E. *Macromolecules* **2007**, *40*, 5689-5697.
(31) Plamper, F. A.; Schmalz, A.; Ballauff, M.; Müller, A. H. E. *J. Am. Chem. Soc.* **2007**, *129*, 14538-14539.
(32) Plamper, F. A.; Ruppel, M.; Schmalz, A.; Borisov, O.; Ballauff, M.; Müller, A. H. E. *Macromolecules* **2007**, *40*, 8361-8366.
(33) Taktak, F. F.; Bütün, V. *Polymer* **2010**, *51*, 3618-3626.
(34) Plamper, F. A.; Becker, H.; Lanzendörfer, M.; Patel, M.; Wittemann, A.; Ballauff, M.; Müller, A. H. E. *Macromol. Chem. Phys.* **2005**, *206*, 1813-1825.
(35) Matyjaszewski, K.; Shipp, D. A.; Wang, J.-L.; Grimaud, T.; Patten, T. E. *Macromolecules* **1998**, *31*, 6836-6840.

(36) Zeng, F.; Shen, Y.; Zhu, S. *Macromol. Rapid Commun.* **2002**, *23*, 1113-1117.
(37) Kujawa, P.; Tanaka, F.; Winnik, F. M. *Macromolecules* **2006**, *39*, 3048-3055.
(38) Jusufi, A.; Likos, C.; Ballauff, M. *Colloid. Polym. Sci.* **2004**, *282*, 910-917.
(39) Das, B.; Guo, X.; Ballauff, M. *Progr. Colloid. Polym. Sci.* **2002**, *121*, 34-38.
(40) Zhou, C.; Hillmyer, M. A.; Lodge, T. P. *Macromolecules* **2011**, *44*, 1635-1641.
(41) Stepánek, P. *J. Chem. Phys.* **1993**, *99*, 6384-6393.
(42) Holthoff, H.; Egelhaaf, S. U.; Borkovec, M.; Schurtenberger, P.; Sticher, H. *Langmuir* **1996**, *12*, 5541-5549.
(43) Chambon, F.; Winter, H. H. *Polym Bull* **1985**, *13*, 499-503.
(44) Nishinari, K. *Prog. Colloid Polym. Sci.* **2009**, *136*, 87-94.
(45) Mours, M.; Winter, H. H. *Adv. Polym. Sci.* **1997**, *134*, 165-234.
(46) Schilli, C. M.; Zhang, M.; Rizzardo, E.; Thang, S. H.; Chong, Y. K.; Edwards, K.; Karlsson, G.; Müller, A. H. E. *Macromolecules* **2004**, *37*, 7861-7866.

4.6. Supporting Information

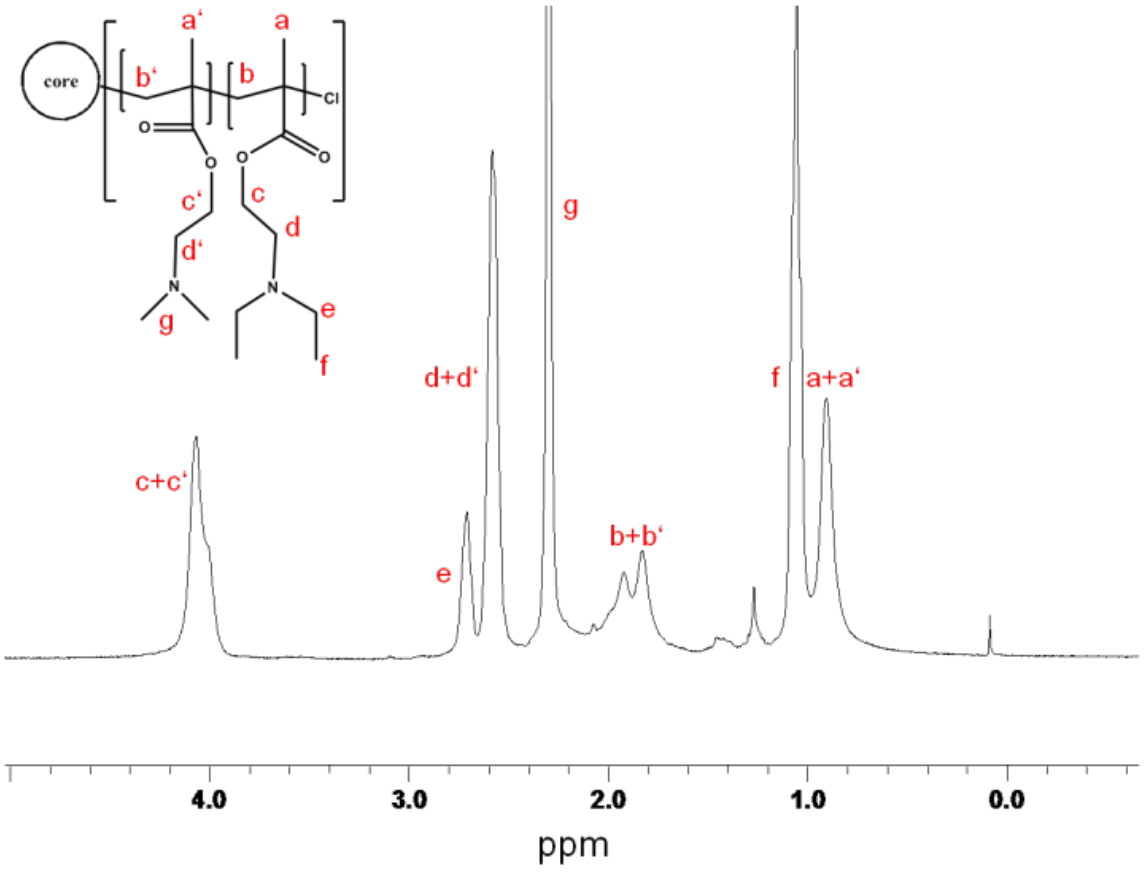

Figure S1. ^{1}H NMR spectrum of $(DMA_{110}DEA_{43})_4$ in $CDCl_3$.

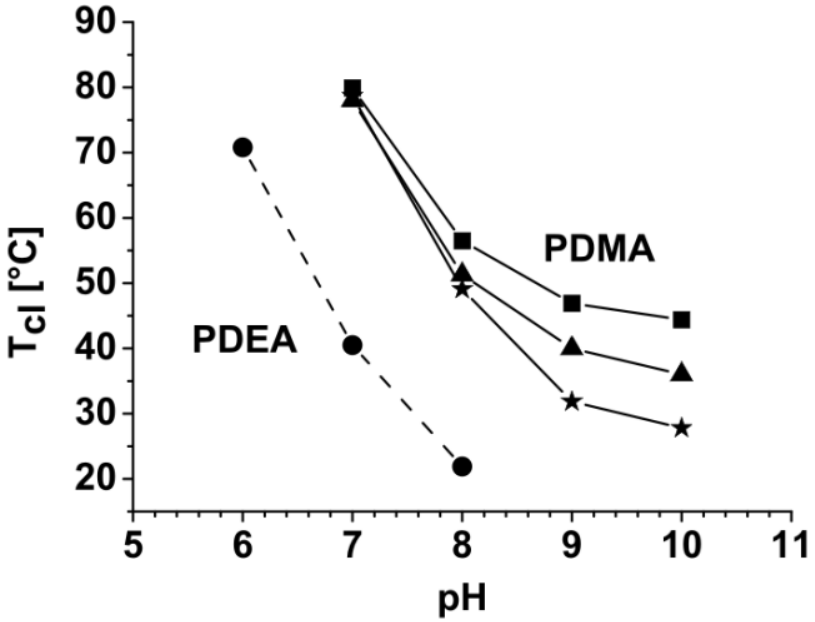

Figure S2. pH-dependent cloud points (T_{cl}) for (●) $(DEA_n)_x$ stars (cloud point is independent of M_n and arm number), (■) $(DMA)_{108}$, (▲) $(DMA_{100})_{3.1}$, and (★) $(DMA_{170})_{18}$.[1,2]

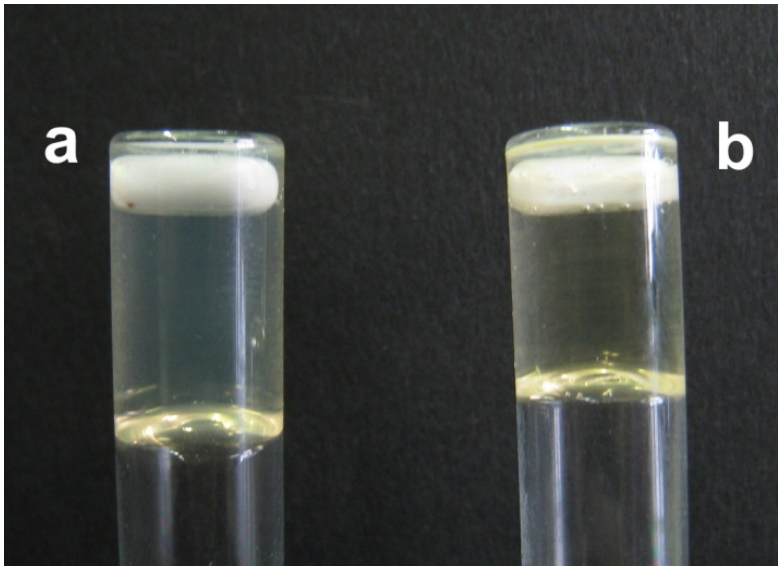

Figure S3. Tube-inversion experiments at pH 8 and 40 °C for a) a 20 wt% solution of $(DMA_{130}DEA_{16})_6$ and b) a 10 wt% solution of $(DMA_{110}DEA_{43})_4$.

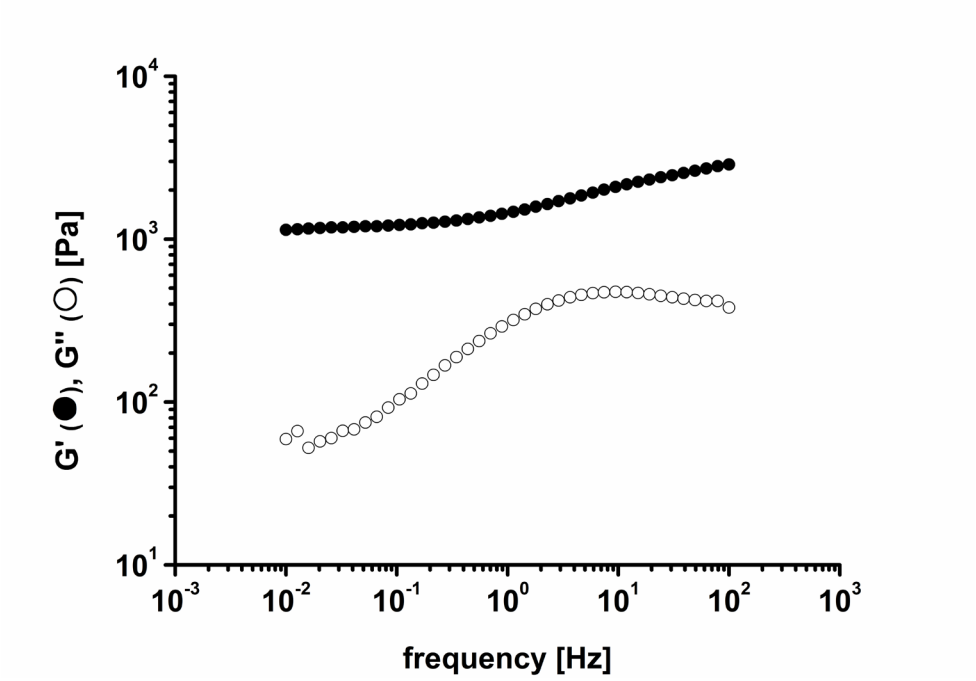

Figure S4. Frequency-dependent storage (*G*') and loss (*G*'') modulus of a 10 wt% solution of $(DMA_{110}DEA_{43})_4$ at pH = 8 in the gel state at 60°C.

References

(1) Schmalz, A.; Hanisch, M.; Schmalz, H.; Müller, A. H. E. *Polymer* **2010**, *51*, 1213-1217.
(2) Plamper, F. A.; Ruppel, M.; Schmalz, A.; Borisov, O.; Ballauff, M.; Müller, A. H. E. *Macromolecules* **2007**, *40*, 8361-8366.

5 Smart Hydrogels Based on Responsive Star-Block Copolymers

Alexander Schmalz, Holger Schmalz*, Axel H. E. Müller*

Makromolekulare Chemie II, Universität Bayreuth, D-95440 Bayreuth

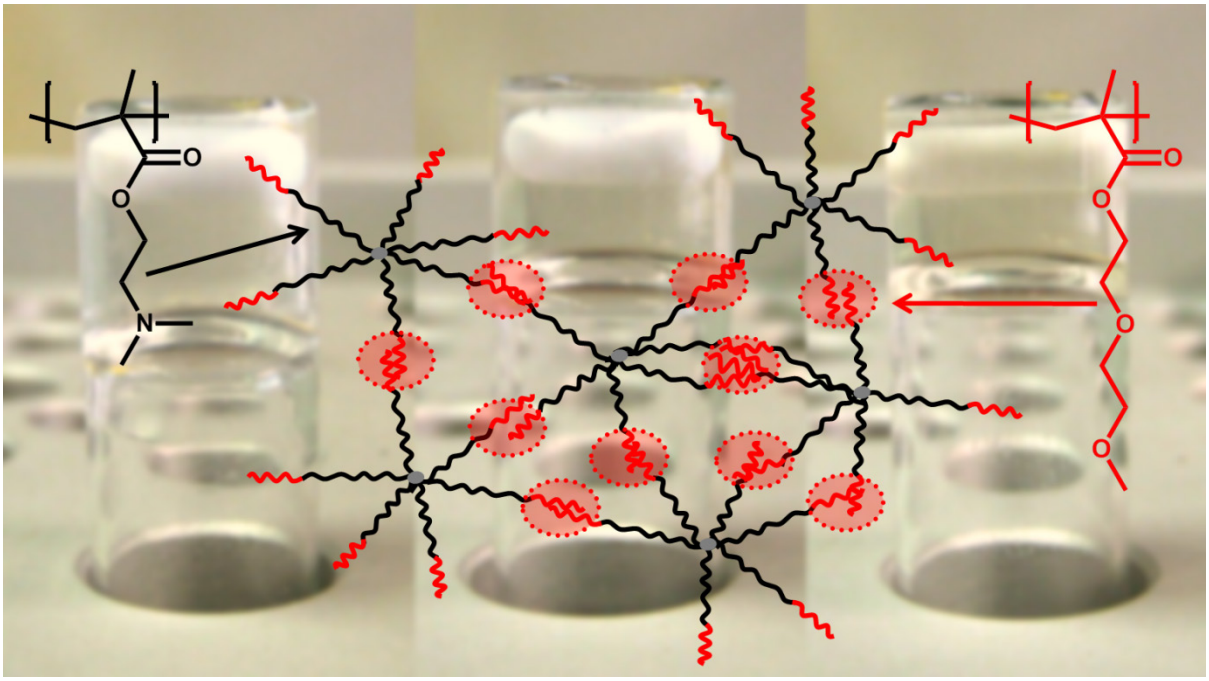

Abstract

A series of smart hydrogels based on dual responsive star block copolymers responding to pH and temperature were prepared via atom transfer radical polymerization (ATRP) employing the core-first method. They consist of poly(2-(dimethylamino)ethyl methacrylate) (PDMA) inner blocks and outer blocks comprised of poly(diethylene glycol methyl ether methacrylate) (PDEGMA). The aggregation behavior of these block copolymer stars is analyzed depending on block length and arm number. The dual responsiveness of the stars is demonstrated by turbimetry as well as dynamic light scattering in dilute aqueous solution, and the gelation behavior of concentrated aqueous solutions is studied by rheology. Above the transition temperature of the PDEGMA outer blocks the stars form flower-like aggregates in dilute solution or free-standing gels at higher concentrations. When the temperature is increased further above the transition temperature of the PDMA inner block, the aggregates start to contract and a weakening of the gels was observed for soft gels, whereas for strong gels no influence on the moduli was detected. The behavior is controlled by both concentration and pH value. In addition, we show that the minimum polymer concentration for gel formation can be lowered by quaternizing the inner block of the stars, but a second response to stimuli is lost during the procedure.

5.1. Introduction

Hydrogels are three-dimensional hydrophilic networks that can bind a large amount of water or biological fluid.[1,2] Stimuli responsive hydrogels, *i.e.*hydrogels responding with a large property change on small variations in their physical and/or chemical environment, have gathered much interest for their use as biomaterials, with applications such as controlled drug release, cell carriers and tissue engineering.[1-5] In general, hydrogels can be classified into two categories depending on their cross-linking method: chemical or physical. The network is usually built of water-soluble macromolecular chains connected either through permanent covalent bonds (chemical cross-linking) or through temporary junction points (physical cross-linking). Chemically crosslinked gels can consist of water-soluble polymers or of polymers that respond to external stimuli such as temperature or pH. Hydrogels based on

crosslinked poly(*N*-isopropylacrylamide) (PNiPAAm) have been studied extensively because its lower critical solution temperature (LCST) is around 32°C in water, making it a promising candidate for biomedical applications.[6-10] Physical gels typically consist of block copolymers where the stimuli responsive blocks are used to form the temporary crosslinking points, *i.e.* switching it insoluble by increasing its hydrophobic interactions. This can be based on a variety of triggers, such as temperature, pH, light, redox reactions or host-guest interactions.[11,12] One reason that much attention is being paid to physical hydrogels is because of their potential for biomedical applications, *e.g.* injectable hydrogels for drug delivery or tissue engineering.[13] However, in most physical hydrogels the "smart" component is only responsible for the formation/disintegration of the gel, most commonly seen in the form of ABA triblock copolymers where the B block only provides solubility.[14,15] The easiest way to introduce dual responsiveness is to copolymerize thermo-sensitive monomers with monomers that are also sensitive to other triggers. This can be achieved by a random copolymerization with a pH-responsive monomer like acrylic acid[16,17] but advances in synthetic protocols have led to more efforts into block-type structures. Until now only a limited number of double temperature-sensitive ABC triblock terpolymers have been synthesized,[18,19] as well as dual temperature- and pH-sensitive ABA diblock copolymers[20-22] and ABC triblock terpolymers.[23] The same advances in synthesis have also opened the way to a more complete control over the polymer architecture, leading to increased interest in *e.g.* star-shaped polymers. Recent publications indicate that a star-shaped gelator is superior to its linear triblock counterpart, *i.e.* they have a lower critical gelation concentration (cgc).[24,25] However, up until now there have been no reports of double responsive gels based on star polymers except our own efforts in that area.[26]

Our group has shown that linear and star-shaped poly(2-(dimethylamino)ethyl methacrylate) (PDMA) as well as poly(2-(diethylamino)ethyl methacrylate) (PDEA) homopolymers are responsive to both pH and temperature.[27-29] We have recently made a first attempt to create hydrogels from star-shaped block copolymers $(A_nB_m)_x$, in which the A block is PDMA and the B block is comprised of PDEA. However, the gelation behavior turned out to be very complex, due to the double responsive nature of both blocks. Thus, we decided to replace

the outer block of the $(A_nB_m)_x$ star block copolymers with a polymer that is responsive to temperature only.

Recently, more and more attention has been given to a new class of thermo-responsive polymers, the poly(oligo(ethylene glycol) methyl ether methacrylate)s (POEGMAs). By copolymerizing different OEGMAs, *i.e.* methacrylates with different numbers of ethylene glycol units in the side chain, such as diethylene glycol methyl ether methacrylate (DEGMA) and OEGMA with 8.5 ethylene glycol units, the cloud point of the copolymer can be tuned according to the molar ratio of the two monomers between 26 °C for pure PDEGMA and 90 °C for pure POEGMA.[30-32] These polymers have proven to be very versatile and have been applied in sensors[33], polymer-protein conjugates[34], photo crosslinkable polymers[35] and the modification of natural polymers.[36] There have already been efforts to directly create chemically cross-linked gels from PDEGMA[37,38] as well as using PDEGMA and PDMA as stimuli responsive blocks in combination with other monomers. PDMA-PDEGMA-PDMA block copolymers[39] have been reported as well as double-responsive ABC triblock terpolymers where the C block was either P(DEGMA-*co*-OEGMA) or PDMA.[40] There has also been work published on star-shaped gelators with PDMA as the responsive outer block.[41]

In this paper we combine these approaches to create new hydrogels based on star-shaped block copolymers consisting of an outer block of thermo-responsive PDEGMA and an inner block of thermo- and pH-responsive PDMA. We propose that gel formation takes place according to an open association mechanism, with a sequential collapse of the blocks starting from the outside upon an increase in temperature. The collapse of the inner PDMA block is controlled by the pH value of the solution, *i.e.* the gel can change its mechanical properties depending on pH. This mechanism is illustrated in Scheme 5.1. Another possibility to utilize the PDMA block is quaternization to turn the inner block into a permanent cationic polyelectrolyte. This should lead to an increase in hydrophilicity along with a stretching of the inner block, *i.e.* an increased volume fraction of the stars in solution, and eliminate the pH-responsiveness.

Scheme 5.1. Aggregation and network formation of dual responsive star block copolymers in dependence on concentration.

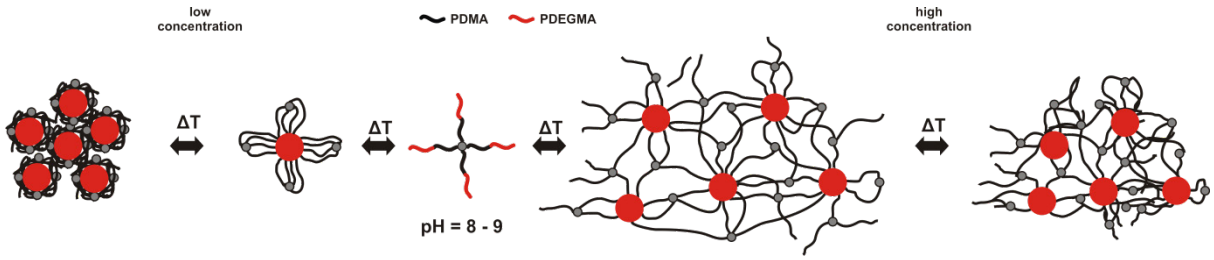

5.2. Experimental

Materials. Ethyl 2-bromoisobutyrate, N,N,N',N'',N''',N'''-hexamethyltriethylenetetramine (HMTETA), copper(I) chloride, 1,3,5-trioxane, iodomethane, and trimethylsilyldiazomethane were purchased from Aldrich and used without further purification. The solvents used were of p.a. quality. The monomers 2-(dimethylamino)ethyl methacrylate (98%, Aldrich) and diethylene glycol methyl ether methacrylate (95%, Aldrich) were destabilized before use by passing through a basic alumina column. The synthesis of the sugar-based initiators with 5 and 8 2-bromoisobutyryl initiation sites, based on glucose and saccharose, respectively, is described in a previous publication.[42] For dialysis, regenerated cellulose membranes (ZelluTrans with MWCO 4000-6000) were used.

Synthesis of star shaped block copolymers. The identical PDMA precursor stars were used as in our previous work, which were synthesized by ATRP with sugar-based initiators.[26]

For the second block the same procedure was applied, except that acetonitrile was used as the solvent instead of anisole. The change of the solvent was necessary to achieve a high blocking efficiency In a typical reaction 2 g of the 4-arm star PDMA macroinitiator (~ 0.084 mmol initiation sites), 4.7 g of the monomer diethylene glycol methyl ether methacrylate (0.025 mol), 16.6 mg Cu(I)Cl (0.168 mmol), 38.7 mg HMTETA (0.168 mmol) and acetonitrile (31.2 g) as solvent were used. The catalyst complex solution was pumped into the reac-

tion vessel, a screw cap vial equipped with a rubber septum, using a double-tipped metal needle with about 0.5 bar of nitrogen pressure to avoid contact with air. The polymerizations were carried out at 50 °C. All reactions for the second block were performed using a fixed ratio between monomer, initiation sites, catalyst and ligand of $[M]_0$:$[I]_0$:[Cat]:[L]=100:1:2:2 at $[M]_0$ ~ 0.063 mol/L.

The arms of the resulting PDMA-*b*-PDEGMA star block copolymers were cleaved off by an alkaline ester hydrolysis at elevated temperatures, using a procedure adapted from Plamper *et.al.*[27] To circumvent the pH independent LCST of the PDEGMA block in water, a method in a non-aqueous solvent was chosen. The cleaving reaction was carried out in a 1M potassium hydroxide solution in methanol (1M KOH in MeOH) at 70 °C. The product of this reaction for both the PDMA and the PDEGMA block is poly(methacrylic acid) (PMAA), as the pendant outer groups get hydrolyzed under the applied conditions. The obtained PMAA was transformed to poly(methyl methacrylate) (PMMA) using trimethylsilyldiazomethane to facilitate molecular characterization. The actual arm number of the precursor PDMA stars was calculated by comparing the theoretical arm length, obtained from conversion, with the experimental M_n of the cleaved arms obtained from MALDI-ToF. The block length of the PDEGMA block was calculated from NMR measurements by comparing the signal of the methoxy group of DEGMA with the signal of the dimethylamino group of DMA. The cleaved-off arms of the block copolymer stars were used to confirm the blocking efficiency as being close to unity.

The quaternization of the PDMA block of the star block copolymers was carried out in a 0.5% w/w solution of acetone. Iodomethane was used as the quaternization agent, with a 1.5 fold excess compared to amino groups. The reaction was stirred overnight at room temperature and the precipitated product was centrifuged off and washed three times with pure acetone.

^{1}H-NMR spectroscopy. All measurements were performed with a Bruker Avance 300 spectrometer using deuterated chloroform or deuterium oxide as solvent.

MALDI-ToF Mass Spectrometry. MALDI-ToF-MS measurements were performed on a Bruker Daltonics Reflex III instrument equipped with an N_2 Laser (337 nm) and an accelera-

tion voltage of 20 kV in positive mode. Sample preparation was done according to the "dried-droplet" method. In detail, matrix (trans-3-indoleacrylic acid, IAA, conc. 2 mg / mL), analyte (conc. 10 mg / mL) were separately dissolved in THF, subsequently mixed in a ratio of 20 : 5 µL. 1.5 µL of the final mixture was applied to the target spot and left to dry under air.

Size Exclusion Chromatography (SEC). The apparent molecular weight distributions of the star shaped homo- and copolymers were determined by SEC using dimethylacetamide (DMAc) with 0.05% lithium bromide as eluent at a flow rate of 0.8 mL/min. The equipment consisted of one pre-column and two analytical columns (PSS GRAM, 10^2 and 10^3 Å pore size, 7 μm particle size) and an Agilent 1200 RI detector. The measurements were performed at 60 °C.

The PMMA samples obtained from the arm cleavage were analyzed using a THF-SEC with a flow rate of 1 mL/min. This setup was equipped with one pre-column, four analytical columns (PSS SDV, 10^2, 10^3, 10^4 and 10^5 Å pore size, 5 μm particle size) and a Shodex 101 RI detector. The measurements were performed at 40 °C. For data evaluation a calibration with linear PMMA standards was used in all cases.

Cloud Point Measurements. The temperature-dependent solution behavior was investigated using a titrator (Titrando 809, Metrohm) equipped with a turbidity probe (Spectrosense, Metrohm, λ_0 = 523 nm) and a temperature sensor (Pt1000, Metrohm). The cloud points (T_{cl}) were determined by dissolving 30 mg of polymer in 30 ml of buffer solutions ranging from pH 7 to pH 9 (NIST buffer, Titrinorm VWR). The solutions were degassed by applying vacuum (50-100 mbar) for 15 min at room temperature in order to minimize bubble formation during the experiments. The measurements were performed using a homemade thermostatable vessel and for the experiments a constant heating rate of 1 K/min was applied using a thermostat (Lauda Ecoline Staredition RE 306, +/- 0.01°C). The cloud points were determined from the intersection of the two tangents applied to the two linear regimes of the transmittance curve at the onset of turbidity.

Dynamic Light Scattering. DLS was performed on an ALV DLS/SLS-SP 5022F compact goniometer system with an ALV 5000/E cross-correlator and a HeNe laser (λ_0 = 632.8 nm). The

solutions were prepared by dissolving 2 mg of polymer in 2 ml of buffer solution of either pH 7 or 8 (NIST buffer, Titrinorm, VWR) and filtered prior to the measurements with 0.45 µm syringe filters (cellulose acetate, Roth). For temperature-dependent measurements, the decaline bath of the instrument was thermostated using a LAUDA Proline RP 845 thermostat. At each temperature the sample was equilibrated for 10 min prior to data acquisition, which was done five times for the duration of 60 sec each. The autocorrelation functions were recorded individually and evaluated using 2^{nd} order cumulant analysis.

Rheology. Rheology measurements were conducted using a Physica MCR 301 rheometer with a cone-and-plate shear cell geometry (D = 50 mm, cone angle = 1°). For the temperature-dependent measurements a frequency of 1 Hz, a heating rate of 0.5 K/min and a strain of 0.5%, which is inside the linear viscoelastic regime, were applied. The temperature was controlled by a Peltier element. For the isothermal frequency sweeps (10^{-2} to 10^{2} Hz) the desired temperature was adjusted by heating the sample at a rate of 0.5 K/min. The samples were prepared using a Ditabis Cooling-Thermomixer MKR13. The polymers were directly dissolved in water at different low pH values, *i.e.*, pH = 2 or 3, to produce solutions with final pH values of pH = 7 or 8, respectively. This procedure avoids additional pH adjustments after sample preparation, which would result in salt (NaCl) formation and consequently might influence the solution behavior of the polyelectrolyte blocks. The samples were shaken in the MKR13 at 10 °C for several hours up to several days until the polymer was completely dissolved, and subsequently stored at 3 °C until use.

Micro Differential Scanning Calorimetry (µ-DSC). The caloric measurements were performed with a Setaram µ-DSC III using closed "batch" cells at a scanning rate of 0.5 K min^{-1}. Millipore water was used as the reference substance.

5.3. Results and Discussion

Synthesis and molecular characterization of star block copolymers. We have synthesized star-shaped block copolymers consisting of a poly(2-(dimethylamino)ethyl methacrylate) (PDMA) inner block and a poly(diethylene glycol methyl ether methacrylate) (PDEGMA) outer block. The synthesis was carried out with slight modifications according to a previously

published protocol employing ATRP with halogen exchange and subsequent monomer addition. A grafting-from approach with functionalized sugar moieties was used.[26] This synthetic route is shown in Scheme 5.2. The synthetic protocol was tested using a monofunctional ATRP initiator, ethyl 2-bromoisobutyrate. Figure 5.1 shows the SEC traces of the synthesized linear PDMA-*b*-PDEGMA block copolymer, $DMA_{75}DEGMA_{140}$, and the corresponding PDMA precursor. The trace of the precursor is monomodal with a narrow distribution (PDI 1.13) while the block copolymer shows a small shoulder at higher elution volume but still has a reasonably narrow distribution (PDI 1.32). This shoulder corresponds to a small amount of unreacted homopolymer but the peak of the block copolymer is completely shifted to lower elution volume.

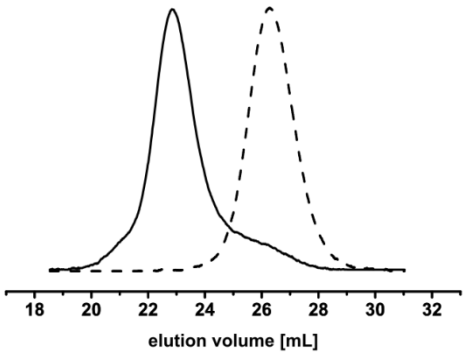

Fig. 5.1. SEC trace of the linear PDMA-*b*-PDEGMA block copolymer (solid line) and the corresponding PDMA precursor (dashed line).

We synthesized two homopolymer star precursors with different arm numbers but almost identical PDMA block lengths. The block lengths for the outer PDEGMA blocks were chosen to produce two different diblock copolymer stars from every precursor. This resulted in a total of 4 diblock copolymer stars with variations in arm number and the length of the outer block while keeping the length of the inner block almost constant.

Scheme 5.2. Synthesis of $(DMA_nDEGMA_m)_x$ star block copolymers

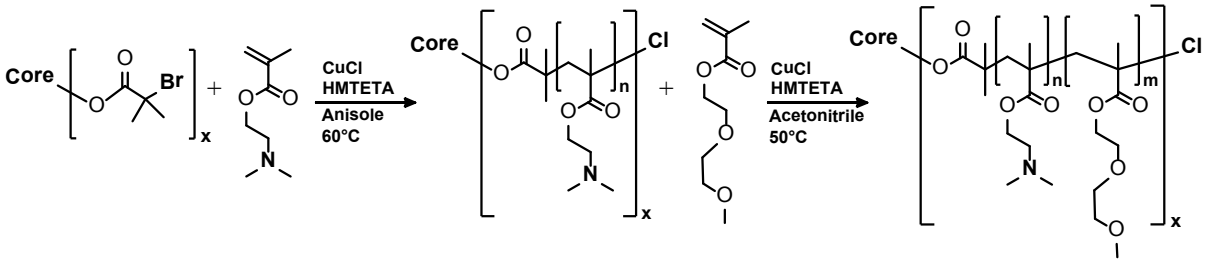

All stars have narrow molecular weight distributions with PDIs ranging from 1.07 to 1.39 (Table 5.1). As an example, the SEC trace of the star $(DMA_{150}DEGMA_{100})_4$ is shown in Figure 5.2a. The shoulder at low elution volume, *i.e.* high molecular weight, indicates some star-star coupling. However, Figure 5.2b shows a monomodal trace for the cleaved off arms of the star block copolymer. This indicates a blocking efficiency close to unity and that the coupling process does not involve recombination of two chain-end radicals but rather the amino side groups of the PDMA block. The side chains of both blocks are cleaved off during the procedure and the coupled connections are removed with them, leading to the mono-modal distribution.

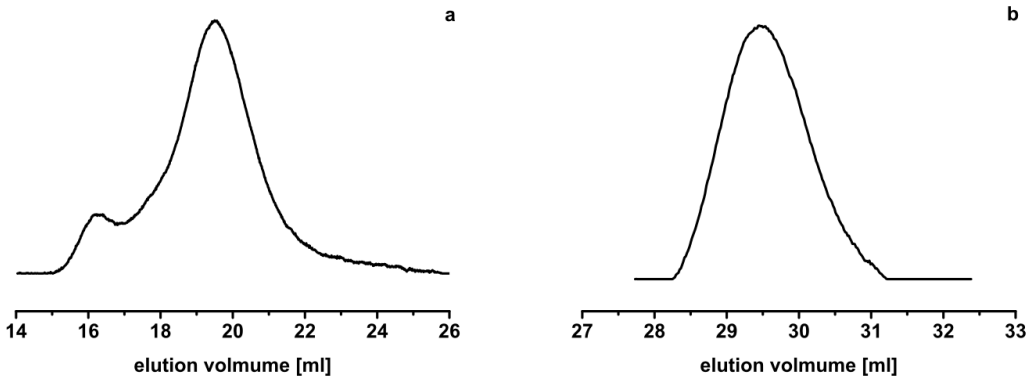

Figure 5.2. SEC traces for a) $(DMA_{150}DEGMA_{100})_4$ in DMAc and b) the corresponding arms, transformed to PMMA and measured in THF.

The molecular characterization of all star polymers is listed in Table 5.1. Later the PDMA blocks of all stars were quaternized with iodomethane to yield a permanent strong polyelectrolyte block (PqDMA). The increased electrostatic repulsion and the osmotic pressure of the counterions inside the PqDMA block[43,44] should lead to a stretching of the arms. Consequently, the volume of the individual stars increases and causes the overall volume fraction of the stars in the solution to rise, which is supposed to result in a decrease of the critical gelation concentration. ^{1}H-NMR measurements were utilized to confirm the structure of the quaternized and nonquaternized block copolymer stars (see Supporting Information p.100, Figure S5.1). The NMR results were also used to calculate the block length of the outer PDEGMA block. The signals at 2.2 and 3.3 ppm, corresponding to the *–N-**(CH$_3$)$_2$*** and *-**OCH$_3$*** groups, respectively, were compared to determine the PDEGMA block length, using the known block length of the inner PDMA block for signal calibration (see Experimental Section). In the case of the quaternized stars, the signals from the peaks at 3.35 ppm and 3.2 ppm, corresponding to the *–O-**CH$_3$*** and the *-N-***(CH$_3$)$_2$** plus the *-N$^+$-**(CH$_3$)$_3$*** groups, respectively, were compared to determine the degree of quaternization of the PDMA blocks (~85%). The expected ratio for complete quaternization can be estimated from the ratio of block length determined from the spectrum of the nonquaternized stars. The difference between the expected ratio and the experimental ratio is the quaternization efficiency.

Table 5.1. Molecular characteristics of the star-shaped (DMA$_n$DEGMA$_m$)$_x$ diblock copolymers and their gelation behavior.

Polymer [a]	M_n [b] [10^3 g/mol]	PDI [c]	f_{DEGMA} [d]	gelation behavior
(DMA$_{150}$DEGMA$_{40}$)$_4$	125	1.39	0.21	no gelation
(DMA$_{130}$DEGMA$_{60}$)$_6$	192	1.09	0.32	free-standing gels
(DMA$_{150}$DEGMA$_{100}$)$_4$	170	1.28	0.40	free-standing gels
(DMA$_{130}$DEGMA$_{140}$)$_6$	282	1.07	0.52	free-standing gels

[a] (DMA$_n$DEGMA$_m$)$_x$: n and m are the number average degrees of polymerization of the respective blocks and x denotes the number average arm number as determined by a combination of SEC and NMR. [b] Number average molecular weight of the stars as determined by a combination of MALDI-ToF and NMR. [c] Apparent polydispersity index as determined by SEC of the star polymers in DMAc. [d] Molar fraction of DEGMA units.

Aggregation of $(DMA_nDEGMA_m)_x$ diblock copolymer stars in dilute solution. The dual responsive nature of the star block copolymers was investigated by turbidity measurements first. Figure 5.3a shows the temperature-dependent transmittance for the star block copolymer $(DMA_{130}DEGMA_{140})_6$ at different pH values. At pH 7, when the cloud point of the PDMA block is around 80 °C,[29] both transitions are visible but strongly separated, with the transition of the PDEGMA block at 24 °C, lower than the cloud point of linear PDEGMA homopolymer.[30] The shift of the transition temperature for the PDEGMA star block copolymer compared to the homopolymer might be due to the fact that the PDMA block is protonated at this pH and hydrogen bonds are formed between the PDMA and PDEGMA blocks, making the stars less soluble.[40,45] At pH 8, there are also two distinct steps in the transmittance, the first around 28 °C and the second around 50 °C. Both correspond very well to the cloud points of the respective homopolymers of the different blocks, 26 °C for PDEGMA homopolymer[30,31] and around 50 °C for PDMA homopolymer at pH 8.[27,29] All star polymers show this behavior at pH 8. Figure 5.3b shows the transition temperatures of all synthesized star block copolymers at various pH values. This agrees with the supposed aggregation mechanism (Scheme 1), *i.e.* a sequential collapse of the blocks takes place upon heating, beginning with the outer PDEGMA block. In dilute solution this leads to the formation of small aggregates. If the temperature is increased further, then, depending on the pH value, the inner PDMA block can collapse, too, leading to precipitation of the whole polymer.

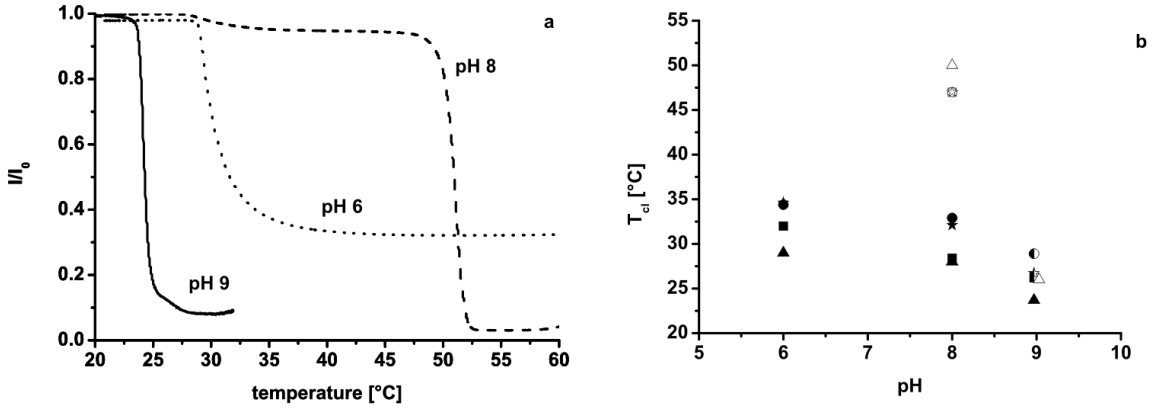

Figure 5.3. Turbidity measurements of a) $(DMA_{130}DEGMA_{140})_6$ and b) transition temperatures of all stars at different pH values with the open symbols representing the inner PDMA block and the filled symbols the transition temperature of the outer PDEGMA block. (●,○) $(DMA_{150}DEGMA_{40})_4$; (■,□) $(DMA_{150}DEGMA_{100})_4$; (★,☆) $(DMA_{130}DEGMA_{60})_6$; (▲,△) $(DMA_{130}DEGMA_{140})_6$. Half-filled symbols indicate that no distinction between the blocks could be made.

However, at pH 9 the cloud point of PDMA is shifted to lower values, around 30 °C,[29] and the block is almost completely deprotonated, making it hydrophobic, which lowers the cloud point of the PDEGMA block.[45] Therefore, the first drop in transmittance observed for $(DMA_{130}DEGMA_{140})_6$ is also attributed to the PDEGMA block Fig. 5.3a). This drop continues to almost zero before a small shoulder appears around 27°C, indicating the collapse of the PDMA block and thus complete collapse of the star. This sequence of collapses is confirmed by µ-DSC measurements (Fig. S5.2, Supporting Information p.101), showing that the transition of the PDEGMA block occurs before the transition of the PDMA block. This behavior shows that the blocks can be triggered independently from each other and the diblock copolymer stars can be mono or dual responsive depending on the pH. However, this is only true for $(DMA_{130}DEGMA_{140})_6$ as the µ-DSC measurements for the other stars show that the transitions of the two blocks overlap.

To further study the aggregation behavior of the stars, dynamic light scattering experiments (DLS) were carried out. Figure 5.4 shows the results for $(DMA_{130}DEGMA_{140})_6$ at pH 7 and 8. In both cases the apparent hydrodynamic radius, $R_{h,app}$, has a value of 19 nm at low temperatures, which is consistent with unimolecularly dissolved stars. Beginning at temperatures

above 20 °C, $R_{h,app}$ increases until a maximum is reached at 30 °C. These maxima are 34 and 29 nm for pH 7 and 8, respectively. The increase in size is in line with the collapse of the outer PDEGMA block and the formation of small flower-like aggregates (Scheme 5.1). At the same time as the size increases the polydispersity index (PDI) of the detected species decreases sharply. This is further evidence for the formation of defined aggregates. The transition temperature is lower than the one determined from turbidity measurements but that is due to the higher sensitivity of the DLS setup, which enables it to detect even small changes in size. At pH 7, $R_{h,app}$ shows a slight decrease from above 30 °C up to 60°C, but no large aggregates because we cannot reach the cloud point at ≈ 80 °C[29] in our experimental setup. The decrease of the radius can be explained by the contraction of the PDMA block due to increased hydrophobicity at elevated temperatures, because the strength of the hydrogen bonds decreases steadily.

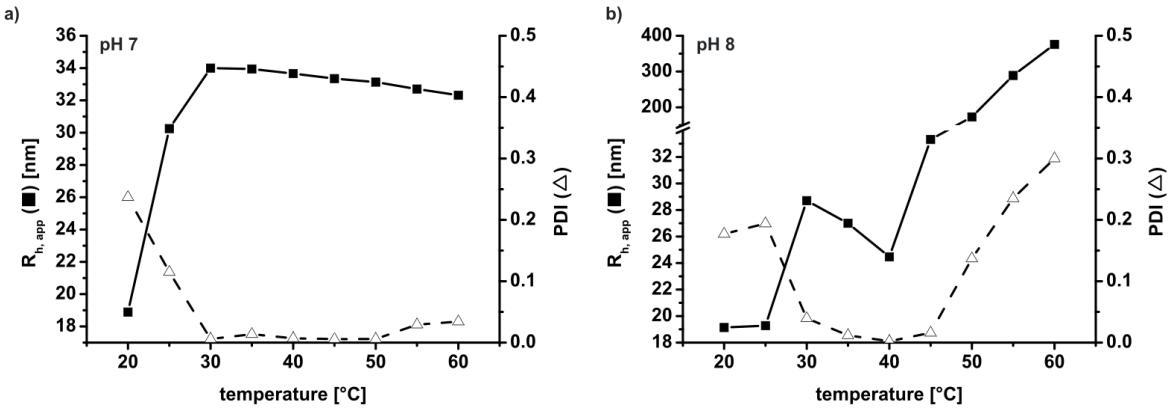

Figure 5.4. Temperature-dependent apparent hydrodynamic radii and polydispersity indices derived from cumulant analysis of $(DMA_{130}DEGMA_{140})_6$ at a) pH 7 and b) pH 8. Measurements were performed in buffer solutions at 1g/L and ϑ = 90°.

At pH 8, $R_{h,app}$ starts to increase at 25 °C, then decreases above 30 °C before rising again above 40 °C and finally reaching values higher than 100 nm for temperatures over 50 °C. The PDI matches this behavior, decreasing between 25 and 30 °C and then increasing again at 50 °C. First, the PDEGMA block starts collapsing above 25 °C and small flower-like aggregates are formed at 30 °C, resulting in the decrease of the PDI. Between 30 and 40 °C, the

inner PDMA block contracts because of the decreasing solvent quality close to its cloud point. However, the flower-like aggregates are stable as indicated by the constant low PDI in this region. At 50 °C the PDMA block reaches its aggregation temperature and collapses, causing intermolecular aggregation as seen by the rapid increase of $R_{h,app}$ and PDI over the remaining measurement, *i.e.* larger and more ill-defined aggregates are formed as the star block copolymers aggregate into clusters. This behavior agrees with our assumptions for dual responsiveness (Scheme 5.1). The DLS measurements of the remaining star block copolymers are shown in Figure S5.3. Their behavior mostly agrees with the one discussed above, except for the star $(DMA_{150}DEGMA_{40})_4$, which has a low arm number and the lowest molar fraction of DEGMA units (21%). The star shows a very broad transition at both pH values, indicating a less defined aggregation. One possible explanation is that due to the small fraction of DEGMA units, stable aggregates are only formed at higher temperatures. This is most pronounced at pH 7, where the PDMA block is hydrophilic and impedes aggregate formation. This would suggest that a minimum fraction of the collapsing outer block is needed to spontaneously form stable aggregates.

Aggregation of quaternized $(qDMA_nDEGMA_m)_x$ diblock copolymer stars in dilute solution. Through quaternization PDMA becomes a strong polyelectrolyte but loses its sensitivity to temperature and pH. Thus the inner block is no longer stimuli-responsive and the diblock copolymer stars can only undergo one transition independent of the pH value, *i.e.* the formation of flower-like aggregates upon the collapse of the PDEGMA block. These aggregates should be stable at elevated temperatures due to the polyelectrolyte nature of the inner block. Figure 4 shows the results for $(qDMA_{130}DEGMA_{140})_6$.

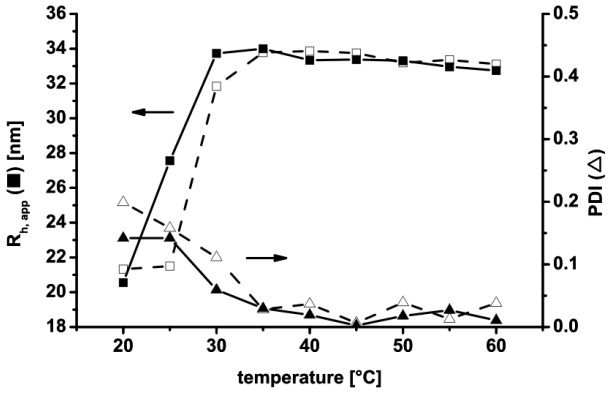

Figure 5.5. Temperature-dependent apparent hydrodynamic radii (■,□) and polydispersity indices (▲,△) derived from cumulant analysis of $(qDMA_{130}DEGMA_{140})_6$ at pH 7 (filled symbols) and pH 8 (open symbols). Measurements performed in buffer solution at 1g/L and Θ = 90°.

At pH 7, $R_{h,app}$ increases above 20 °C and reaches the same plateau value of 34 nm as the nonquaternized diblock star (Figures 5.5). The value then stays almost constant within the investigated temperature range. Coinciding with this increase in radius is again a decrease of the PDI, supporting the assumption that the PDEGMA block collapses and small flower-like aggregates are formed which are stable even at elevated temperatures. The results for pH 8 are practically equal to those at pH 7, as expected because the inner PqDMA block has no LCST anymore. Hence, the aggregation behavior of the quaternized stars is markedly different to that for the nonquaternized stars as there is only one transition visible between 20 and 30 °C.

The results obtained from turbidity measurements and dynamic light scattering experiments prove the double responsive nature of the diblock copolymer stars in dilute solutions and that the outer block can be triggered independently of the inner block. This behavior should lead to hydrogel formation in concentrated solutions upon heating, independent of the solution pH as long as the outer block collapses first. To investigate the behavior of the diblock stars in concentrated solutions, tube-inversion experiments and rheology measurements were performed.

Gel formation of $(DMA_nDEGMA_m)_x$ diblock copolymer stars at pH ≈ 8. All samples were prepared by dissolving the polymers in water of appropriate low pH to obtain the desired pH value close to 8, because here the transition temperature of PDMA is in the accessible temperature range (≈50 °C).[29] Thus, gel formation is supposed to take place triggered by the collapse of the outer PDEGMA block and upon reaching the transition temperature of the inner PDMA block, the mechanical properties of the gel should change because of the contraction of the PDMA block (Scheme 1). Tube-inversion revealed that at pH values around 8 all the stars, except the one with the lowest PDEGMA fraction, $(DMA_{150}DEGMA_{40})_4$, formed free-standing hydrogels starting from 15 wt%. $(DMA_{150}DEGMA_{40})_4$ does not form gels at any concentration and pH value tested. DLS showed that this star has a very broad transition in dilute solution, making it likely that the physical crosslinks initially formed by this star are not strong enough to enable gelation. On the other hand, the star with the highest DEGMA fraction, $(DMA_{130}DEGMA_{140})_6$, forms free-standing even at concentrations as low as 10 wt%.

To obtain a more detailed picture of the gelation behavior of the block copolymer stars selected samples were investigated by rheology. We applied an oscillatory stress to the sample using a cone-plate shear cell geometry.

Regimes where the storage modulus, G', exceeds the loss modulus, G'', are defined as the gel state according to the common definitions. The sol state is defined by $G' < G''$, and $G' > 1$ kPa is taken as a characteristic value for strong, free-standing gels. [46-48] The point at which G' and G'' intersect is defined as the sol-gel transition temperature, T_{sg}.

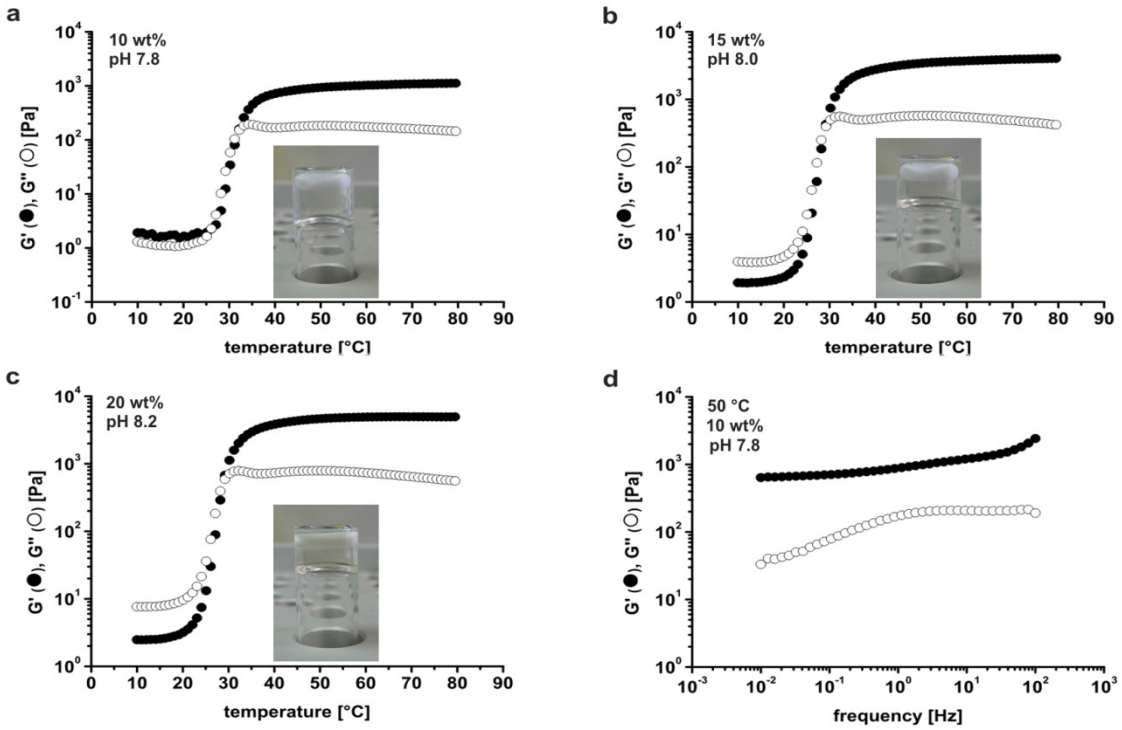

Figure 5.6. Temperature-dependent storage and loss moduli for $(DMA_{130}DEGMA_{140})_6$ in a) a 10 wt% solution at pH 7.8, b) a 15 wt% solution at pH 8.0, c) a 20 wt% solution at pH 8.2 and d) an isothermal frequency sweep at 50 °C of the 10 wt% sample. Insets depict digital photographs of tube-inversion experiments of the respective samples at 50 °C.

Figure 5.6 shows typical plots of the temperature-dependent storage and loss moduli for $(DMA_{130}DEGMA_{140})_6$ at different concentrations and one isothermal frequency sweep. At temperatures below 25 °C *G''* exceeds *G'* and the solution is in the sol state, as both blocks are beneath their transition temperature and thus fully soluble in water. With increasing temperature both moduli increase and at 30 °C, the transition temperature of DEGMA, the solution crosses into the gel state. Eventually *G'* reaches a plateau with *G'* > 1 kPa, indicating a strong gel (Table 5.2). This is supported by Figure 5.6d, which shows the frequency dependent measurements at 50 °C, for the sample depicted in Figure 5.6a. *G'* is higher than *G''* over the whole measured frequency range, proving that free-standing gels are formed. Increasing the polymer concentration from 10 wt% to 20 wt% (Figure 5.6a-c) leads to a substantial increase in the gel strength because the number of physical crosslinks in the gel increases accordingly. Unexpectedly, the moduli show no change when the temperature is

increased above 50 °C, the transition temperature of DMA, which is attributed to the high gel strength (G' > 1 kPa).

Table 5.2. Gelation behavior of $(DMA_nDEGMA_m)_x$ and $(qDMA_nDEGMA_m)_x$ diblock stars.

5 wt%				
	f_{DEGMA} [a]	pH [b]	T_{sg} [°C] [c]	G' [kPa] [d]
$(qDMA_{130}DEGMA_{60})_6$ [e]	0.32	quat.	55	0.73
$(qDMA_{150}DEGMA_{100})_4$ [e]	0.40	quat.	42	0.35
$(qDMA_{130}DEGMA_{140})_6$ [e]	0.52	quat.	36	0.79
10 wt%				
	f_{DEGMA} [a]	pH [b]	T_{sg} [°C] [c]	G' [kPa] [d]
$(qDMA_{130}DEGMA_{60})_6$ [e]	0.32	quat.	53	2.0
$(qDMA_{150}DEGMA_{100})_4$ [e]	0.40	quat.	41	1.0
$(qDMA_{130}DEGMA_{140})_6$ [e]	0.52	quat.	36	1.8
$(DMA_{130}DEGMA_{140})_6$	0.52	7.8	32	1.1
15 wt%				
	f_{DEGMA} [a]	pH [b]	T_{sg} [°C] [c]	G' [kPa] [d]
$(DMA_{130}DEGMA_{60})_6$	0.32	8.2	41	2.8
$(DMA_{150}DEGMA_{100})_4$	0.40	8.2	35	1.7
$(DMA_{130}DEGMA_{140})_6$	0.52	8.0	29	3.9
$(DMA_{130}DEGMA_{140})_6$	0.52	8.8	32	0.07 (0.27[f])
20 wt%				
	f_{DEGMA} [a]	pH [b]	T_{sg} [°C] [c]	G' [kPa] [d]
$(DMA_{130}DEGMA_{60})_6$	0.32	8.3	40	2.8
$(DMA_{150}DEGMA_{100})_4$	0.40	8.4	34	1.9
$(DMA_{130}DEGMA_{140})_6$	0.52	8.2	29	5.0
$(DMA_{130}DEGMA_{140})_6$	0.52	8.7	31	0.13 (0.55[f])

[a] molar fraction of DEGMA units. [b] solution pH measured before rheology. [c] sol-gel transition temperature, defined as the temperature when G' and G'' cross over. [d] value of G' in the plateau region taken at 70 °C. [e] the degree of quaternization is 85 – 88%. [f] value at maximum.

Table 5.2 summarizes the results of the rheology experiments for all measured samples of the star block copolymers and the corresponding plots of G' and G'' can be found in Figures 5.6-5.8 and S5.5- S5.7. There are some general trends noticeable. The first trend is that an increase in the polymer concentration results in a strengthening of the hydrogels. The second important characteristic is the molar fraction of DEGMA units, f_{DEGMA}, which plays a

very important role in the formation of hydrogels for these diblock copolymer stars. As mentioned above, $(DMA_{150}DEGMA_{40})_4$ does not form any hydrogels under the conditions investigated. This leads to the conclusion that a minimum f_{DEGMA} is necessary for hydrogel formation, but most importantly, f_{DEGMA} controls the sol-gel transition temperature (Table 2). Turbidity measurements show that the cloud point decreases with the DEGMA block length, thus T_{sg} should decrease accordingly. The gel strength on the other hand, is influenced by both f_{DEGMA} and the arm number of the star. This is reasonable, as f_{DEGMA} is proportional to the block length of the DEGMA block and a longer hydrophobic block leads to stronger gels. The arm number determines the number of possible crosslinking points so that a higher arm number means more crosslinking points and thus a stronger gel. However, the effect of the arm number is more pronounced, as the 6-arm star with the lowest f_{DEGMA} forms stronger gels than the 4-arm star with a higher f_{DEGMA} at all concentrations measured. This suggests that the concentration of crosslinking points is more important than the strength of the hydrophobic interactions. The transition temperature of the inner PDMA block is around 50 °C for pH values around 8, so we expected the dynamic-mechanical behavior of the gels to change upon heating above 50 °C but there is no visible change in G' and G'' for the investigated hydrogels (Figures 5.6 and S5.5). The high strength of the gels around pH 8 makes them too rigid to respond to the increase in temperature above the transition temperature of PDMA. This is similar to behavior we observed for gels based on PDMA-*b*-PDEA block copolymer stars.[26] For that reason we decided to investigate gels at higher pH.

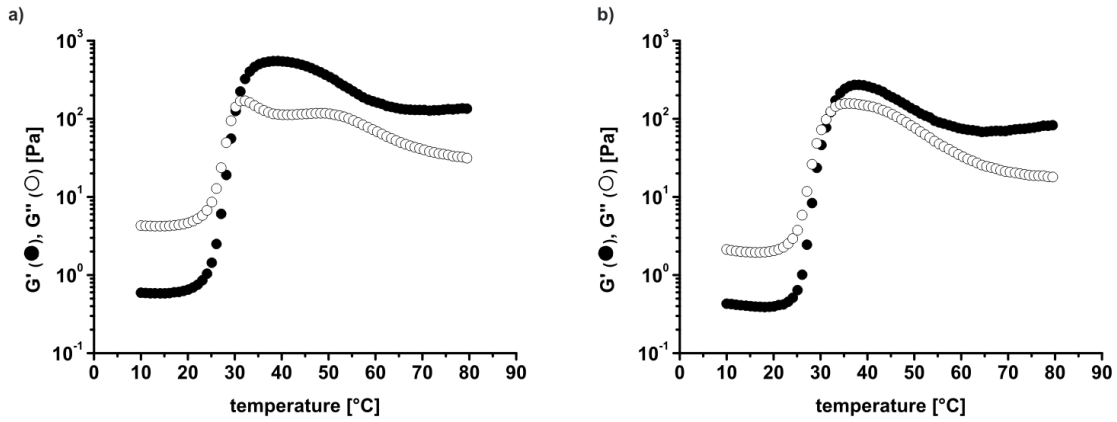

Figure 5.7. Temperature-dependent storage and loss moduli for $(DMA_{130}DEGMA_{140})_6$ in a) a 15 wt% solution at pH 8.8 and b) a 20 wt% solution at pH 8.7.

Gel formation of $(DMA_nDEGMA_m)_x$ diblock copolymer stars at pH ≈ 9. Figure 5.7 shows the results of the rheology measurements of $(DMA_{130}DEGMA_{140})_6$ at pH values close to 9. The increase of the pH value has two consequences: first, the cloud point of the PDMA block is lowered to around 30 °C and second, the DMA chains are less stretched because the DMA blocks are less protonated. The lower degree of protonation together with the contraction of the chains causes a decrease of the effective volume fraction of the stars, making the gels at high pH softer compared to the gels at lower pH values. Again, gelation occurs around 30 °C. Both samples have a lower maximum value of *G'* compared to their counterparts at pH ≈ 8. The difference to the behavior at pH ≈ 8 becomes visible immediately after the crossover (Figure 6). *G'* decreases after reaching a maximum at 35 °C (for 15 wt%) and 40 °C (for 20 wt%) before leveling off again at T > 60 °C. This indicates a further contraction of the PDMA block after gelation because the solvent quality of the water decreases steadily with increasing temperature, making this gel dual responsive in its formation process and its mechanical properties in the gel state. The contraction of the chains is in agreement with the behavior of the PDMA blocks at elevated temperatures in DLS. However, since the polymer is already in the gel state the PDMA blocks cannot completely collapse, which leads to the plateau of *G'* at elevated temperatures.

In contrast, $(DMA_{150}DEGMA_{100})_4$ and $(DMA_{130}DEGMA_{60})_6$ do not form a gel under these conditions ($G'_{max} < 10$ Pa, Figure S6). A possible explanation is that $(DMA_{130}DEGMA_{140})_6$ is the only star where the turbidity and μ-DSC measurements show two distinct transitions even at

pH 9 (Figures 5.3b, S5.2a). The transition temperatures of the PDMA blocks of the other stars coincide with those of the PDEGMA blocks, making successful hydrogel formation impossible (Figures 5.3, S5.2b). The measurements depicted in Figure S5.6 all show an increase in *G'* around 30 °C, the transition temperature of DEGMA, but before a gel can be formed the moduli drop sharply. This is attributed to the collapse of the PDMA block shortly after the PDEGMA block has collapsed. In these cases stable crosslinking points cannot be formed, making network formation impossible.

Gel formation of quaternized ($qDMA_nDEGMA_m)_x$ diblock copolymer stars. In this system hydrogel formation takes place upon the collapse of the outer PDEGMA block, the same as for the nonquaternized diblock copolymer stars. The resulting gels will not be dual responsive as the thermo- and pH-responsiveness of the inner PDMA block is lost upon quaternization. This prediction is confirmed by both tube inversion and rheology measurements. Tube-inversion experiments show a significant decrease of the critical gelation concentration as compared to the nonquaternized stars. As an example, gel formation for $(qDMA_{130}DEGMA_{140})_6$ takes place at concentrations as low as 2 wt%. This is due to the increased stretching of the PqDMA block because of the much higher charge density and the increased osmotic pressure of the counterions. However, the rheology measurements of $(qDMA_{130}DEGMA_{140})_6$ show that the gels formed at 5 wt% and lower cannot be categorized as strong free-standing gels but rather are considered to be soft gels ($G' < 1$ kPa).

Figure 5.8 shows the rheology measurements of $(qDMA_{130}DEGMA_{140})_6$ at concentrations of 5 wt% and 10 wt% and the other quaternized stars are shown in Figure S5.7. In Figure 5.8 a sol-gel transition is observed upon heating the samples and the storage modulus does not decrease again after reaching the gel state.

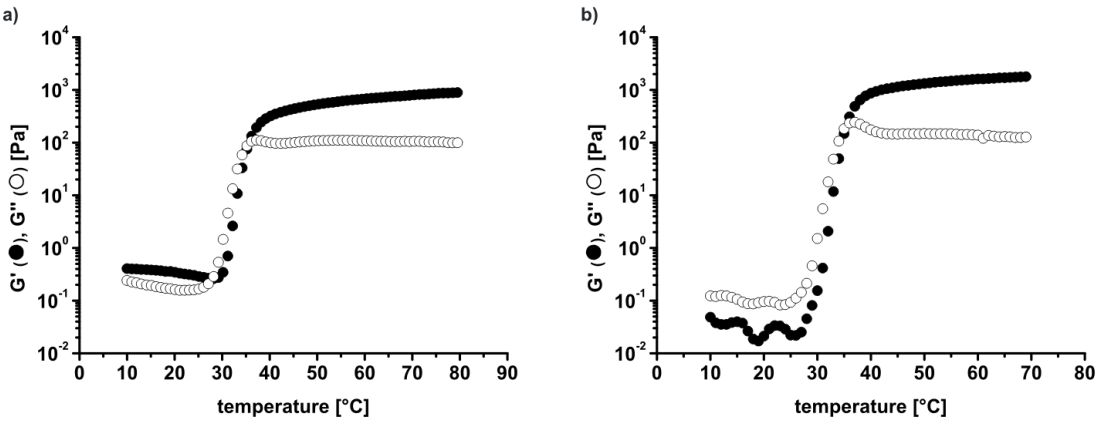

Figure 5.8. Temperature-dependent storage and loss moduli for a) a 5 wt% solution and b) a 10 wt% solution of $(qDMA_{130}DEGMA_{140})_6$.

An increase in the polymer concentration also leads to a strengthening of the gel in analogy to the behavior of the nonquaternized stars. Here we can directly compare 10 wt% samples of $(DMA_{130}DEGMA_{140})_6$ and $(qDMA_{130}DEGMA_{140})_6$ in terms of sol-gel transition temperature and gel strength (Table 2). Through quaternization, T_{sg} shifts to slightly higher temperatures because of the hydrophilic PqDMA block, *i.e.* the transition temperature of the PDEGMA block is increased, and the gel strength increases due to the higher effective volume fraction of the quaternized stars. The behavior of the quaternized stars is similar to that of the non-quaternized stars, insofar as T_{sg} is solely controlled by f_{DEGMA} and the gel strength is mainly controlled by the arm number of the stars and to a lesser extent by f_{DEGMA}.

5.4. Conclusions

Turbidimetry and dynamic light scattering have confirmed that $(DMA_nDEGMA_m)_x$ diblock copolymer stars are double-responsive in dilute aqueous solution. Upon heating the outer PDEGMA block collapses first and flower-like aggregates are formed. When the temperature is increased further, the inner PDMA block responds depending on the pH value. If the pH is chosen correctly, a sequential collapse starting with the outer block can be triggered. Therefore, in concentrated aqueous solutions, hydrogel formation takes place upon the collapse of the outer PDEGMA block and the mechanical properties of the gel can be manipulated

further by temperature. Unexpectedly, the gels formed at pH ≈ 8 do not show a change in their moduli when the temperature is increased above the transition temperature of PDMA. This is attributed to the fact that in these cases strong gels are formed (G'_{max} > 1 kPa), which are too rigid to be affected. However, when the gels are prepared at pH ≈ 9 they exhibit a significantly reduced gel strength and thus a drop of the moduli upon heating over the transition temperature of PDMA can be observed.

To further prove the versatility of our system, the inner PDMA blocks were quaternized to from PqDMA, a strong polycation. Further advantages of a quaternized block are the possibilities to incorporate nanoparticles or to introduce a light sensitivity through multivalent counterions.[28,49] During the quaternization the temperature and pH responsiveness of the inner block is lost but so are the restrictions on the solution pH value. The increased effective volume fraction of the quaternized diblock stars leads to a significant decrease in the critical gelation concentration.

Acknowledgements. The German Science Foundation (DFG) is acknowledged for financial support within the priority program SPP 1259. We thank Florian Stegmann for his help in the synthesis, Ingo Rehberg and Reinhard Richter (Experimental Physics V, University of Bayreuth) for providing us with access to their rheometer and Marietta Böhm (Macromolecular Chemistry II, University of Bayreuth) for performing the SEC measurements.

References

(1) He, C.; Kim, S. W.; Lee, D. S. *J. Controlled Release* **2008**, *127*, 189-207.

(2) Hoffman, A. S. *Adv. Drug Deliv. Rev.* **2002**, *54*, 3-12.

(3) Alarcon, C.; de Las, H.; Pennadam, S.; Alexander, C. *Chem. Soc. Rev.* **2005**, *34*, 276-285.

(4) Ruel-Gariepy, E.; Leroux, J.-C. *Eur. J. Pharm. Biopharm.* **2004**, *58*, 409-426.

(5) Peppas, N. A.; Hilt, J.; Khademhosseini, A.; Langer, R. *Adv. Mater.* **2006**, *18*, 1345-1360.

(6) Okano, T.; Yamada, N.; Okuhara, M.; Sakai, H.; Sakurei, Y. *Biomaterials* **1995**, *16*, 297-303.

(7) Stayton, P. S.; Shimoboji, T.; Long, C.; Chilkoti, A.; Ghen, G.; Harris, J. M.; Hoffman, A. S. *Nature* **1995**, *378*, 472-474.

(8) Zhang, J.; Peppas, N. A. *Macromolecules* **2000**, *33*, 102-107.

(9) Jeong, B.; Kim, S. W.; Bae, Y. H. *Adv. Drug Deliv. Rev.* **2002**, *54*, 37-51.

(10) Kikuchi, A.; Okano, T. *Prog. Polym. Sci.* **2002**, *27*, 1165-1193.

(11) Tsitsilianis, C. *Soft Matter* **2010**, *6*, 2372-2388.

(12) Ahn, S.-K.; Kasi, R. M.; Kim, S.-C.; Sharma, N.; Zhou, Y. *Soft Matter* **2008**, *4*, 1151-1157.

(13) Yu, L.; Ding, J. *Chem. Soc. Rev.* **2008**, *37*, 1473-1481.

(14) Li, C.; Tang, Y.; Armes, S. P.; Morris, C. J.; Rose, S. F.; Lloyd, A. W.; Lewis, A. L. *Biomacromolecules* **2005**, *6*, 994-999.

(15) Yu, L.; Chang, G.; Zhang, H.; Ding, J. *J. Polym. Sci., Part A: Polym. Chem.* **2007**, *45*, 1122-1133.

(16) Jones, M. S. *Eur. Polym. J.* **1999**, *35*, 795-801.

(17) O'Lenick, T. G.; Jin, N.; Woodcock, J. W.; Zhao, B. *J. Phys. Chem. B* **2011**, *115*, 2870-2881.

(18) Li, C.; Buurma, N. J.; Haq, I.; Turner, C.; Armes, S. P.; Castelletto, V.; Hamley, I. W.; Lewis, A. L. *Langmuir* **2005**, *21*, 11026-11033.

(19) Sugihara, S.; Kanaoka, S.; Aoshima, S. *J. Polym. Sci., Part A: Polym. Chem.* **2004**, *42*, 2601-2611.

(20) Nguyen, M. K.; Park, D. K.; Lee, D. S. *Biomacromolecules* **2009**, *10*, 728-731.

(21) Angelopoulos, S. A.; Tsitsilianis, C. *Macromol. Chem. Phys.* **2006**, *207*, 2188-2194.

(22) Bossard, F.; Tsitsilianis, C.; Yannopoulos, S. N.; Petekidis, G.; Sfika, V. *Macromolecules* **2005**, *38*, 2883-2888.

(23) Reinicke, S.; Schmelz, J.; Lapp, A.; Karg, M.; Hellweg, T.; Schmalz, H. *Soft Matter* **2009**, *5*, 2648-2657.

(24) Fechler, N.; Badi, N.; Schade, K.; Pfeifer, S.; Lutz, J.-F. *Macromolecules* **2009**, *42*, 33-36.

(25) Lin, H.-H.; Cheng, Y.-L. *Macromolecules* **2001**, *34*, 3710-3715.

(26) Schmalz, A.; Schmalz, H.; Müller, A. H. E. *Z. Phys. Chem.* **2012**, *accepted*.

(27) Plamper, F. A.; Schmalz, A.; Penott-Chang, E.; Drechsler, M.; Jusufi, A.; Ballauff, M.; Müller, A. H. E. *Macromolecules* **2007**, *40*, 5689-5697.

(28) Plamper, F. A.; Schmalz, A.; Ballauff, M.; Müller, A. H. E. *J. Am. Chem. Soc.* **2007**, *129*, 14538-14539.

(29) Plamper, F. A.; Ruppel, M.; Schmalz, A.; Borisov, O.; Ballauff, M.; Müller, A. H. E. *Macromolecules* **2007**, *40*, 8361-8366.

(30) Hoth, A.; Lutz, J. F. *Macromolecules* **2006**, *39*, 893-896.

(31) Akdemir, Ö.; Hoth, A.; Lutz, J. F. *J. Am. Chem. Soc.* **2006**, *128*, 13046-13047.

(32) Han, S.; Hagiwara, M.; Ishizone, T. *Macromolecules* **2003**, *36*, 8312-8319.

(33) Pietsch, C.; Hoogenboom, R.; Schubert, U. S. *Angew. Chem. Int. Ed.* **2009**, *48*, 5653-5656.

(34) Jones, M. W.; Gibson, M. I.; Mantovani, G.; Haddleton, D. M. *Polym. Chem.* **2011**, *2*, 572-574.

(35) Park, S.; Cho, H. Y.; Yoon, J. A.; Kwak, Y.; Srinivasan, A.; Hollinger, J. O.; Paik, H.-j.; Matyjaszewski, K. *Biomacromolecules* **2010**, *11*, 2647-2652.

(36) Porsch, C.; Hansson, S.; Nordgren, N.; Malmstrom, E. *Polym. Chem.* **2011**, *2*, 1114-1123.

(37) Kumano, N.; Seki, T.; Ishii, M.; Nakamura, H.; Takeoka, Y. *Angew. Chem. Int. Ed.* **2011**, *50*, 4012-4015.

(38) Yoon, J. A.; Gayathri, C.; Gil, R. R.; Kowalewski, T.; Matyjaszewski, K. *Macromolecules* **2010**, *43*, 4791-4797.

(39) Munoz-Bonilla, A.; Fernandez-Garcia, M.; Haddleton, D. M. *Soft Matter* **2007**, *3*, 725-731.

(40) Reinicke, S.; Schmalz, H. *Colloid. Polym. Sci.* **2011**, *289*, 497-512.

(41) Li, Y.; Tang, Y.; Narain, R.; Lewis, A. L.; Armes, S. P. *Langmuir* **2005**, *21*, 9946-9954.

(42) Plamper, F. A.; Becker, H.; Lanzendörfer, M.; Patel, M.; Wittemann, A.; Ballauff, M.; Müller, A. H. E. *Macromol. Chem. Phys.* **2005**, *206*, 1813-1825.

(43) Jusufi, A.; Likos, C.; Ballauff, M. *Colloid. Polym. Sci.* **2004**, *282*, 910-917.

(44) Das, B.; Guo, X.; Ballauff, M. *Progr. Colloid. Polym. Sci.* **2002**, *121*, 34-38.

(45) Roth, P. J.; Jochum, F. D.; Forst, F. R.; Zentel, R.; Theato, P. *Macromolecules* **2010**, *43*, 4638-4645.

(46) Chambon, F.; Winter, H. H. *Polym Bull* **1985**, *13*, 499-503.

(47) Mours, M.; Winter, H. H. *Adv. Polym. Sci.* **1997**, *134*, 165-234.

(48) Nishinari, K. *Prog. Colloid Polym. Sci.* **2009**, *136*, 87-94.

(49) Plamper, F. A.; Walther, A.; Müller, A. H. E.; Ballauff, M. *Nano Letters* **2007**, *7*, 167-171.

5.5. Supporting Information

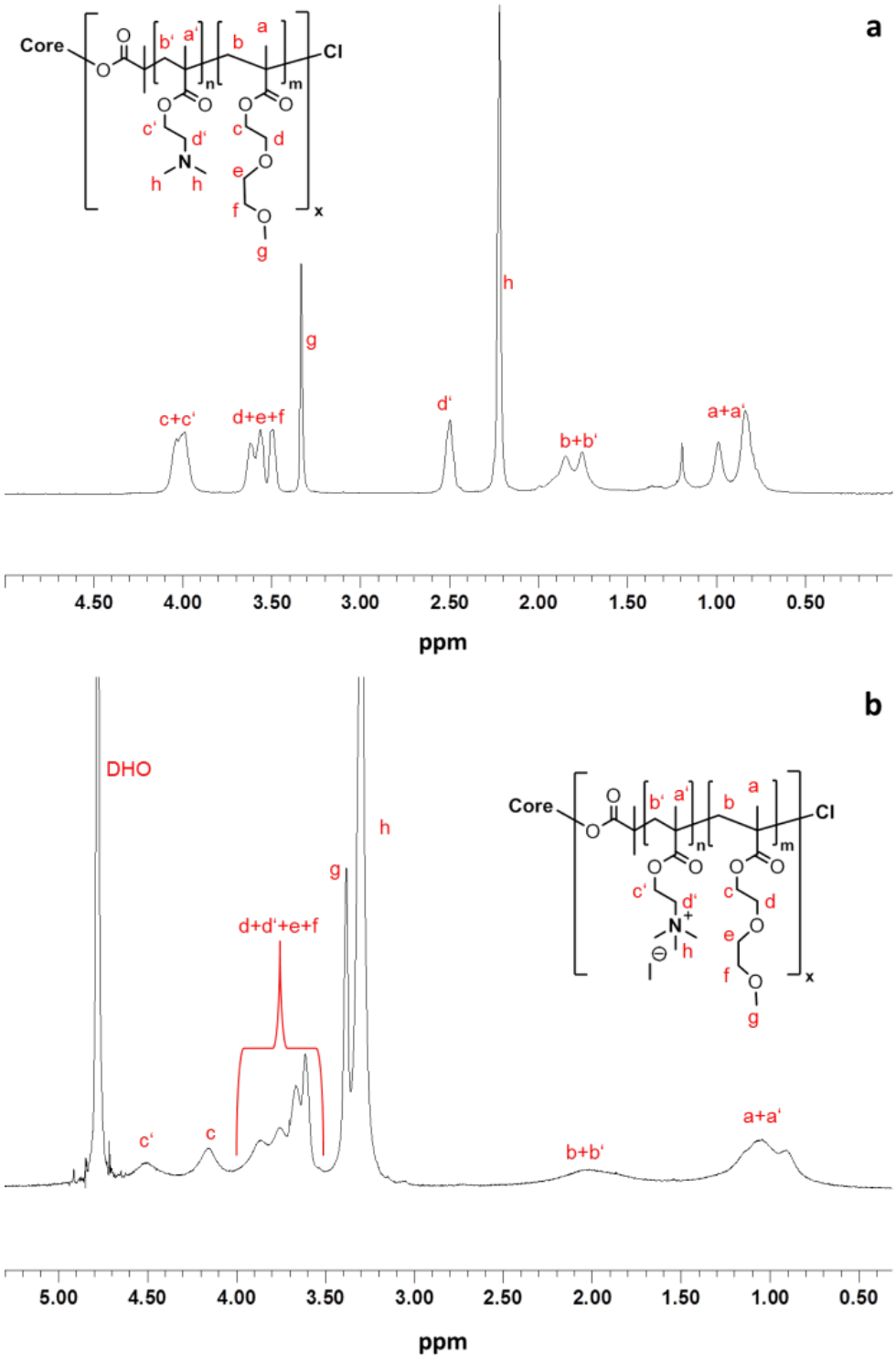

Figure S5.1. ^{1}H-NMR spectra of a) $(DMA_{150}DEGMA_{100})_4$ in $CDCl_3$ and b) quaternized $(qDMA_{150}DEGMA_{100})_4$ in D_2O.

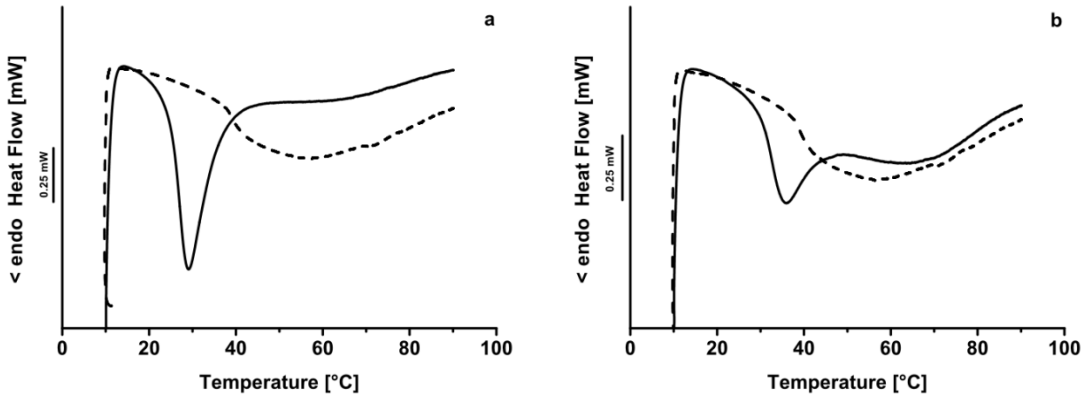

Figure S5.2. Micro differential scanning calorimetry measurements for a) $(DMA_{130}DEGMA_{140})_6$ and b) $(DMA_{130}DEGMA_{60})_6$ at pH 9 (solid line) compared to $(DMA_{130})_6$ (dashed line). Measurement performed at 20 wt% for the diblock stars and 10 wt% for the homopolymer star and with a heating rate of 0.5K/min.

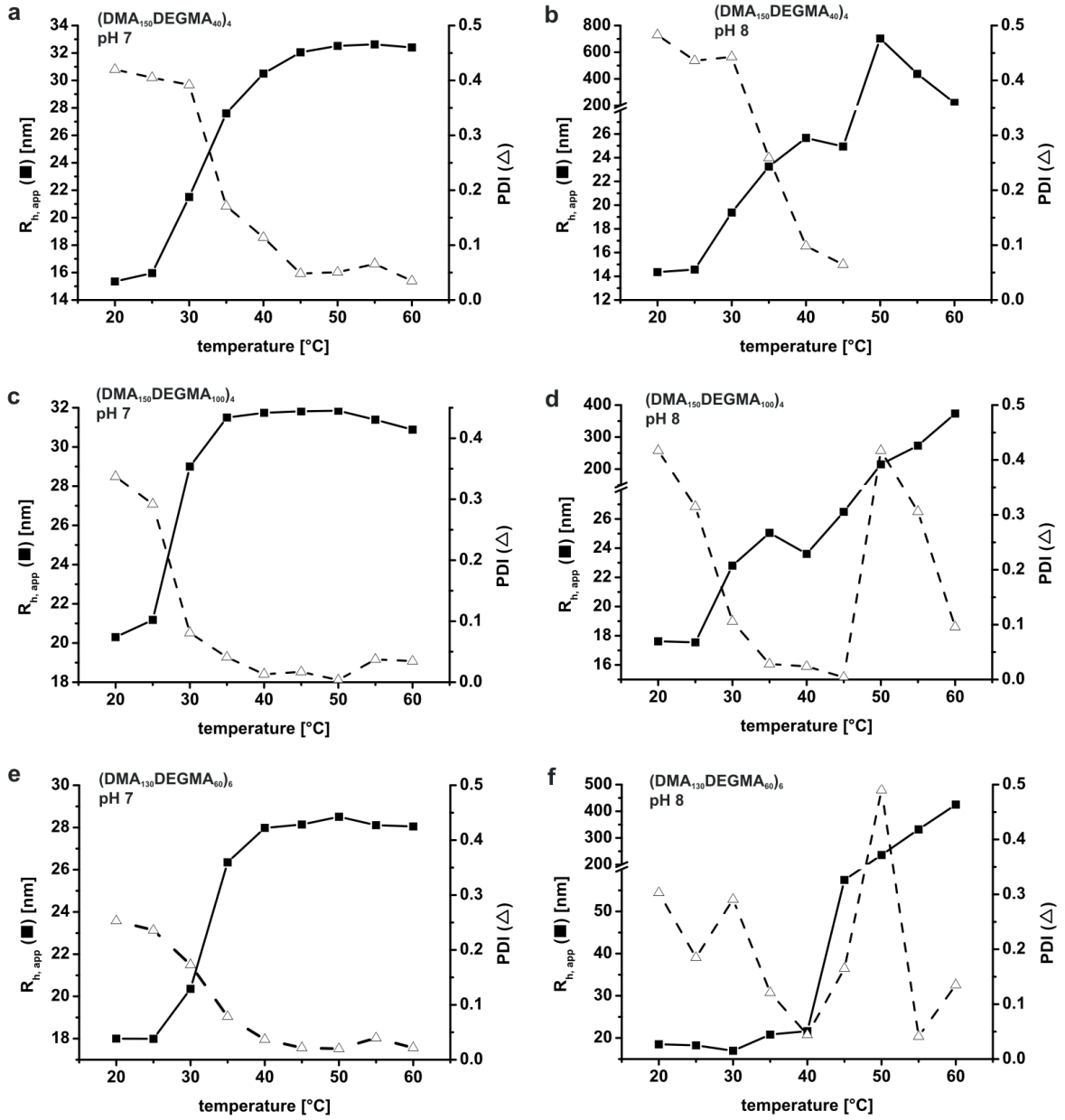

Figure S5.3. Temperature-dependent apparent hydrodynamic radii and polydispersity indices derived from cumulant analysis for $(DMA_{150}DEGMA_{40})_4$ at a) pH 7 and b) pH 8, $(DMA_{150}DEGMA_{100})_4$ at c) pH 7 and d) pH 8 and $(DMA_{130}DEGMA_{60})_6$ at e) pH 7 and f) pH 8. Measurements performed in buffer solution at 1g/L and Θ = 90°.

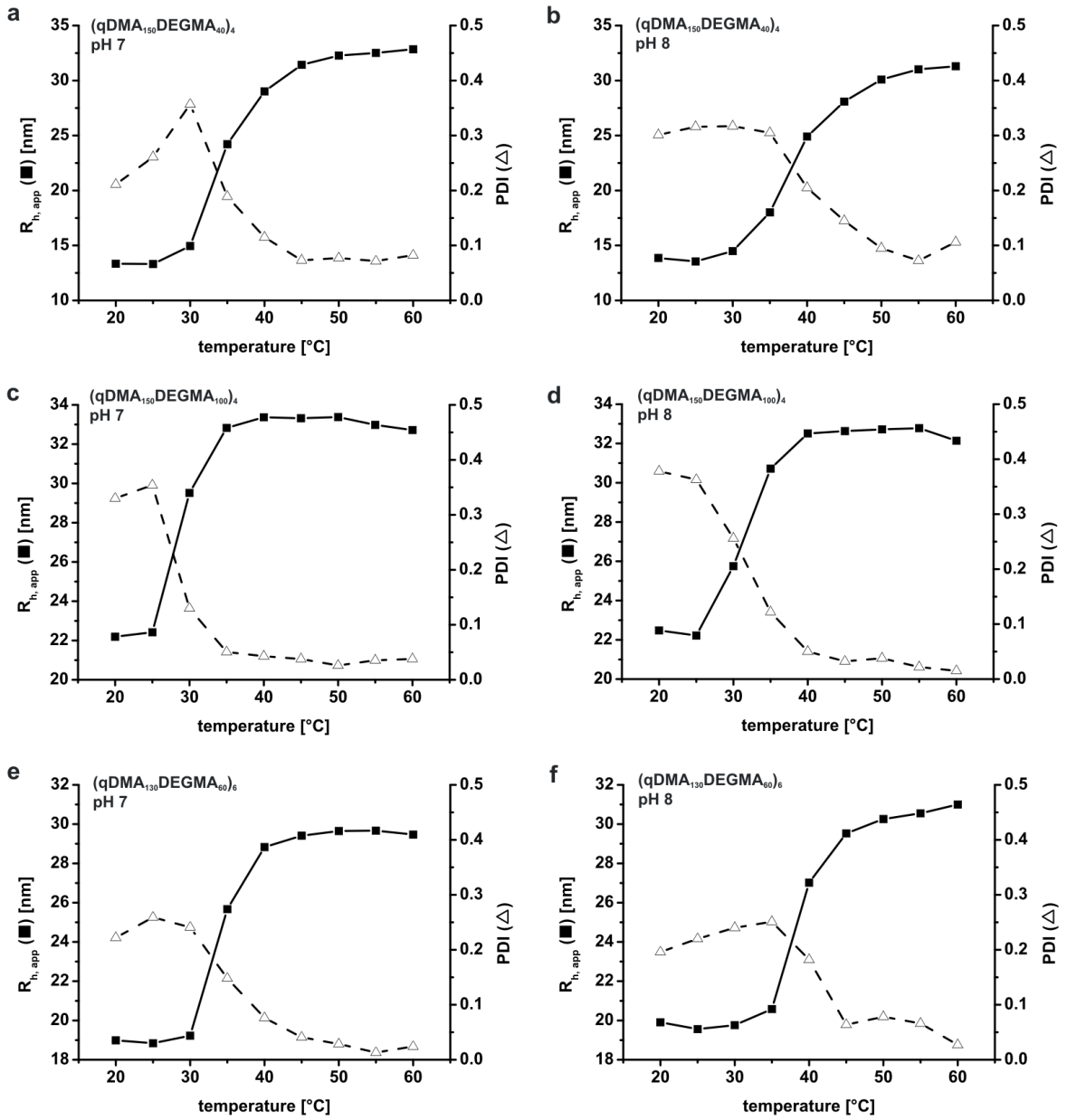

Figure S5.4. Temperature-dependent apparent hydrodynamic radii and polydispersity indices derived from cumulant analysis for $(qDMA_{150}DEGMA_{40})_4$ at a) pH 7 and b) pH 8, $(qDMA_{150}DEGMA_{100})_4$ at c) pH 7 and d) pH 8 and $(qDMA_{130}DEGMA_{60})_6$ at e) pH 7 and f) pH 8. Measurements performed in buffer solution at 1g/L and Θ = 90°.

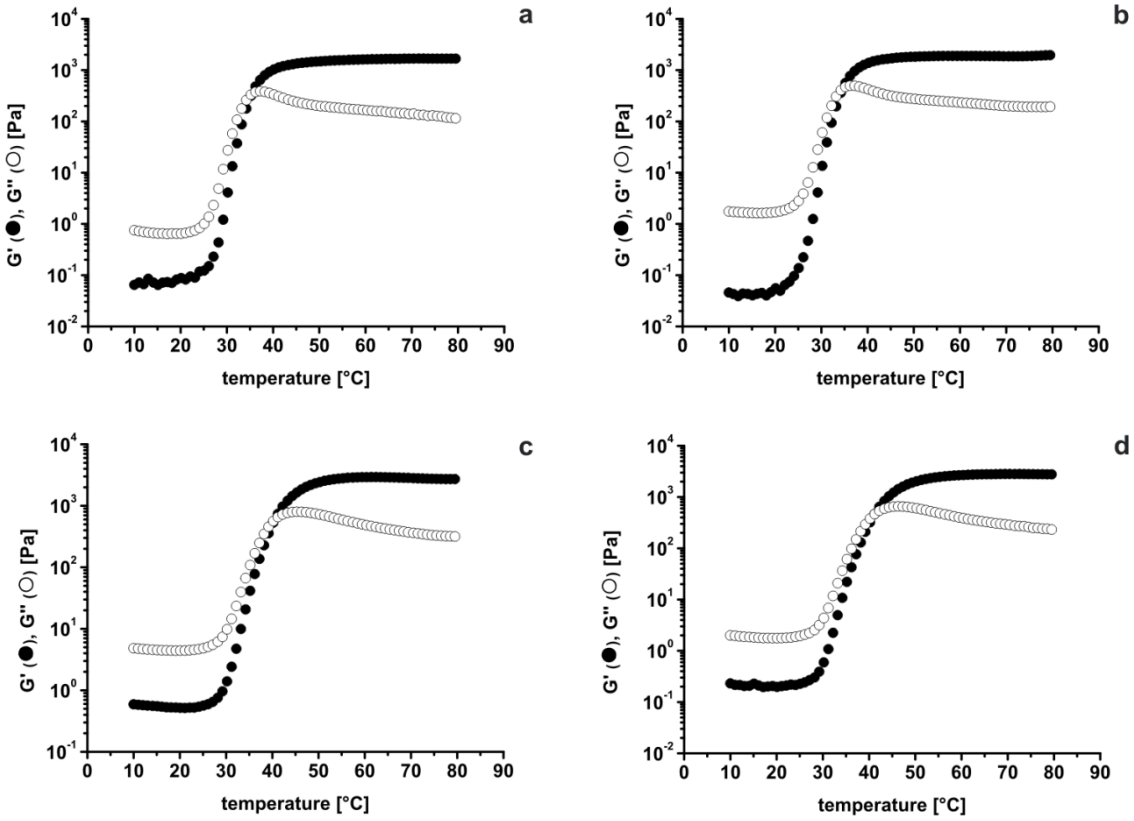

Figure S5.5. Temperature-dependent storage (*G'*) and loss moduli (*G''*) of $(DMA_{150}DEGMA_{100})_4$ in a) a 15 wt% solution at pH 8.2 and b) a 20 wt% solution at pH 8.4 and of $(DMA_{130}DEGMA_{60})_6$ in c) a 15 wt% solution at pH 8.2 and d) a 20 wt% solution at pH 8.3.

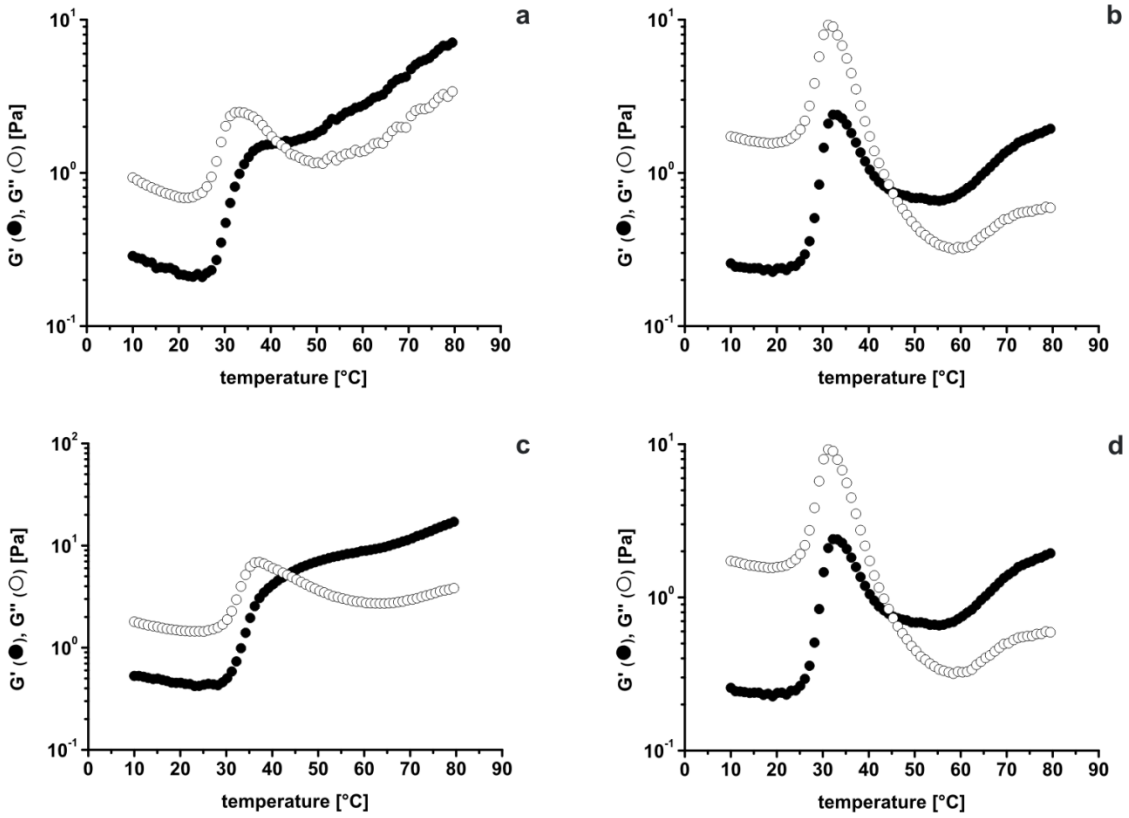

Figure S5.6. Temperature-dependent storage (*G'*) and loss moduli (*G''*) of $(DMA_{150}DEGMA_{100})_4$ in a) a 15 wt% solution at pH 8.9 and b) a 20 wt% solution at pH 8.9 and of $(DMA_{130}DEGMA_{60})_6$ in c) a 15 wt% solution at pH 9.0 and d) a 20 wt% solution at pH 8.7.

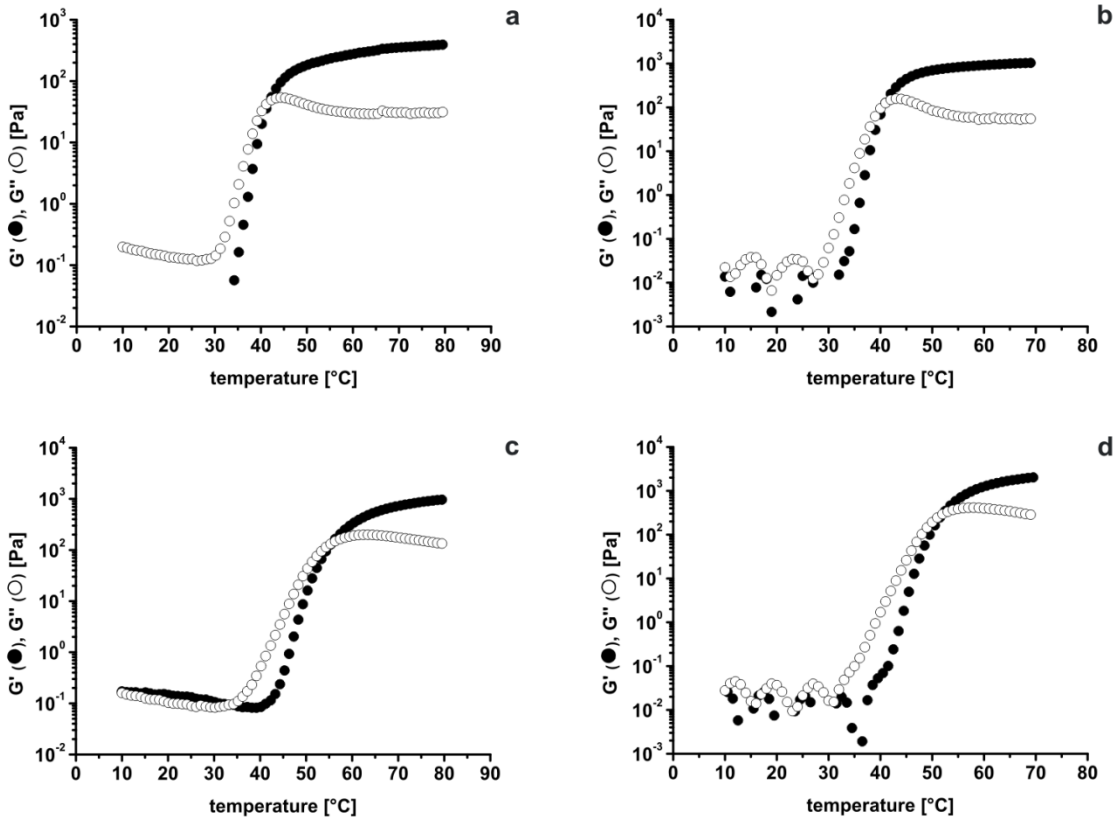

Figure S5.7. Temperature-dependent storage (*G'*) and loss moduli (*G''*) of $(qDMA_{150}DEGMA_{100})_4$ in a) a 5 wt% solution and b) a 10 wt% solution and of $(qDMA_{130}DEGMA_{60})_6$ in c) a 5 wt% solution and d) a 10 wt% solution.

6 Summary

The work presented in this thesis is focused on the synthesis of double-responsive star-shaped block copolymers and their formation of smart hydrogels in response to different external stimuli, specifically temperature and pH. Our concept was based on $(AB)_x$ diblock copolymer stars where both blocks are responsive to temperature and pH. This approach led to physically crosslinked hydrogels, which could form/disintegrate in response to a first trigger, *i.e.* the outer B blocks are alternating between hydrophilic and hydrophobic. The mechanical properties of the gels could still be manipulated by a second, independent trigger, *i.e.* upon applying the second trigger, the inner A blocks contract, leading to a change in mechanical properties.

The first part deals with the synthesis and characterization of linear and star-shaped poly((2-diethylamino)ethyl methacrylate) (PDEA) to investigate its double-responsive behavior and its potential for the design of double-responsive gelators. This polymer responds to variations in both pH and temperature, just like the analogous poly((2-dimethylamino)ethyl methacrylate) (PDMA). At a given temperature PDEA exhibits a critical pH value above which the chains collapse and aggregation takes place. The temperature-responsive behavior of PDEA does not depend on molecular weight or architecture, *i.e.* arm number. However, the cloud point does strongly depend on pH, as it affects the overall charge of the star.

For the second part we combined PDMA and PDEA to create double-responsive star-shaped block copolymers $(DMA\text{-}DEA)_x$ where both blocks are responsive to pH and temperature. The collapse of the PDEA outer blocks is first selectively triggered by heating. This has been proven by dynamic light scattering and is due to the significantly lower cloud point of PDEA with respect to that of PDMA at identical pH. The gelation behavior was investigated in dependence on block length and arm number. At high concentrations hydrogel formation was observed under conditions where only the PDEA outer blocks are insoluble. Rheology measurements showed that a minimum DEA fraction is necessary for gel formation and that the DEA fraction strongly influences the properties of the gels. Another factor controlling the gelation behavior of the diblock copolymer stars is the pH value, as the sol-gel transition temperature at a given concentration is shifted to lower values upon increasing the pH. The

mechanical properties of some gel can be manipulated, as a decrease in the storage modulus was only observed for soft gels, if the temperature is increased above the transition temperature of the inner PDMA block, *i.e.* when the PDMA blocks contract. Thus, we successfully created double-responsive star-shaped gelators which formed reversible hydrogels that were still able to respond to a second trigger. However, the aggregation and hydrogel formation turned to out to be quite complex, due to the high number of parameters controlling them.

Finally, our concept was extended to other polymers and simplified by changing the outer block of the block copolymer stars to a polymer that is only responsive to temperature. This allows for an easier tuning of the sol-gel transition, as only one parameter is involved. The new diblock stars are comprised of PDMA inner blocks and outer blocks of poly(diethylene glycol methyl ether methacrylate) (PDEGMA), which can be triggered independently of each other as confirmed by turbidimetry and dynamic light scattering. They form hydrogels at relatively low concentrations upon heating above the transition temperature of PDEGMA independent of the pH value. The fraction of DEGMA is an important parameter for the gelation behavior of the $(DMA\text{-}DEGMA)_x$ stars, the same as the DEA fraction was for the $(DMA\text{-}DEA)_x$ stars. Unexpectedly, the mechanical properties of these gels can also not be changed by heating above the transition temperature of PDMA at pH values around 8. The gels formed in this pH region are strong and too rigid to be affected, similar to strong gels formed from $(DMA\text{-}DEA)_x$ stars. Only when the pH is increased close to 9 and the subsequently formed gels are softer, a decrease in the moduli is observed.

We also quaternized the inner PDMA blocks of the $(DMA\text{-}DEGMA)_x$ stars to transform them it into strong polycations. This leads to an increase in the effective volume fraction of the stars and consequently to a significant decrease of the critical gelation concentration. The quaternization opens our concept up to the introduction of light sensitivity through multivalent counterions and the incorporation of nanoparticles.

Zusammenfassung

Die vorliegende Arbeit befasste sich mit der Synthese von doppelt responsiven sternförmigen Blockcopolymeren und deren Verwendung zur Herstellung von intelligenten Hydrogelen die auf mehrere Reize reagieren können, im Besonderen Temperatur und pH-Wert. Unser Konzept basiert auf $(AB)_x$ Blockcopolymer-Sternen bei denen beide Blöcke auf Temperatur und pH-Wert reagieren können. Diese Vorgehensweise führt zu physikalisch vernetzten Hydrogelen deren Bildung/Auflösung durch einen externen Reiz geschaltet werden kann, d.h. die äußeren B Blöcke wechseln zwischen hdrophil und hydrophob hin und her. Die mechanischen Eigenschaften der Gele können von einem unabhängigen zweiten Reiz verändert werden, d.h. die inneren A Blöcke schrumpfen als Reaktion auf den zweiten Reiz.

Als erstes wurden lineare und sternförmige Poly((2-diethylamino)ethylmethacrylat)e (PDEA) synthetisiert und deren doppelt responsives Verhalten und das Potential zur Herstellung von doppelt responsiven Gelatoren untersucht. Das Polymere reagiert auf Änderungen der Temperatur und des pH-Wertes ähnlich wie das analoge Poly((2-dimethylamino)ethyl methacrylat) (PDMA). Je nach Temperatur besitzt PDEA einen kritischen pH-Wert, oberhalb dessen die Ketten kollabieren und Aggregation auftritt. Das temperatur-responsive Verhalten von PDEA ist nicht vom Molekulargewicht oder der Architektur, d.h. der Zahl der Arme, abhängig. Allerdings hängt der Trübungspunkt stark vom pH-Wert ab, da dieser die gesamte Ladung des Sterns beeinflusst.

Im Anschluss wurden PDMA und PDEA kombiniert um doppelt responsive sternförmige Blockcopolymere $(DMA\text{-}DEA)_x$ herzustellen, deren beide Blöcke auf pH-Wert- und Temperaturänderungen reagieren. Der Kollaps des äußeren PDEA Blocks kann beim Heizen selektiv als erstes ausgelöst werden. Dies wurde durch dynamische Lichtstreuexperimente bewiesen und liegt an dem signifikant tiefer liegenden Trübungspunkt von PDEA in Vergleich zu PDMA, bei identischem pH-Wert. Das Gelierungsverhalten wurde auf seine Abhängigkeit von Blocklänge und Armzahl hin untersucht. Hydrogele bilden sich in konzentrierten Lösungen unter Bedingungen bei denen nur der äußere PDEA Block unlöslich ist. Rheologische Messungen haben gezeigt dass ein bestimmter minimaler DEA-Anteil nötig ist um Gele zu bilden und dass der Anteil an DEA einen großen Einfluss auf die Eigenschaften

der Gele hat. Ein weiterer Faktor, der das Verhalten beeinflusst, ist der pH-Wert, da der Sol-Gel Übergang sich bei gegebener Konzentration und steigendem pH-Wert zu niedrigeren Temperaturen verschiebt. Die mechanischen Eigenschaften einiger der Gele können verändert werden, da der Speichermodul nur bei weichen Gelen abnimmt, wenn die Temperatur über die Übergangstemperatur des PDMA Blocks erhöht wird. Somit haben wir erfolgreich doppelt responsive sternförmige Gelatoren hergestellt, die reversible Hydrogele bilden, die auf einen zweiten Reiz reagieren können.

Anschließend haben wir unser Konzept auf andere Polymere erweitert und es vereinfacht indem der äußere Block durch ein Polymer ersetzt wurde das nur auf Temperatur reagiert. Die zweite Maßnahme erlaubt eine einfachere Anpassung des Sol-Gel Übergangs, da nur ein einziger Parameter beteiligt ist. Die neuen Diblock-Sterne bestehen im Inneren aus PDMA Blöcken und aus äußeren Blöcken aus Poly(diethylenglycol methylether methacrylat) (PDEGMA), welche unabhängig voneinander geschalten werden können. Sie bilden bei relativ niedrigen Konzentrationen Hydrogele, sobald die Temperatur über die Übergangstemperatur von PDEGMA erhöht wird, unabhängig vom pH-Wert. Der Anteil an DEGMA ist ein wichtiger Parameter für das Gelierungsverhalten der $(DMA\text{-}DEGMA)_x$ Sterne, genauso wie es der Anteil an DEA für die $(DMA\text{-}DEA)_x$ Sterne war. Entgegen unserer Erwartungen konnten die mechanischen Eigenschaften der Gele bei pH 8 nicht durch Erwärmen oberhalb der Übergangstemperatur des PDMA Blocks beeinflusst werden. Die Gele die in diesem pH Bereich gebildet werden sind stark und zu fest um manipuliert zu werden, ähnlich den Gelen die von $(DMA\text{-}DEA)_x$ Sternen gebildet werden. Nur wenn der pH-Wert auf fast 9 erhöht wird und die dabei entstehenden Gele weicher sind, wurde eine Abnahme der Moduli beobachtet.

Abschließend wurden die inneren PDMA Blöcke der $(DMA\text{-}DEGMA)_x$ Sterne quaternisiert um sie in starke Polykationen umzuwandeln. Dies hat eine Zunahme des effektiven Volumenbruchs der Sterne zur Folge und führt zu einer deutlichen Abnahme der kritischen Gelierungskonzentration. Die Quaternisierung eröffnet die Möglichkeit unser Konzept zu erweitern, mittels der Einführung von Lichtsensitivität durch mehrwertige Gegenionen und der Integration von Nanopartikeln.

7 List of Publications

During the course of this thesis the following paper have been published:

1. Plamper, F.A.; **Schmalz, A.**; Penott-Chang, E.K.; Drechsler, M.; Jusufi, A.; Ballauff, M.; Müller, A.H.E., *Synthesis and Characterization of Star-Shaped Poly(N,N-dimethylaminoethyl methacrylate) and Its Quaternized Ammonium Salts*, **Macromolecules**, 2007, *40*, 5689-5697.

2. Plamper, F.A.; Ruppel, M.; **Schmalz, A.**; Borisov, O.; Ballauff, M.; Müller, A.H.E., *Tuning the Thermoresponsive Properties of Weak Polyelectrolytes: Aqueous Solutions of Star-Shaped and Linear Poly(N,N-dimethylaminoethyl methacrylate)*, **Macromolecules**, 2007, *40*, 8361-8366.

3. Plamper, F.A.; **Schmalz, A.**; Ballauff, M.; Müller, A.H.E., *Tuning the Thermoresponsivness of Weak Polyelectrolytes by pH and Light: Lower and Upper Critical Solution Temperature of Poly(N,N-dimethylaminoethyl methacrylate)*, **J. Am. Chem. Soc.**, 2007, *129*, 14538-14539.

4. **Schmalz, A.**; Hanisch, M.; Schmalz, H.; Müller, A.H.E., *Double Stimuli-Responsive Behavior of Linear and Star-Shaped Poly(N,N-diethylaminoethyl methacrylate) in Aqueous Solution*, 2010, **Polymer**, *51*, 1213-1217.

5. **Schmalz, A.**; Schmalz, H.; Müller, A.H.E., *Double Responsive Hydrogels Based on Tertiary Amine Methacrylate Star Block Copolymers*, **Z. Phys. Chem**., 2012, *226* (7-8), 695-709.

6. **Schmalz, A.**; Schmalz, H.; Müller, A.H.E., *Smart Hydrogels Based on Responsive Star-Block Copolymers*, **Soft Matter**, 2012, *8* (36), 9436-9445.

Acknowledgements

First of all, I would like to thank my supervisor Professor Axel H. E. Müller for giving me the opportunity to work in his group. I appreciate all the help he has provided me during the course of my thesis and the time he has taken for discussions and for all the useful tips. I am grateful for the numerous opportunities he has offered me, including sending me to several international conferences to present my work.

Special thanks go to Dr. Holger Schmalz, who has been of immense help to me during my research. Thank you for all the time spent in discussions and helping me correct my manuscripts.

I want to thank Professor Ingo Rehberg and Dr. Reinhard Richter for providing access to their rheometer and Tobias Lang for helping me with all my problems with it.

I would also like to thank Dr. Felix Plamper for teaching me most of what I know about the synthesis of stars and for the time spent in the lab together.

Most of all I have to thank the whole MC^2 group for being such an incredibly funny and interesting place to spend my time during my thesis. First are the technical assistants Melanie Förtsch, Marietta Böhm, Annika Pfaffenberger, Annette Krökel, Sabine Wunder and Susanne Edinger for doing all my measurements for SEC, TEM, MALDI and for all the countless other things they did for me. In addition, I thank Gaby Oliver for all her help with administrative problems and for all the humor she had with me.

A big thank you goes to all my former and present coworkers who managed to make this experience into something amazing. For all the time spent in our “group activities” either in the lab or outside, which made all the difference. So in no particular order: André Pfaff, Sandrine Tea, Thomas Ruhland, Markus Müllner, André Gröschel, Alexander Majewski, Stephan Weiß, Joachim Schmelz, Christopher Synatschke, Eva Betthausen, Andrea Wolf, Zhicheng Zheng, Stefan Reinicke, Hans-Joachim Voigtländer, Felix Plamper, Felix Schacher, Markus Ruppel, Markus Burkhadt, Anja Goldmann, Jiayin Yuan, Youyong Xu, Manuela Schuhmacher, Michael Witt and many more…

I also thank the Chemiker Spass Gesellschaft, CSG e.V., and all the people involved for providing me and a lot of others with many, many great evenings and activities. I had a lot of fun and hope that I will continue to do so as a member over the years.

Most importantly I have to thank my parents, my brother and tina for their unwavering support and encouragement over the years, without which I couldn’t have made it to where I am today.

Erklärung

Die vorliegende Arbeit wurde von mir selbstständig verfasst und ich habe dabei keine anderen als die angegebenen Hilfsmittel und Quellen benutzt.

Ferner habe ich nicht versucht anderweitig, mit oder ohne Erfolg, eine Dissertation einzureichen oder mich der Doktorprüfung zu unterziehen.

Bayreuth, den 06.12.2011

(Alexander Schmalz)